ARTICLE IN PRESS
GR-02448; No of Pages 41

Gondwana Research 90 (2021) xxx

Contents lists available at ScienceDirect

Gondwana Research

journal homepage: www.elsevier.com/locate/gr

GR Focus Review

The Sveconorwegian orogeny

Bernard Bingen [a,*], Giulio Viola [b], Charlotte Möller [c], Jacqueline Vander Auwera [d], Antonin Laurent [e], Keewook Yi [f]

[a] Geological Survey of Norway, 7491 Trondheim, Norway
[b] Department of Biological, Geological and Environmental Sciences, BiGeA, University of Bologna, 40126 Bologna, Italy
[c] Department of Geology, Lund University, Sölvegatan 12, SE-223 62 Lund, Sweden
[d] Department of Geology, University of Liège, 4000 Liège, Belgium
[e] Université de Lyon, UJM-Saint-Etienne, CNRS, UCA, IRD, LMV UMR 6524, F-42023 Saint-Etienne, France
[f] Korea Basic Science Institute, 363-883, Chungbuk, South Korea

ARTICLE INFO

Article history:
Received 2 March 2020
Received in revised form 21 October 2020
Accepted 31 October 2020
Available online 24 November 2020

Keywords:
Sveconorwegian
Mesoproterozoic
Rodinia
Continental collision
Orogenic plateau - lithospheric mantle delamination

ABSTRACT

This article reviews the geology of the Sveconorwegian orogen in south Scandinavia and existing tectonic models for the Mesoproterozoic to Neoproterozoic Sveconorwegian orogeny. It proposes an updated geodynamic scenario of large, hot, long-duration continental collision starting at c. 1065 Ma between proto-Baltica and another plate, presumably Amazonia, in a Rodinia-forming context. An orogenic plateau formed at 1280 Ma as a back-arc Cordillera-style plateau, and then grew further stepwise after 1065 Ma, as a collisional Tibetan-style plateau. Voluminous mantle- and crustal-derived Sveconorwegian magmatism took place in the hinterland in the west of the orogen, mainly: (i) bimodal magmatism at 1280–1145 Ma, overlapping with extensional intramontane basin sedimentation, (ii) the calc-alkaline Sirdal magmatic belt at 1065–1020 Ma, (iii) the hydrous ferroan hornblende-biotite granite (HBG) suite at 985–925 Ma and (iv) the anhydrous ferroan massif-type anorthosite-mangerite-charnockite (AMC) suite at 935–915 Ma. High-alumina orthopyroxene megacrysts in anorthosite imply mafic underplating at 1040 Ma and remelting of the underplates at 930 Ma. Overlapping with magmatism, protracted low-pressure, granulite-facies metamorphism reached twice ultra-high temperature conditions of 0.6 GPa-920 °C at 1030–1005 Ma and 0.4 GPa-920 °C at 930 Ma, respectively. These features imply shallow asthenosphere under the crust. Towards the foreland in the east, metamorphism shows an increasing high-pressure signature eastwards with time, with peak P-T values of 1.15 GPa-850 °C at 1150–1120 Ma in the Bamble-Kongsberg lithotectonic units, 1.5 GPa-740 °C at c. 1050 Ma in the Idefjorden lithotectonic unit, and 1.8 GPa-870 °C at c. 990 Ma in the Eastern Segment under eclogite-facies conditions. These are attributed to retreating delamination of the dense sub-continental lithospheric mantle and growth of the orogenic plateau towards the foreland. After c. 930 Ma, convergence came to a halt, the orogenic plateau collapsed, and 16 km of overburden was removed by extension and erosion.

Contents

* Corresponding author.
E-mail addresses: bernard.bingen@ngu.no (B. Bingen), giulio.viola3@unibo.it (G. Viola), charlotte.moller@geol.lu.se (C. Möller), jvdauwera@uliege.be (J. Vander Auwera), antonin.laurent@univ-st-etienne.fr (A. Laurent), kyi@kbsi.re.kr (K. Yi).

https://doi.org/10.1016/j.gr.2020.10.014
1342-937X/

Please cite this article as: B. Bingen, G. Viola, C. Möller, et al., The Sveconorwegian orogeny, Gondwana Research, https://doi.org/10.1016/j.gr.2020.10.014

1. Introduction

Late-Mesoproterozoic orogenic belts are interpreted as products of the closure of oceanic realms and the collision between continents to form supercontinent Rodinia at the end of the Mesoproterozoic (Hoffman 1991; Li et al. 2008). The Rodinia paradigm is robust, and supported by a peak in the abundance of late Mesoproterozoic detrital zircons (Hawkesworth et al. 2009). This notwithstanding, paleogeographic models for Rodinia configuration and plate tectonic models for Rodinia assembly remain in essence ill-defined (Torsvik 2003). Proto-Baltica (Proterozoic Baltica = East European Craton, here after called Baltica) is a core piece of Rodinia in almost all models (Fig. 1) (Li et al. 2008; Merdith et al. 2017), and the Sveconorwegian orogen at the western margin of Baltica provides key geological evidence for the assembly of Rodinia (Bingen et al. 2008a; Bingen et al. 2008c; Bogdanova et al. 2008; Cawood and Pisarevsky 2017; Cawood et al. 2010; Falkum and Petersen 1980; Gee et al. 2015; Gower et al. 2008; Hartz and Torsvik 2002; He et al. 2018; Ibanez-Mejia et al. 2011; Johansson, 2009; Johansson, 2014; Lorenz et al. 2012; Pisarevsky et al. 2014; Roberts 2013; Roberts and Slagstad 2015; Slagstad et al. 2019; Slagstad et al. 2020; Slagstad et al. 2018; Slagstad et al. 2017; Spencer et al., 2019; Stephens and Wahlgren 2020b; Torsvik et al. 1996; Weber et al. 2010).

The Sveconorwegian orogen is well exposed and accessible in its type area in southwest Scandinavia (south Norway and southwest Sweden). It represents therefore an excellent natural laboratory to study Precambrian geodynamics (Bingen and Viola 2018; Laurent et al. 2018a; Möller and Andersson 2018; Slagstad et al. 2018; Stephens and Wahlgren 2020b; Vander Auwera et al. 2011; Viola and Henderson 2010).

The body of geological data on the Sveconorwegian orogen has been steadily growing over the last 20 years, leading to contrasting conceptual models. This article reviews the existing structural, metamorphic, magmatic, geochronological and isotopic record across the entire Sveconorwegian orogen, and discusses the orogenic models that have been proposed in the literature. In fact, there is a lively debate in the literature on whether the Sveconorwegian orogeny was a collisional (Himalaya-Tibet type) or a non-collisional (Andean type) orogeny (Bingen et al. 2008a; Möller and Andersson 2018; Slagstad et al. 2020; Slagstad et al. 2017; Slagstad et al. 2013; Stephens and Wahlgren 2020b). We address this debate and conclude proposing an updated model of large, hot, and long-duration continent-continent collision

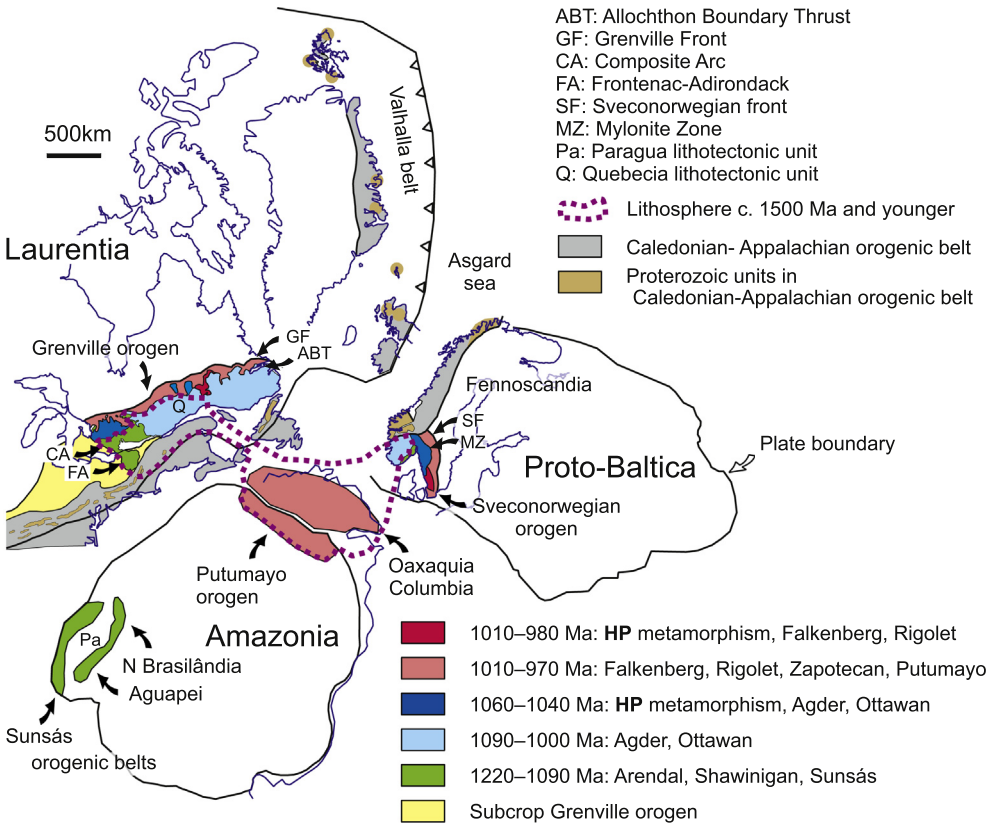

Fig. 1. Archetypal paleogeographic reconstruction of proto-Baltica (Baltica), Laurentia and Amazonia in their Rodinia framework at the Mesoproterozoic-Neoproterozoic boundary (Cawood and Pisarevsky 2017; Hoffman 1991; Li et al. 2008). The first order architecture of the Meso- to Neoproterozoic orogenic belts is shown, with emphasis on the geochronology of metamorphism (Hynes and Rivers 2010; Ibanez-Mejia et al. 2011; Rivers 2008; Tohver et al. 2005). The high-pressure (HP) metamorphic belts are shown separately. The names of the main tectonometamorphic phases in the different orogens are listed in the legend, with Arendal, Agder, Falkenberg for the Sveconorwegian orogen, Shawinigan, Ottawan, Rigolet for the Grenville orogen, Putumayo for the Putumayo orogenic belt, Zapotecan for the Oaxaquia lithotectonic unit, and Sunsás for the Sunsás, Aguapei and N Brasilândia belts.

for the Sveconorwegian orogeny at the margin of Baltica. This model involves the stepwise propagation of an orogenic plateau towards the foreland and hinterland of the orogen, associated with retreating delamination of the continental lithospheric mantle. It takes into account a number of key features of the orogeny, including the zoning of metamorphism, the distribution of magmatism and the genesis of massif-type anorthosites.

2. Context

2.1. The Sveconorwegian orogen and Sveconorwegian orogeny

The Sveconorwegian orogen is located along the southwestern margin of Fennoscandia (Fennoscandia is the northern part of proto-Baltica/Baltica) (Figs. 1, 2; Table 1) (Bogdanova et al. 2008; Koistinen et al.

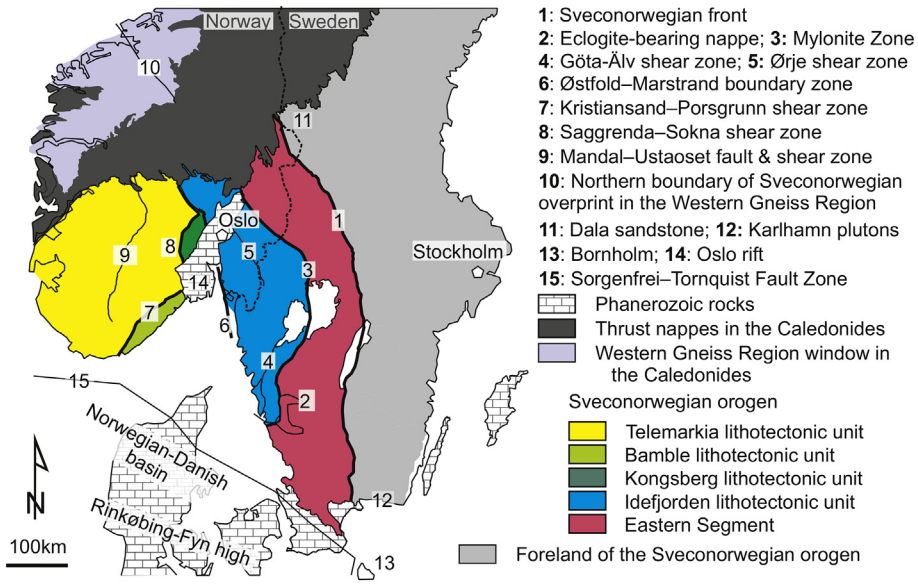

Fig. 2. Sketch map of the Sveconorwegian orogen, with nomenclature of lithotectonic units and main shear and fault zones.

2001; Stephens et al. 2020). The Sveconorwegian orogen consists of Paleoproterozoic to Mesoproterozoic continental lithosphere reworked during the Sveconorwegian orogeny at the transition between the Mesoproterozoic and the Neoproterozoic (Stenian to Tonian). This lithosphere was generated during the Svecokarelian (1910–1750 Ma), post-Svecokarelian (1710–1660 Ma), Gothian (1660–1520 Ma), Telemarkian (1520–1480 Ma) and Hallandian (1465–1380 Ma) accretionary orogenies.

The exposed Sveconorwegian orogen is presently c. 550 km wide and has a general N–S structural grain (Fig. 2) (Berthelsen 1980; Demaiffe and Michot 1985; Falkum 1985; Falkum and Petersen 1980). In the east, it is separated from the Paleoproterozoic foreland by the nearly 700 km long Sveconorwegian front (Möller and Andersson 2018; Möller et al. 2015; Stephens and Wahlgren 2020a; Wahlgren et al. 1994).

In the north, the Sveconorwegian orogen was reworked during the Caledonian orogeny (Fig. 2). Precambrian rocks with a Mesoproterozoic to Neoproterozoic overprint are observed in the Western Gneiss Region, the largest basement window in the Caledonides (Røhr et al. 2013; Tucker et al. 1990) and are also found in Caledonian thrust nappes of the Lower and Middle Allochthons of the Caledonides (Augland et al. 2014; Corfu 2019; Lundmark and Corfu 2008; Roffeis and Corfu 2014; Wiest et al. 2018). In the south, the Sveconorwegian basement is overlain by Phanerozoic sedimentary rocks and affected by Carboniferous-Permian and younger faulting and rifting along the WNW–ESE trending Sorgenfrei-Tornquist Fault Zone and NNE–SSW trending Oslo rift (Fig. 2) (Bergerat et al. 2007; Erlström 2020; Larsen et al. 2008; Torgersen et al. 2015). As inferred from geophysical data and a few deep wells in Denmark, a Sveconorwegian basement probably underlies the Norwegian-Danish Basin (Ringkøbing-Fyn high), reaching the southern boundary of the Baltica plate (Trans-European Suture Zone and Elbe line) (Lassen and Thybo 2012; Olesen et al. 2004; Olivarius et al. 2015; Thybo 2001).

The Sveconorwegian orogen can be conceptually subdivided into five, orogen-parallel lithotectonic units (INSPIRE_Directive, 2007), called, from east to west, the Eastern Segment, and the Idefjorden, Kongsberg, Bamble, and Telemarkia lithotectonic units (also referred to as units in short in the following text) (Fig. 2) (Bingen et al. 2008c). These lithotectonic units are separated by major Sveconorwegian shear zones and are characterized by distinct geological histories.

The first high-grade metamorphism attributed to the Sveconorwegian orogeny dates back to between 1150 and 1120 Ma and is recorded in the Bamble and Kongsberg lithotectonic units. It is referred to as the Arendal phase in Bingen et al. (2008a, 2008c). As elaborated further below, this early-Sveconorwegian event can be interpreted as the outcome of a geodynamic evolution starting after the Hallandian orogeny, i.e. after c. 1340 Ma, and is hereafter referred to as the pre-Sveconorwegian. The main Sveconorwegian orogeny started at c. 1065 Ma, and can be summarized by three orogenic phases (Bingen et al. 2008a; Bingen et al. 2008c): the Agder phase (1065–1000 Ma), the Falkenberg phase (1000–970 Ma) and the Dalane phase (970–900 Ma). As more geological data become available, however, these three phases are becoming increasingly difficult to discriminate in time and they are not used systematically in the following text. Intrusion of pegmatite fields and lamprophyre dykes sealed the orogeny at c. 915–900 Ma (Müller et al. 2015; Müller et al. 2017; Wahlgren et al., 2016).

2.2. Rodinia assembly

Several paleogeographic and tectonic models have been proposed for the configuration and assembly of supercontinent Rodinia at the end of the Mesoproterozoic (Hoffman 1991; Li et al. 2008; Merdith et al. 2017; Torsvik 2003). Classical models (Fig. 1), integrating paleomagnetic data and geological information from the Proterozoic to the Phanerozoic, suggest that Rodinia formed by the reassembly of

Table 1
Chart of geological events in the Sveconorwegian orogen.

Name	Geochronology [5 Ma bins]	P [GPa]	T [°C]	Lithotectonic unit	Reference
Visingsö Group deposition	885–740			Foreland	Moczydłowska et al. 2018
Sveconorwegian orogeny	1150–900				
Main Sveconorwegian orogeny	1065–900				
Falkenberg and Dalane phases	990–900				
Rare mineral pegmatites	915–900			Telemarkia	Müller et al. 2017
Flå-Bohus-Blomskog granite plutons	930–915	0.4		Idefjorden	Eliasson et al. 2003
UHT-LP granulite-facies metamorphism	935–930	0.4	910	Telemarkia, Rogaland-Vest Agder	Laurent et al., 2018a
Bjerkreim-Sokndal layered intrusion	930–920	≤ 0.5		Telemarkia, Rogaland-Vest Agder	Vander Auwera and Longhi 1994
Anorthosite-mangerite-charnockite suite	935–915	0.5		Telemarkia, Rogaland-Vest Agder	Charlier et al. 2010
Almesåkra Group deposition	980–945			Foreland	Ripa and Stephens, 2020d
Blekinge-Dalarna dolerites	980–945			Foreland	Söderlund et al. 2005
Hornblende-biotite granite suite	985–925	0.2–0.4		Telemarkia	Vander Auwera et al., 2014a
HP Granulite-facies metamorphism	980–960	1.1	850	Eastern Segment	Möller and Andersson, 2018
Eclogite-facies metamorphism	990	1.65–1.9	850–900	Eastern Segment	Tual et al. 2017
Agder phase	1065–1000				
UHT-LP granulite-facies metamorphism	1030–1005	0.55–0.7	950	Telemarkia, Rogaland-Vest Agder	Laurent et al., 2018b
Amphibolite-facies metamorphism	1040–995	0.9–1.2	730–790	Idefjorden	This work; Austin Hegardt, 2010
HP granulite-facies metamorphism	1045	1.5	740–780	Idefjorden	Söderlund et al., 2008a
Kalhovd Formation deposition	<1055			Telemarkia, Telemark	Bingen et al. 2003
Mafic underplate, HAOM crystallization	1040	1.3		Telemarkia, Rogaland-Vest Agder	Bybee et al. 2014
Sirdal magmatic belt, Feda suite	1065–1020	0.38–0.48		Telemarkia, Rogaland-Vest Agder	Coint et al. 2015
Early Sveconorwegian orogeny	1150–1080			Bamble, Kongsberg	
Arendal phase					
Eidsborg Formation deposition	<1105			Telemarkia, Telemark	Lamminen 2011
MP-MT granulite-facies metamorphism	1150–1120	1.15	850	Bamble, Kongsberg	Engvik et al. 2016
Pre-Sveconorwegian	1340–1150				
Hallandian orogeny	1465–1385			Eastern Segment and foreland	
Seljord, Modum, Kragerø, Nidelva deposition	1480–1340			Telemarkia, Bamble, Kongsberg	
Telemarkian orogeny	1520–1480			Telemarkia	
Gothian orogeny	1660–1520			Idefjorden	
Post-Svecokarelian magmatism	1710–1660			Eastern Segment	

continents previously merged into supercontinent Nuna (Columbia) during the Paleoproterozoic and Mesoproterozoic (Evans and Mitchell 2011; Johansson 2009; Pisarevsky et al. 2014; Rogers and Santosh 2002; Zhang et al. 2012). These models place Laurentia in the centre of Rodinia, with Baltica to the east and Amazonia to the south of Laurentia, respectively (Fig. 1) (Cawood and Pisarevsky 2017; Dalziel 1997; Gong et al. 2018; Hoffman 1991; Li et al. 2008; Merdith et al. 2017; Torsvik et al. 1996). Alternative Baltica–Laurentia reconstructions are proposed by Torsvik (2003), Lorenz et al. (2012) and Slagstad et al. (2019).

It is beyond the scope of this paper to review Rodinia assembly models. In the following text and in several figures, updated geological, geochronological and isotopic data from the Sveconorwegian orogen are compared with data from the Grenville orogen of Laurentia, the Putumayo and Sunsás orogens of Amazonia and Mesoproterozoic lithotectonic units in the Andes (Garzón, Las Minas inliers) and Mexico (Oaxaquia). The goal is to show that it is realistic to consider the Sveconorwegian orogen as part of a large orogenic zone between Laurentia, Amazonia and Baltica (Fig. 1). The comparative analysis offers a broader perspective for the Sveconorwegian orogeny in a Rodinia context.

2.3. A diversity of orogenic models

Many large-scale tectonic models have been proposed to explain the Sveconorwegian orogenic evolution. In Fig. 3, six possible conceptual end-member models are sketched in map view. They range from collisional (Himalaya-Tibet type) to non-collisional (Andean type), and some involve accretion of exotic lithotectonic units to Fennoscandia. In Fig. 3a, the early-Sveconorwegian closure of an ocean between the Telemarkia and Idefjorden lithotectonic units resulted in the formation of the Bamble-Kongsberg lithotectonic units at c. 1150–1120 Ma, and accretion of an exotic Telemarkia lithotectonic unit (Bingen et al. 2005). In Fig. 3b, the five lithotectonic units are all endemic to Fennoscandia. Only large-scale movements between them are considered, steered by large scale wrench tectonics, which is controlled by strike-slip shearing along the main Sveconorwegian shear zones (Bingen et al. 2005; Lamminen and Köykkä 2010; Stephens and Wahlgren 2020b). In Fig. 3c, closure of an oceanic basin at c. 990 Ma between the Eastern Segment and the Idefjorden lithotectonic unit (along the Mylonite Zone) resulted in the collision between Baltica (Fennoscandia) and a continent composed of the four western lithotectonic units of the orogen ('Sveconorwegia') (Möller and Andersson 2018; Petersson et al. 2015b). In Fig. 3d, an (Himalaya-Tibet type) collision at and after c. 1065 Ma between Baltica (Fennoscandia) and one (or several) continental plate(s) (possibly Amazonia, Laurentia, and intervening terranes exposed in Mexico and the Andes of Colombia) involved closure of oceanic basins to the west of the exposed orogen (Bingen et al. 2008c; Bogdanova et al. 2008; Cawood and Pisarevsky 2017; Ibanez-Mejia et al. 2011; Stephens and Wahlgren 2020b; Weber et al. 2010). In Fig. 3e and f, non-collisional (Andean type) models feature an eastward subduction of an oceanic plate below the western margin of Baltica (Fennoscandia) during the entire Sveconorwegian orogeny, from 1150 to 900 Ma, without a final collision. The lithotectonic units in the orogen were either already assembled before the Sveconorwegian orogeny (Fig. 3e) (Falkum and Petersen 1980; Slagstad et al. 2013) or, alternatively, they were dispersed during the pre-Sveconorwegian time interval (1340–1150 Ma) and then re-assembled during the Sveconorwegian orogeny after 1150 Ma (Fig. 3f) (Slagstad et al. 2020). These six models are not mutually exclusive because terrane assembly (Fig. 3a, c) can be anticipated before a collision (Fig. 3d) or during a protracted subduction history (Fig. 3e, f), and because deformation partitioning (Fig. 3b) can take place before, during and after a collision or during protracted subduction. Arguments supporting or dismissing aspects of each of these orogenic models are discussed in more detail below.

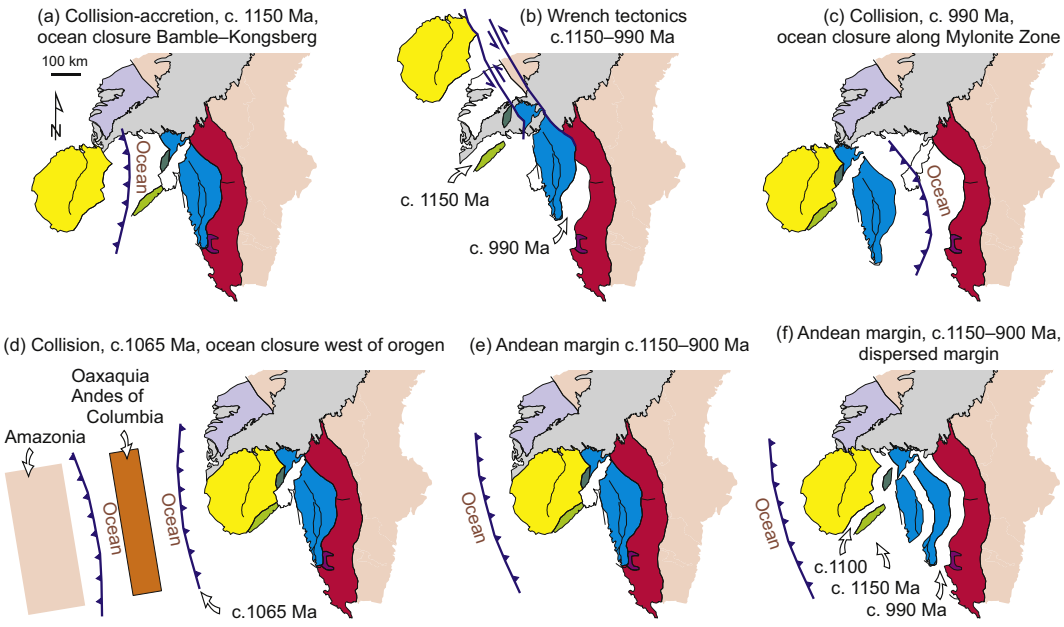

Fig. 3. Conceptual tectonic models, in map view, of the Sveconorwegian orogeny, reviewed in this paper. Same colour coding as in Fig. 2. (a) Early-Sveconorwegian accretion of the Telemarkia lithotectonic unit, with suturing along the Bamble-Kongsberg lithotectonic units (Bingen et al. 2005). (b) Wrench tectonics involving large strike-slip displacements between the five lithotectonic units of the orogen, all endemic to Fennoscandia (Lamminen and Köykkä 2010; Stephens and Wahlgren 2020b). (c) Collision at c. 990 Ma between Baltica (Fennoscandia) and a continent comprising the four western lithotectonic units of the orogen (Möller and Andersson 2018; Petersson et al. 2015b). (d) Collision at c. 1065 Ma between Baltica (Fennoscandia) and another continental plate (Amazonia) with closure of oceanic basins to the west of the exposed orogen (Bogdanova et al. 2008; Cawood and Pisarevsky 2017; Ibanez-Mejia et al. 2011). (e, f) non-collisional (Andean type) models, with orogeny controlled by a subduction system outboard of Fennoscandia during the entire duration of orogeny from c. 1150 to 900 Ma. (e) The margin was either well assembled before the orogeny (Falkum and Petersen 1980; Slagstad et al. 2013) or (f) dispersed and re-assembled during the orogeny (Slagstad et al. 2020).

2.4. Secular evolution of the Earth, mantle delamination and orogenic plateau

Estimates of heat flow and heat production through Earth history suggest that the asthenosphere was c. 100 °C hotter in the Mesoproterozoic than at present (Gerya 2014; Herzberg et al. 2010; Johnson et al. 2013; Korenaga 2008; Sizova et al. 2014). A hotter asthenosphere implies a weaker rheology of lithospheric plates. The tectonic consequences of a hotter asthenosphere on the dynamics of orogeny are multiple and include, but are not limited to, ductile thick-skinned deformation, lower topography, more proximal sedimentation, shallower slab break-off, widespread partial melting in the lower to middle crust, widespread syn-orogenic magmatism, ultrahigh temperature granulite-facies metamorphism (above 900 °C), decoupling between crust and lithospheric mantle, and remelting of basaltic underplates to produce anorthosite plutons (Brown 2006, 2013; Gerya 2014; Rey and Houseman 2006; Sizova et al. 2014; Vander Auwera et al. 2011; Vanderhaeghe 2012). These consequences can be evaluated qualitatively in the Proterozoic geological record (Cagnard et al. 2011; Chardon et al. 2009). However, they are difficult to assess and quantify individually (Sizova et al. 2014).

There is wide consensus that after the Archean, plate tectonics has imposed dominant horizontal movements to orogenies. However, an evaluation of the composition and temperature of the lithosphere through Earth history suggests that, after the Archean, the sub-continental lithospheric mantle was, on average, denser than the asthenosphere (Griffin et al. 2009; Poudjom Djomani et al. 2001). The sub-continental lithospheric mantle was therefore gravitationally unstable in the Proterozoic, like in the Phanerozoic, and prone to delamination and foundering (subduction) (Bird 1979; Chen et al. 2017; Krystopowicz and Currie 2013). Delamination of the lithospheric mantle is compensated by upwelling of asthenosphere. The parameters and geometry of delamination in convergent orogens were explored numerically by Li et al. (2016). Delamination is promoted by the density contrast between the lithospheric mantle and the asthenosphere, rheological weakness of the lower crust and the lithospheric mantle, convergence rate, and eclogitization of the lower crust.

The Sveconorwegian orogeny is characterized by widespread crustal partial melting, low-pressure–ultrahigh-temperature metamorphism and massif-type anorthosite plutonism, typical of hot orogens. Orogenic models for the Sveconorwegian orogeny should integrate the evolution of the mantle (and not only the crust). They require consideration of vertical movements of the lithospheric mantle and the asthenosphere in addition to horizontal movements of the lithospheric plates.

Orogenic plateaus are a hallmark of large and hot convergent orogens (Beaumont et al. 2006; Godin et al. 2006; Jamieson and Beaumont 2013; Li et al. 2016; Rey et al. 2001; Royden et al. 2008; Vanderhaeghe 2012). An orogenic plateau consists of elevated and thickened crust spreading by gravitational forces above a lithospheric mantle thinned by delamination. Temperature in the crust is regulated by self-heating and basal heating from the mantle. The crust of a plateau is characterized by a little viscous low- to middle-crust, weakened by partial melting, called infrastructure, overlain by a brittle upper crust, called superstructure or orogenic lid (Jamieson and Beaumont 2013; Rey et al. 2001; Vanderhaeghe 2012). In the infrastructure, metamorphism typically carries a high-temperature signature, overprinting pre-plateau metamorphic signatures (for example early high-pressure metamorphism) (Godin et al. 2006). Due to the difference in viscosity, the infrastructure and superstructure are structurally decoupled. The infrastructure can flow under the superstructure (channel flow), leading to a situation where the superstructure is in extension, while the infrastructure is in compression. An orogenic plateau can be anticipated to grow with time if convergence is maintained (Li et al. 2016; Royden et al. 2008).

The Sveconorwegian orogen consists of a patchwork of high-grade gneiss complexes and low-grade rocks (Fig. 4). In this paper, these are interpreted as the remnants of the infrastructure and superstructure of an orogenic plateau, respectively.

3. Geology of the Sveconorwegian orogen

The geology of the Sveconorwegian orogen is reviewed below from east to west, using the nomenclature summarized in Table 1 and the maps of Figs. 2, 4-6. A compilation of the geochronology of magmatic rocks is provided in Fig. 7, and a compilation of Lu–Hf isotopic data in Fig. 8.

3.1. Fennoscandian foreland

The Fennoscandian foreland of the Sveconorwegian orogen (Fig. 2) comprises mainly metamorphosed Paleoproterozoic magmatic rocks (plutonic and volcanic rocks) and siliciclastic sedimentary rocks, dating back to between c. 1960 Ma and 1740 Ma (Bergman et al. 2008; Korja et al. 2006; Lahtinen et al. 2009; Stephens 2020). These rocks were assembled during the accretionary Svecokarelian orogeny. They were unconformably overlain and crosscut by post-Svecokarelian volcanic and plutonic complexes formed between c. 1710 and 1680 Ma (Appelquist et al. 2011; Brander et al. 2012; Högdahl et al. 2004; Ripa and Stephens 2020a). These rocks are attributed in the literature to the Phase 2 of the Transcandinavian Igneous Belt and are little deformed to undeformed. They are interpreted to have formed in a supra-subduction geodynamic setting after the Svecokarelian orogeny. Younger Mesoproterozoic magmatic rocks intruded this basement, including granitic plutons (1530–1220 Ma; Andersson et al. 2002b; Brander and Söderlund 2009; Cecys and Benn 2007; Johansson et al. 2016), dolerites (c. 1460 Ma; Söderlund et al. 2005), and the so-called Central Scandinavian dolerites (1271 ± 1 to 1246 ± 2 Ma; Brander et al. 2011; Ripa and Stephens 2020c; Söderlund et al. 2006).

The c. 1 km thick unconformable Jotnian sandstone was deposited in a gentle continental sag basin between c. 1580 Ma and 1270 Ma and it is not deformed (Lundmark and Lamminen 2016; Ripa and Stephens 2020b). The southernmost part of the Fennoscandian foreland was reworked during the Hallandian orogenic event between 1465 and 1385 Ma (Fig. 6) (Bogdanova et al. 2008; Brander and Söderlund 2009; Ulmius et al. 2015; Wahlgren and Stephens 2020).

Sveconorwegian-related brittle deformation reached far into the Fennoscandian foreland (Andréasson and Rodhe 1994; Elminen et al. 2018; Mattila and Viola 2014; Saintot et al. 2011; Viola et al. 2009; Viola et al. 2013). The Blekinge-Dalarna dolerites form a weakly arcuate N-S trending dyke swarm parallel to the Sveconorwegian front (Figs. 4, 5). They intruded between 978 ± 2 and 946 ± 1 Ma, in the easternmost part of the Sveconorwegian orogen and its foreland (Gong et al. 2018; Ripa and Stephens 2020d; Söderlund et al. 2005). The c. 1200 m thick, sandstone dominated, Almesåkra Group represents possible remnants of a Sveconorwegian fold-and-thrust belt, to the east of the Sveconorwegian front (Fig. 5) (Ripa and Stephens 2020d; Rodhe 1987). Locally preserved peperitic contacts between the Blekinge-Dalarna dolerites and these sediments suggest that the sandstone was unconsolidated during intrusion of the dolerites and therefore that the two rock types are broadly coeval.

The Neoproterozoic, c. 1400 m thick, microfossil-bearing, Visingsö Group is exposed along the Sveconorwegian front in Sweden (Fig. 5). Its deposition is bracketed between 886 ± 9 Ma (detrital zircon U–Pb data) and c. 740 Ma (biostratigraphy). It can be considered as the infill of a post-Sveconorwegian, fault-controlled basin (Loron and Moczydłowska 2018; Moczydłowska et al. 2018; Pulsipher and Dehler 2019; Wickström and Stephens 2020).

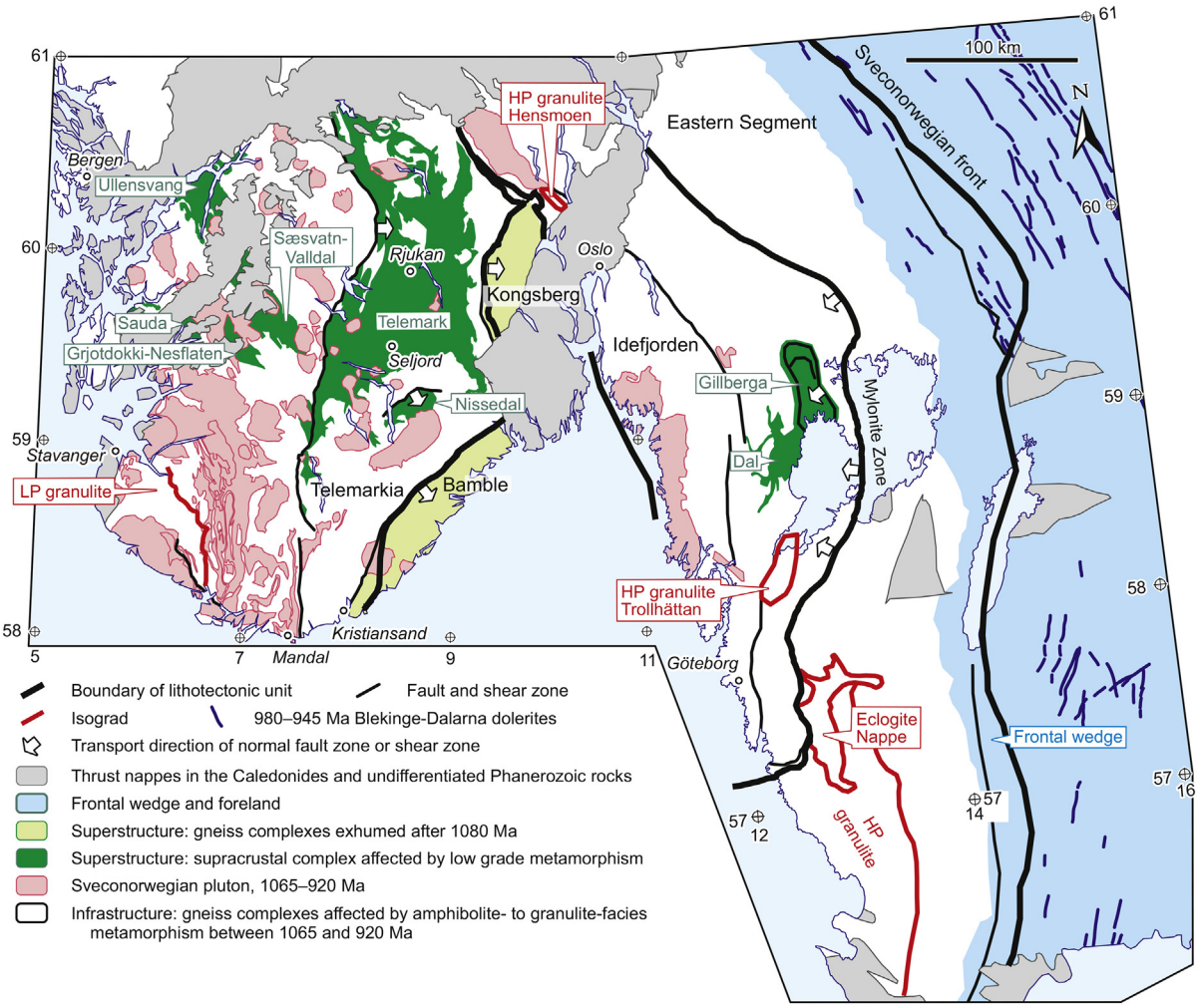

Fig. 4. Sketch map of the Sveconorwegian orogen, showing the extent of the infrastructure and superstructure (orogenic lid) of the orogen during the main Sveconorwegian orogeny (1065–920 Ma) and the Sveconorwegian plutons (1065–920 Ma).

3.2. Eastern segment

3.2.1. Svecokarelian and post-Svecokarelian evolution

The Eastern Segment is a 60 to 120 km wide, N–S trending lithotectonic unit mainly consisting of granitic to quartz-monzonitic orthogneiss (Fig. 2) (Berthelsen 1980; Möller and Andersson 2018; Stephens and Wahlgren 2020a). The protoliths formed between c. 1900 and 1660 Ma, with a strong frequency maximum of crystallization ages between 1710 and 1660 Ma (Fig. 7). They have an alkali-calcic geochemical composition and are characterized by a mildly positive ε_{Hf} and ε_{Nd} isotopic signature (average $\varepsilon_{Hf} = +3.0$ at 1700 Ma; Fig. 8) (Appelquist et al. 2011; Appelquist et al. 2008; Brander et al. 2012; Gorbatschev and Bogdanova 2006; Petersson et al. 2015a; Söderlund et al. 1999; Söderlund et al. 2002; Stephens and Wahlgren 2020a). They represent the western continuation of the Paleoproterozoic crust exposed in the foreland of the Sveconorwegian orogen, especially the post-Svecokarelian 1710–1680 Ma magmatic rocks exposed just east of the Sveconorwegian front (Petersson et al. 2015a; Ripa and Stephens 2020a; Stephens and Wahlgren 2020a). They were presumably formed in the same geodynamic setting along the same active continental margin.

3.2.2. Hallandian and pre-Sveconorwegian evolution

After an event of mafic magmatism at c. 1565 Ma (Beckman et al. 2017; Söderlund et al. 2004; Söderlund et al. 2005), the southern part of the Eastern Segment and the Sveconorwegian foreland were both affected by the Hallandian orogeny (Figs. 6, 7). The Hallandian orogeny involved low-pressure amphibolite- to granulite-facies metamorphism, migmatitization and deformation between c. 1465 and 1385 Ma (Brander et al. 2012; Möller et al. 2007; Piñán-Llamas et al. 2015; Söderlund et al. 2002; Ulmius et al. 2015), and was accompanied by magmatism during the same time interval (Fig. 7) (Åhäll et al. 1997; Andersson et al. 1999; Brander and Söderlund 2009; Cecys et al. 2002; Christoffel et al. 1999; Möller et al. 2015; Ulmius et al. 2015). The final stage of Hallandian magmatism includes a suite of charnockite-mangerite, granite and anorthosite plutons formed between c. 1400 and 1380 Ma (Åhäll et al. 1997; Christoffel et al. 1999; Harlov et al. 2013; Möller et al. 2015). The Hallandian orogeny may have involved subduction along the southern margin of Baltica and may record a change in the configuration of subduction zones around Baltica, from E-dipping before 1480 Ma to N-dipping after 1465 Ma (Pisarevsky et al. 2014; Roberts and Slagstad 2015; Stephens and Wahlgren 2020b; Ulmius et al. 2015).

Post-Hallandian bimodal plutonism took place between 1225 and 1180 Ma, including dolerites (Protogine zone dolerites) and syenitic to granitic plutons (e.g. the Vaggeryd syenite; Fig. 6) (Larsson and Söderlund 2005; Petersson et al. 2015a; Söderlund and Ask 2006; Söderlund et al. 2005). These rocks are characterized by a suprachondritic (radiogenic) ε_{Hf} isotopic signature ($+1.2 < \varepsilon_{Hf} < +6.6$) implying an influx of depleted mantle derived magmas along the

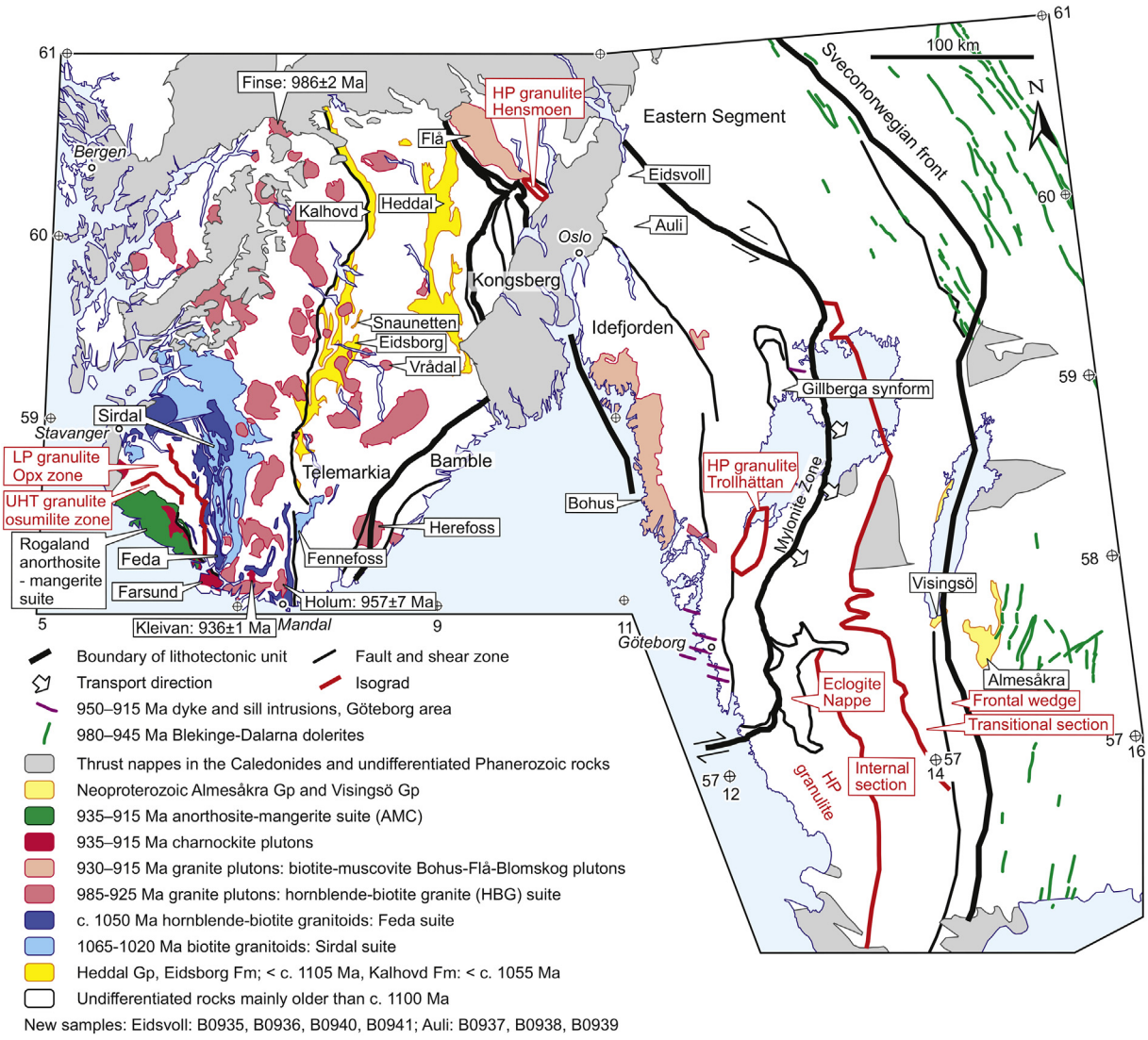

Fig. 5. Sketch map of the Sveconorwegian orogen, with emphasis on Sveconorwegian events younger than c. 1100 Ma. Localities of samples in Auli and Eidsvoll analysed in this study are shown. Age bins in the legend are rounded to 5 Ma intervals.

Sveconorwegian front (Fig. 8) (Petersson et al. 2015a; Söderlund et al. 2005).

3.2.3. Sveconorwegian orogeny

The Sveconorwegian metamorphic grade in the Eastern Segment increases towards the WSW (Fig. 5) (Johansson et al. 1991; Möller and Andersson 2018; Möller et al. 2015; Piñán-Llamas et al. 2015). Four zones of distinct metamorphic and structural reworking can be defined from east to west: (i) a frontal wedge, (ii) a transitional section, (iii) an internal section and (iv) an eclogite-bearing ductile nappe (Möller and Andersson 2018; Möller et al. 2015).

The frontal wedge (i) is a zone of non-penetrative Sveconorwegian deformation forming a steep or fan-shaped structure in cross section that narrows and steepens towards the south (Möller and Andersson 2018; Stephens and Wahlgren 2020a; Wahlgren et al. 1994). The zone comprises a network of thin (<100 m), N–S trending, steeply dipping, greenschist- to amphibolite-facies ductile shear zones with mainly western-block-up kinematics (Andréasson and Dallmeyer 1995; Brander et al. 2012; Gorbatschev and Bogdanova 2006; Söderlund et al. 2004; Wahlgren et al. 1994). The frontal wedge is bound in the east by the Sveconorwegian front, which in the north is a system of discontinuous west dipping shear zones with a reverse, top-to-east sense of shear (Wahlgren et al. 1994). In the northernmost part of the Eastern Segment in Norway, the frontal wedge is poorly documented.

The transitional section (ii) exhibits a near-penetrative amphibolite-facies overprint, with little evidence of partial melting (Beckman et al. 2017; Möller and Andersson 2018; Söderlund et al. 1999). The internal section (iii) is characterized by upper-amphibolite-facies conditions increasing westwards to high-pressure granulite-facies conditions (1.1 GPa - 850 °C; Fig. 5). This metamorphic evolution caused widespread migmatitization and transposition leading to mafic and felsic gneissic layering (banding), dynamic recrystallization of original magmatic textures, as well as reworking of earlier Hallandian structures, where present (Andersson et al. 1999; Connelly et al. 1996; Hansen et al. 2015; Möller et al. 2015; Möller et al. 2007; Piñán-Llamas et al. 2015). The regional aeromagnetic map (Geological Survey of Sweden) unveils prominent, regional scale fold interference patterns, with E-W trending and gently-plunging fold axes and trains of N–S trending folds (Möller et al. 2007; Stephens and Wahlgren 2020a; Viola et al. 2011). Several generations of folds can be recognised (F1 to F4), including km-scale asymmetric to recumbent folds and late upright folds (Möller and Andersson 2018; Möller et al. 2015; Piñán-Llamas et al. 2015; Tual et al. 2015). These different generations record continued deformation under high-grade metamorphic conditions.

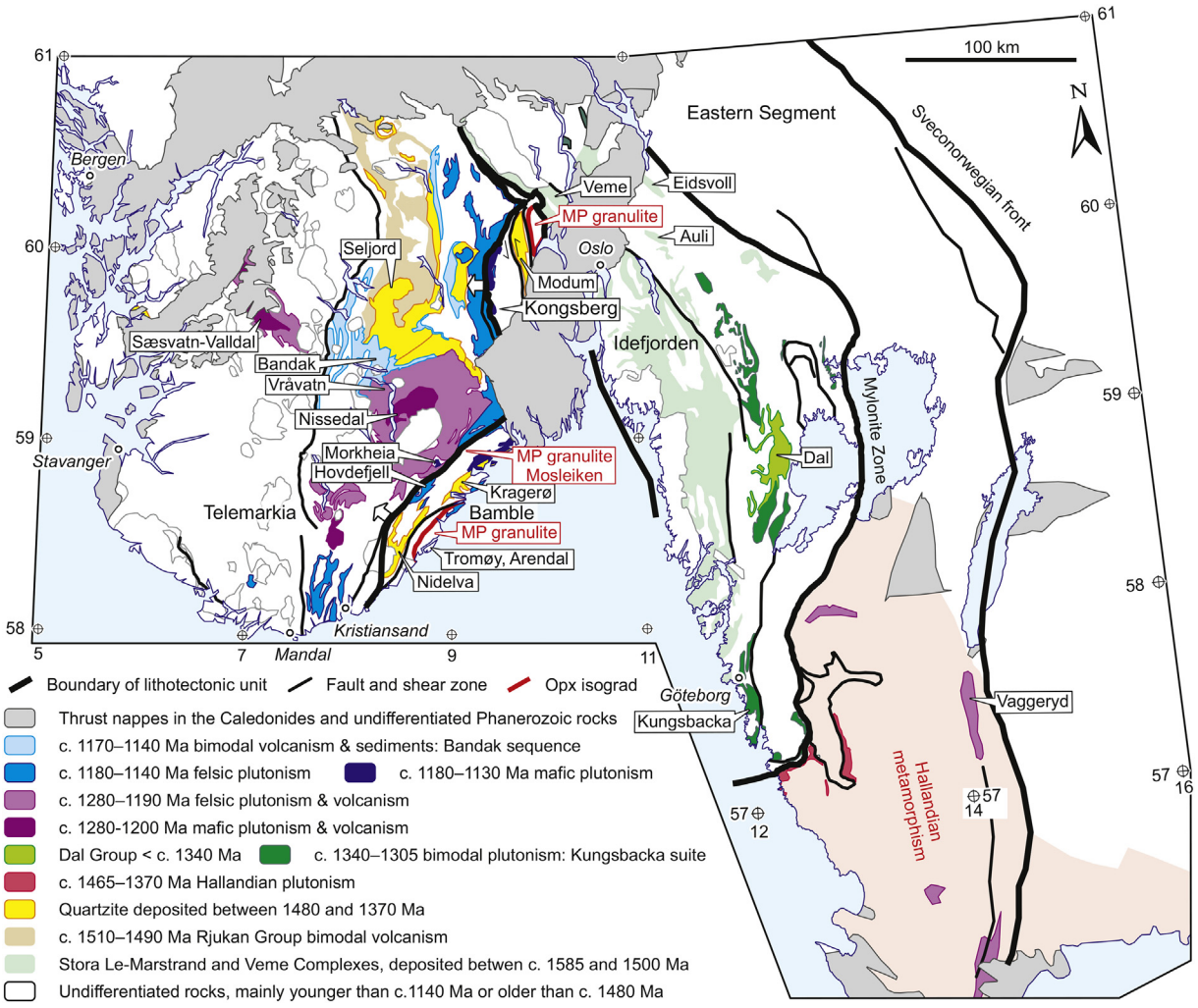

Fig. 6. Sketch map of the Sveconorwegian orogen, with emphasis on pre- and early- Sveconorwegian events and rocks.

The eclogite-bearing ductile nappe (iv) is hosted in the innermost section of the Eastern Segment as an E-vergent ductile nappe, folded into a c. 50 x 75 km large recumbent fold (Fig. 5) (Möller et al. 2015; Tual et al. 2015). It is well defined on the regional aeromagnetic map and bordered (on the southern and eastern flanks) by a sheet of c. 1380 Ma granite (Fig. 6). The ductile nappe hosts retro-eclogite bodies up to 2 km in length (Möller 1998, 1999; Möller and Andersson 2018; Möller et al. 2015; Tual et al. 2015). The retro-eclogite bodies are layered mafic rocks, including two characteristic varieties, a Mg-Al-rich kyanite-bearing variety and a Fe-Ti-rich variety. Retro-eclogites preserve prograde growth zoning of garnet and show widespread retrogression of omphacite and kyanite into granulite-facies symplectites (clinopyroxene + plagioclase, orthopyroxene + plagioclase, and anorthite + sapphirine + corundum) (Fig. 9a). They constrain a narrow (hairpin) clockwise pressure-temperature path at high temperature. Eclogite-facies peak conditions of 1.65–1.9 GPa and 850–900 °C were followed by near-isothermal decompression (Tual et al. 2017). Eclogite boudins are hosted in strongly deformed, partly migmatitic, gneisses characterized by a pervasive foliation, E–W stretching lineation, and S- to E-vergent folds (Möller et al. 2015; Tual et al. 2015). Two post-eclogite-facies deformation phases (D1-D2) are described as successively documenting an early stage of exhumation and east-directed transport of the ductile nappe, lubricated by partial melts.

A zircon U–Pb age from an eclogite sample defines a maximum age for eclogite-facies metamorphism at 988 ± 6 Ma (Möller et al. 2015). Zircon in felsic and mafic gneiss, migmatite and syn-kinematic granite in the entire Eastern Segment, including the eclogite-bearing nappe, yields a consistent age interval between 978 ± 7 and 961 ± 6 Ma for amphibolite- to granulite-facies metamorphism, deformation and partial melting (Andersson et al. 2002a; Beckman et al. 2017; Hansen et al. 2015; Möller et al. 2015; Möller et al. 2007; Piñán-Llamas et al. 2015; Söderlund et al. 2002). Cross-cutting pegmatite dykes intruded between 961 ± 13 and 934 ± 6 Ma (Andersson et al. 1999; Möller et al. 2007; Möller and Söderlund 1997; Söderlund et al. 2008b; Söderlund et al. 2002). Titanite U–Pb ages range from c. 976 ± 4 to 923 ± 3 Ma, with the oldest age recorded in the northern part of the transitional section and the youngest ages in the internal section (Connelly et al. 1996; Johansson et al. 2001; Söderlund et al. 1999; Wang et al. 1998). Hornblende and biotite $^{40}Ar/^{39}Ar$ plateau ages in the internal section are interpreted to date regional cooling between c. 530 and 330 °C between c. 901 ± 2 and 893 ± 3 Ma (Ulmius et al. 2018). Biotite and muscovite $^{40}Ar/^{39}Ar$ plateau ages collected in the frontal wedge range from 930 ± 6 to 882 ± 2 Ma (Andréasson and Dallmeyer 1995; Page et al. 1996a; Ulmius et al. 2018). The youngest ages are recorded in the southernmost exposed section of the orogen. These ages either record discrete events of (re)crystallization or cooling

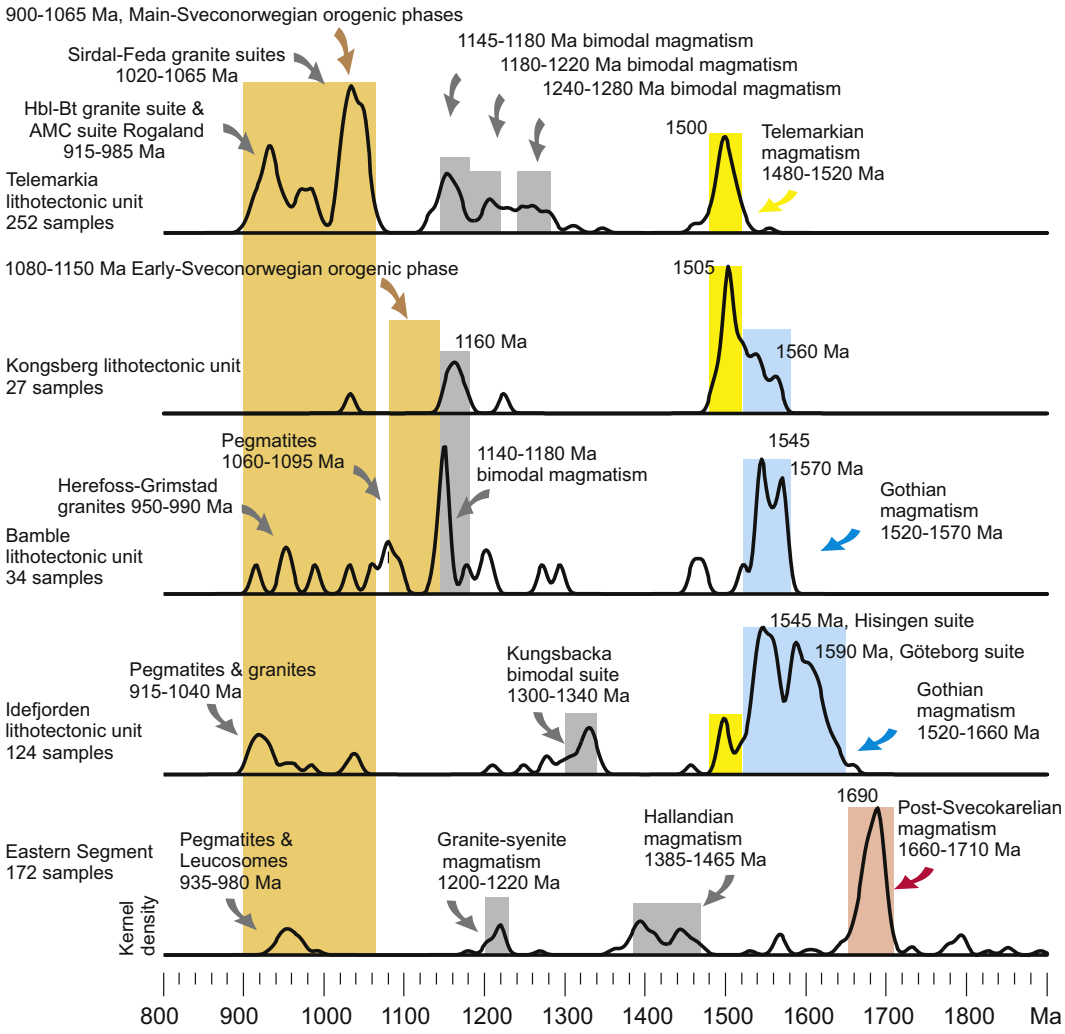

Fig. 7. Kernel density estimators summarizing the geochronology of magmatic rocks in the five lithotectonic units of the Sveconorwegian orogen based on a compilation of published data. The plots are generated with "DensityPlotter" (Vermeesch 2012) (each published age is entered as one value, with a bandwidth of 6 Ma; the height of the five curves is identical and normalized to that of the largest peak). The compilation is provided in the supplementary material, with referencing.

after deformation by shear zones at the front of the orogen (Andréasson and Dallmeyer 1995; Page et al. 1996a; Ulmius et al. 2018).

3.3. Idefjorden lithotectonic unit

The Idefjorden lithotectonic unit is a c. 140 km wide unit exposed west of the Eastern Segment on either side of the Permian Oslo Rift (Fig. 2, Fig. 5) (Åhäll and Connelly 2008; Åhäll and Gower 1997; Bergström et al. 2020; Bingen et al. 2001; Park et al. 1991; Viola et al. 2011). It is bounded in the east by the 450 km long, west dipping, Mylonite Zone.

3.3.1. Gothian and pre-Sveconorwegian evolution

The Idefjorden lithotectonic unit is made up of plutonic and volcanic rocks formed during the Gothian accretionary orogeny mainly between 1660 and 1520 Ma and associated with metasedimentary rocks (Fig. 7) (Åhäll and Connelly 2008; Åhäll and Larson 2000; Ahlin et al. 2006; Andersen et al. 2004a; Bergström et al. 2020; Bingen et al. 2005; Brewer et al. 1998; Graversen and Pedersen 1999). From east to west, three complexes (called formations or belts in the literature) are described as younging towards the west (Åhäll and Connelly 2008; Brewer et al. 1998): (i) the 1660–1640 Ma metavolcanic Horred Complex, (ii) the 1630–1590 Ma metavolcanic and metasedimentary Åmål Complex associated with the Göteborg granite suite, and (iii) the 1590–1520 Ma metasedimentary and metavolcanic Stora Le-Marstrand Complex, associated with the 1580–1520 Ma plutonic Hisingen Suite. The Stora Le-Marstrand Complex, exposed east of the Oslo Rift, correlates with the Veme Complex west of the Oslo Rift (Fig. 6) (Bingen et al. 2001). The Stora Le-Marstrand and Veme complexes comprise several metasedimentary successions (Åhäll and Connelly 2008), consisting of thick packages of turbiditic psammite and greywacke metamorphosed under amphibolite-facies conditions (Bingen et al. 2001). Sedimentation started before c. 1585 Ma (metagreywacke xenoliths in a 1584 ± 7 Ma granite pluton) and continued to after c. 1500 Ma (detrital zircon geochronology in 12 samples) (Åhäll and Connelly 2008; Åhäll et al. 1998; Andersen et al. 2004a; Bingen et al. 2001; Bingen and Viola 2018). The paragneisses analysed in this study just east of the Oslo Rift (Eidsvoll and Auli; Figs. 5, 6, 10) are attributed to the Stora Le-Marstrand Complex.

The c. 1660–1520 Ma (Gothian) magmatic suites (Fig. 7) are characterized by low- to medium-K calc-alkaline geochemical compositions, with supra-chondritic Hf and Nd isotopic signature (average $\varepsilon_{Hf} = +4.8$ in the Idefjorden lithotectonic unit at 1570 Ma; Fig. 8), reflecting continental and oceanic volcanic arc magmatism (Andersen et al. 2004a; Andersen et al. 2002b; Bergström et al. 2020; Brewer et al. 1998; Petersson et al. 2015b). Metabasalts interlayered in the Stora

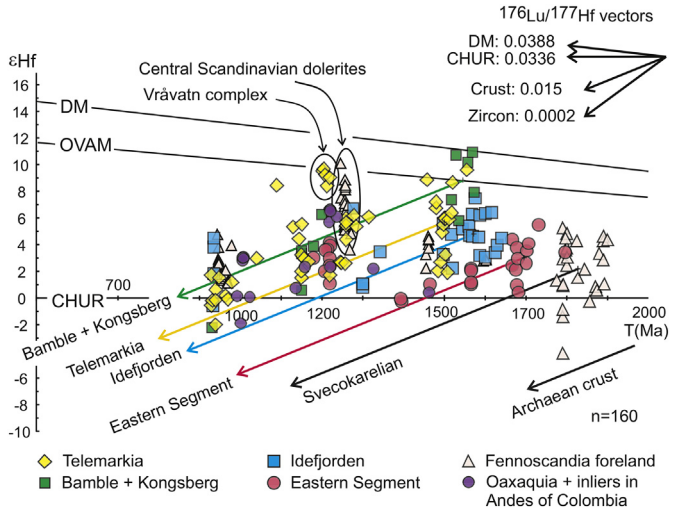

Fig. 8. Hafnium isotopic composition of magmatic rocks in the Sveconorwegian orogen and Fennoscandian foreland, expressed as ε_{Hf} (initial value) as a function of intrusion age. Interpretations of the distribution of data are discussed in the text. The five lithotectonic units are shown with distinct colours and summarized by an evolution vector. The Oaxaquia lithotectonic unit (Mexico) and the inliers in the Andes of Colombia are shown for comparison. Each symbol represents the average value for one sample, of the isotopic composition of several analyses of zircon or baddeleyite or of one whole-rock analysis (only a few samples), at the recommended time of intrusion (zircon or baddeleyite U–Pb age). Total of 220 samples. Sources of data: Sveconorwegian orogen and foreland: Andersen et al. (2009, 2002b, 2007), Lamminen et al. (2011), Pedersen et al. (2009), Petersson et al. (2015a, 2015b), Roberts et al. (2013); Söderlund et al. (2005); Oaxaquia and inliers in the Andes of Colombia: Ibanez-Mejia et al. (2015), Weber et al. (2010); DM: depleted mantle (Griffin et al. 2000); OVAM: oceanic volcanic arc mantle (Dhuime et al. 2011); CHUR: chondritic reservoir (Bouvier et al. 2008). The top right inset shows the $^{176}Lu/^{177}Hf$ ratio and evolution vectors of isotopic reservoirs and typical zircon.

Le-Marstrand rocks are tholeiitic and interpreted as oceanic back-arc magmatism (Brewer et al. 1998).

The c. 1660–1520 Ma rocks were assembled during the Gothian accretionary orogenic event (Åhäll and Connelly 2008; Andersen et al. 2004a; Petersson et al. 2015b; Roberts and Slagstad 2015). Convincing evidence for Gothian regional deformation and metamorphism includes crosscutting relationships (folded xenoliths in a 1584 ± 7 Ma pluton) and U–Pb geochronological data in zircon and monazite ranging from 1546 ± 5 to 1539 ± 8 Ma from a few localities in the Veme and Stora Le-Marstrand complexes (Åhäll and Connelly 1998, 2008; Bingen et al. 2008b; Bingen and Viola 2018; Connelly and Åhäll 1996).

The 1660–1520 Ma rocks are intruded by the 1457 ± 6 Ma, N–S trending Orust tholeiitic dolerite dykes (Åhäll and Connelly 1998), and the 1340–1305 Ma bimodal Kungsbacka suite (Fig. 6) (Austin Hegardt et al. 2007). The Dal Group (or Dalsland Group) is a c. 2 km thick succession of low-grade clastic sedimentary rocks and tholeiitic basalt, exposed in a syncline structure, overlying (and therefore younger than) the Kungsbacka suite (Fig. 6) (Brewer et al. 2002). The Dal Group is poorly characterized. However, it may provide critical evidence for the tectonic evolution of the Idefjorden lithotectonic unit before the Sveconorwegian orogeny (Brewer et al. 2002) and therefore would warrant new investigations.

3.3.2. Sveconorwegian orogeny

In the Idefjorden lithotectonic unit, the Sveconorwegian deformation is associated with a N–S to NW–SE structural grain and has variable strain intensity. Several shear zones, including the prominent Ørje and Göta Älv shear zones (Fig. 2), are parallel to this structural grain (Bergström et al. 2020; Park et al. 1991; Viola et al. 2011; Wahlgren et al., 2016). Metamorphism ranges from greenschist- to granulite-facies. The low-grade rocks are exposed in syncline structures (Fig. 4). For example, between the Göta Älv shear zone and the Mylonite Zone, the Gillberga syncline hosts the Glaskogen low-grade complex, bounded by low-angle shear zones (Lindh et al. 1998), and the Åmal volcanic rocks (1614 ± 7 Ma), known for good preservation of primary volcanic structures (Lundqvist and Skiöld 1993). In the amphibolite-facies gneiss complexes east and west of the Göta-Älv shear zone, garnet amphibolites provide pressure-temperatures estimates of 0.9 to 1.2 GPa – 730 to 790 °C (3 samples; Austin Hegardt 2010). High-pressure garnet–clinopyroxene-bearing granulite-facies assemblages are reported from metadolerite dykes hosted in amphibolite-facies gneisses from several localities east of the Göta-Älv shear zone (Trollhättan, Fig. 5) (Söderlund et al. 2008a). Geothermobarometry coupled with zircon U–Pb data and mineral isochron data from two dykes indicate conditions of c. 1.5 GPa – 740 °C at 1046 ± 6 Ma and c. 1.0 GPa – 700 °C at 1026 ± 5 Ma (Söderlund et al. 2008a). In the Veme Complex, west of the Oslo rift in Norway, a kyanite-garnet-rutile paragneiss hosting clinopyroxene-garnet-plagioclase-rutile mafic boudins also records high-pressure granulite-facies conditions, with pressure-temperature estimates of 1.2 GPa – 780 °C (Hensmoen, Fig. 5) (Bingen et al.

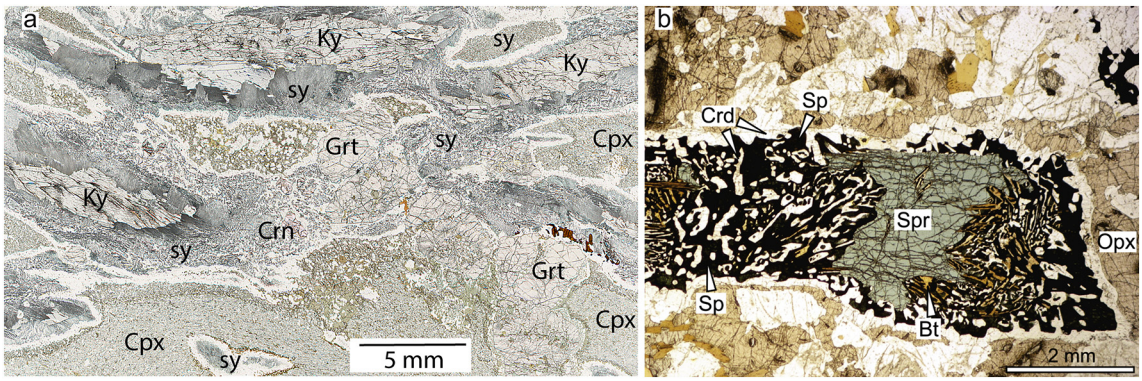

Fig. 9. Microphotographs of thin sections showing the contrast between high-pressure (eclogite facies) and ultrahigh temperature (granulite facies) metamorphism, east and west of the Sveconorwegian orogen, respectively, at c. 1000 Ma. (a) Kyanite-bearing (retro)eclogite from the eclogite-bearing nappe in the Eastern Segment (Möller and Andersson 2018). The thin section shows a partly preserved peak eclogite-facies assemblage of garnet (Grt) + omphacite (Cpx) + kyanite (Ky) + amphibole + rutile (1.8 GPa - 870 °C - 988 ± 6 Ma) breaking down into a symplectitic (sy) assemblage during isothermal decompression. Symplectites (sy) include a sapphirine + corundum + anorthite reaction rim around kyanite, an orthopyroxene + plagioclase + amphibole reaction rim around clinopyroxene, and plagioclase expulsion symplectite in former omphacite (Cpx). Garnet preserves a prograde (pre-eclogite facies) zoning, and the rock shows evidence for a hairpin P-T path (Tual et al. 2017). (b) Sapphirine + orthopyroxene granulite from the Ivesdal locality, in the ultra-high temperature (UHT) zone of Rogaland, in the Telemarkia lithotectonic unit (Laurent et al. 2018b). The thin section shows the peak assemblage of sapphirine (Spr) mantled by orthopyroxene (Opx) (0.6 GPa - 920 °C - 1029 ± 9 to 1006 ± 8 Ma) breaking down into an assemblage of cordierite (Crd) + hercynite (Sp) with additional biotite (Bt) (4.5 GPa – 900 °C) constraining a clockwise P-T path.

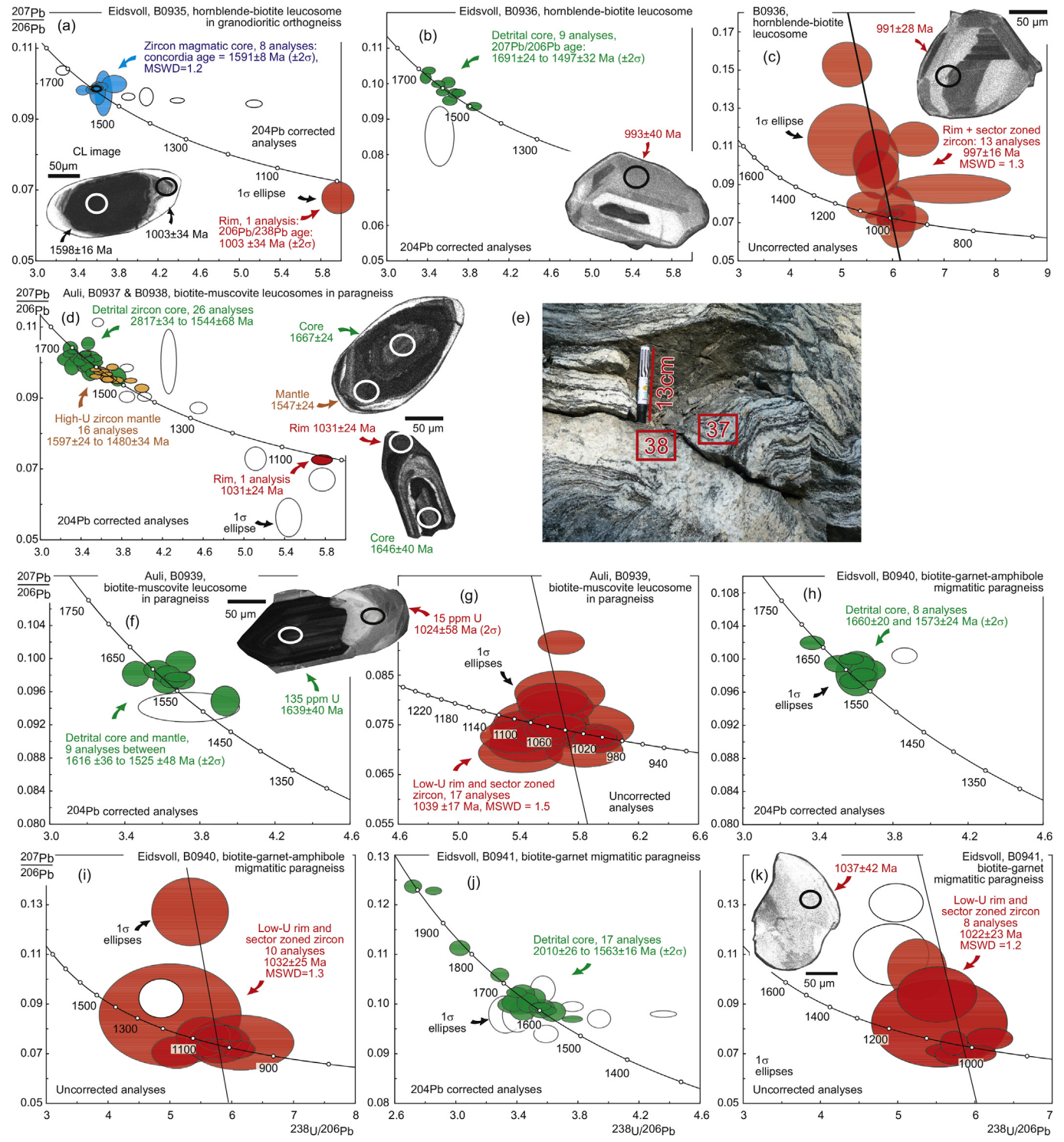

Fig. 10. New geochronological data of migmatitic gneisses in the Eidsvoll-Auli area, Idefjorden lithotectonic unit (Fig. 5). (a–k) Tera-Wasserburg concordia diagrams with zircon SIMS U–Pb analyses and a selection of CL images of zircon with position of analyses. Blue ellipses for magmatic zircon cores, green ellipses for detrital zircon cores, and red ellipses for low-U sector zoned zircon and zircon rims attributed to migmatitization. One sigma error ellipses. (e) Photo of outcrop where two samples represent two generations of leucosomes, with B0938 crosscutting B0937. Interpretation: migmatites from the five studied localities are characterized by abundant, interconnected leucosomes (stromatic texture) parallel to the gneissic foliation. Zircon contains an inherited core (magmatic or detrital), a CL-dark mantle and a CL-bright rim. Analyses of the mantle overlap with those of the core and define a significant spread in each sample. The spread of apparent ages can be interpreted to represent partial recrystallization of the core during partial melting. Newly formed CL-bright rims or large crystals with oscillatory to weakly sector zoning reflect crystallization of zircon related to migmatitization (Harley et al. 2007; Kelsey et al. 2008; Rubatto et al. 2009) between 1039 ± 17 and 997 ± 16 Ma (a, c, g, i, k). In this c. 40 Myr time interval, the biotite-muscovite and biotite-garnet leucosomes range from 1039 ± 17 to 1022 ± 23 Ma (d, g, i, k), while the hornblende-biotite-bearing leucosomes are marginally to significantly younger with ages of 1003 ± 34 and 997 ± 16 Ma (a, c). This difference suggests that muscovite and biotite dehydration melting took place before amphibole dehydration melting, in what can be interpreted as reflecting increasing temperature or isothermal decompression.

2008b). Monazite in the kyanite-rutile-gneiss records peak metamorphism at 1052 ± 4 Ma (Bingen et al. 2008b).

East of the Oslo rift in Norway, amphibolite-facies metamorphism is associated with a foliation dipping unimodally to the NE and with folds verging to the W to SW (Viola et al. 2011). The timing of this metamorphism is provided by the new U–Pb data from zircon rims in migmatitic samples (Eidsvoll–Auli area, Figs. 5, 10, Table 2). The dates range from 1039 ± 17 to 997 ± 16 Ma, in seven samples affected by both muscovite- biotite- and amphibole-dehydration melting. The dates are interpreted to record crystallization of the leucosomes. This interval overlaps with published zircon and titanite U–Pb data and a Sm-Nd mineral isochron interpreted to record high-grade metamorphism between 1043 ± 11 Ma and 1024 ± 9 (7 samples; Åhäll et al. 1998; Austin Hegardt 2010; Austin Hegardt et al. 2007; Bingen et al. 2008b), and also with intrusion of rare-mineral pegmatites between 1041 ± 2 and 984 ± 6 Ma (Romer and Smeds 1996).

Several mafic to felsic magmatic intrusions, with a consistent WNW–ESE trend and dated between 951 ± 7 and 915 ± 1 Ma, crosscut the regional amphibolite-facies ductile fabric in the coastal area of Sweden (Årebäck et al. 2008; Hellström et al. 2004; Scherstén et al. 2000; Wahlgren et al., 2016). These include a lamprophyre dyke (915 ± 1 Ma) (Wahlgren et al., 2016) and the small Hakefjorden norite-anorthosite complex (916 ± 11 Ma), carrying evidence for extensive fractional crystallization (Årebäck and Stigh 2000). The Flå and Bohus biotite-muscovite granite plutons intruded between 932 ± 8 and 922 ± 3 Ma, as large tabular bodies, in pressure conditions of c. 0.4 GPa (Fig. 5) (Eliasson et al. 2003; Eliasson and Schöberg 1991; Lamminen et al. 2011). A final batch of rare-mineral pegmatite formed between 909 ± 1 and 906 ± 6 Ma (Müller et al. 2017).

3.3.3. The Mylonite Zone

The Mylonite Zone is a generally west dipping shear zone juxtaposing the Eastern Segment and Idefjorden lithotectonic unit. It is several km thick, continuous for some 450 km and characterized by a widespread greenschist- to upper amphibolite-facies mylonitic fabric (Figs. 2, 5) (Andersson et al. 2002a; Bergström et al. 2020; Möller et al. 2015; Park et al. 1991; Stephens et al. 1996; Viola and Henderson 2010; Viola et al. 2011). It possibly roots in the mantle (EUGENO-S-working-group 1988).

The Mylonite Zone is interpreted as a Sveconorwegian mid-crustal thrust zone placing the Idefjorden lithotectonic unit on top of the Eastern Segment, with an overall southeastward transport direction oblique to the orogen (Stephens et al. 1996; Viola and Henderson 2010; Viola et al. 2011). Shear zones inside the Idefjorden lithotectonic unit, including the Ørje and Göta Älv shear zones (Fig. 2) are similarly interpreted as transpressional thrust zones (Park et al. 1991; Viola et al. 2011; Wahlgren et al., 2016).

In the north (in Norway), the Mylonite Zone trends NW–SE and has a steep attitude with sinistral strike-slip kinematics. This segment has been interpreted as the sinistral lateral ramp to the thrust frontal ramp farther to the southeast. The frontal ramp dips gently to moderately to the west and bears a NW plunging stretching lineation associated with dominant top-to-southeast reverse kinematics. In the southernmost part, the shear zone turns quite abruptly E–W, dipping gently to the north, and accommodating a dominant component of dextral strike-slip shearing. This part is interpreted as a dextral lateral ramp of the thrust zone (Viola and Henderson 2010; Viola et al. 2011). The importance of the southernmost dextral lateral ramp is downplayed by Bergström et al. (2020), who interpret the Mylonite Zone, as a whole, as a sinistral transpressional thrust zone. Zircon U–Pb data in the Mylonite Zone and close hanging wall and footwall record amphibolite-facies migmatitization and associated ductile deformation between 980 ± 13 and 969 ± 13 Ma (Andersson et al. 2002a).

The Mylonite Zone was reactivated in extension with top-to-the-west kinematics along a network of localized shear zones, contributing to exhumation of the Eastern Segment in the footwall (Viola and Henderson 2010; Viola et al. 2011). Muscovite and biotite $^{40}Ar/^{39}Ar$ data suggest that this deformation took place between 923 ± 4 and 861 ± 5 Ma (Viola et al. 2011).

3.4. Kongsberg and Bamble lithotectonic units

The Bamble and Kongsberg lithotectonic units are two narrow c. 25 km wide units situated in the center of the exposed Sveconorwegian orogen (Fig. 2). Kongsberg trends N–S while Bamble trends NE–SW. These two lithotectonic units share a number of features, including evidence for early-Sveconorwegian metamorphism (1150-1120 Ma) (Bingen et al. 2008b; Bingen and Viola 2018; Engvik et al. 2016; Knudsen et al. 1997; Nijland et al. 2014; Starmer 1985; Viola et al. 2016).

Table 2
Summary of sampling and zircon U-Pb data for migmatitic gneisses, Eidsvoll-Auli area, Idefjorden lithotectonic unit.

Sample	Sample definition	Zircon zone	n	Data reduction	Correction	Age [Ma ± 2s]	Figure	X	Y	Longitude	Latitude
B0935	Hornblende-biotite leucosome in granodioritic orthogneiss, Eidsvoll	Magmatic core	9	Concordia age	204Pb	1591 ± 8	Fig. 10a	618558	6688342	11.14619	60.31428
		Rim	1	206Pb/238U age	207Pb	1003 ± 34	Fig. 10a				
B0936	Hornblende-biotite leucosome in paragneiss, Eidsvoll	Clastic core	9	207Pb/206Pb age	204Pb	1691 ± 24 to 1497 ± 32	Fig. 10b	621108	6690771	11.19377	60.33532
		Rim	13	Intercept age	207Pb	997 ± 16	Fig. 10c				
B0937+B0938	Biotite-muscovite leucosomes in paragneiss, Auli	Clastic core	28	207Pb/206Pb age	204Pb	2817 ± 34 to 1544 ± 68	Fig. 10d	630848	6657581	11.34866	60.03453
		Rim	1	206Pb/238U age	207Pb	1031 ± 24	Fig. 10d				
B0939	Biotite-muscovite leucosome in paragneiss, Auli	Clastic core	8	207Pb/206Pb age	204Pb	1616 ± 32 to 1525 ± 48	Fig. 10f	629773	6657536	11.32936	60.03447
		Rim	17	Intercept age	207Pb	1039 ± 17	Fig. 10g				
B0940	Biotite-garnet-amphibole migmatitic paragneiss, Eidsvoll	Clastic core	8	207Pb/206Pb age	204Pb	1660 ± 20 to 1573 ± 24	Fig. 10h	624788	6689196	11.25939	60.32007
		Rim	10	Intercept age	207Pb	1032 ± 25	Fig. 10i				
B0941	Biotite-garnet migmatitic paragneiss, Eidsvoll	Clastic core	17	207Pb/206Pb age	204Pb	2010 ± 26 to 1563 ± 16	Fig. 10j	624754	6689204	11.25878	60.32016
		Rim	8	Intercept age	207Pb	1022 ± 23	Fig. 10k				

n: number of analyses; Correction: common Pb correction, "204Pb" means "common Pb correction on the basis of 204Pb signal, if 204Pb signal is above background". "207Pb" means "projection of the uncorrected analysis on the concordia curve from a common Pb anchor point"; X, Y: UTM coordinates, zone 32.

3.4.1. Gothian–Telemarkian evolution

Two main lithological complexes are present in the Bamble and Kongsberg lithotectonic units, (i) an orthogneiss complex, referred to as Kongsberg Complex in Kongsberg and Bamble Complex in Bamble, and (ii) a quartzite-dominated metasedimentary complex, called Modum Complex in Kongsberg and Nidelva and Kragerø Complexes in Bamble (Fig. 6). (i) The orthogneiss complex consists of penetratively deformed orthogneisses with composition ranging from dioritic to tonalitic, to granitic, and more competent gabbro plutons (Holleia and Blengsvatn; Bingen and Viola 2018; Nijland et al. 2000). The orthogneisses are interlayered with comparatively heterogeneous layered gneisses (referred to as banded gneiss in the field), commonly migmatitic, and generally fine-grained. The layered gneisses derive probably from both volcanic and sedimentary protoliths. Thin sulfide-rich or graphite-rich schistose layers are common (falhbands) (Broekmans et al. 1994; Gammon 1966). The protoliths of the orthogneisses range in age from 1575 ± 44 to 1460 ± 21 Ma, with two frequency maxima around 1545 and 1505 Ma (Fig. 7) (Andersen et al. 2004a; Bingen and Viola 2018; Engvik et al. 2016). The orthogneisses have tholeiitic to low-K calc-alkaline geochemical signature, typical of volcanic arc magmatism (Andersen et al. 2004a). Their Hf isotopic signature is very radiogenic, with an average $\varepsilon_{Hf} = +8.8$ ($+7 < \varepsilon_{Hf} < +11$), approaching the depleted mantle reservoir at 1550 Ma (Fig. 8) (Andersen et al. 2002b). (ii) The metasedimentary complexes (Fig. 6) consist of coarse quartzite, interlayered with mica schist, sillimanite gneiss and sulfide-rich schist (Morton 1971; Nijland et al. 2014; Nijland et al. 1993). They host metasomatic rocks such as orthoamphibole-cordierite gneiss, talc schist, albitite, scapolitite and dolomite, generally located at the interface with gabbro bodies (Dahlgren et al. 1993; Engvik et al. 2014; Munz 1990; Munz et al. 1994). Deposition of the sedimentary protoliths took place after 1467 ± 33 Ma (detrital zircon U–Pb data in quartzite samples), implying that they represent part of a cover to the orthogneiss basement (Åhäll et al. 1998; Bingen et al. 2001).

3.4.2. Pre- to early-Sveconorwegian plutonism

The orthogneiss and quartzite-rich metasedimentary complexes are intruded by variably sized, gabbroic plutons. These plutons are commonly zoned, with (sub)ophitic picritic gabbro in the core and garnet amphibolite along the margin (Munz and Morvik 1991). Two such gabbro plutons have been dated by the Sm-Nd method at 1224 ± 15 and 1207 ± 14 Ma (Morud and Vestre Dale gabbro, not represented in Fig. 7; deHaas et al. 2002b; Munz and Morvik 1991), and two have been dated with the U–Pb method at 1164 ± 12 and 1149 ± 7 Ma (Vinoren and Ringsjø; Bingen and Viola 2018; Engvik et al. 2011). Felsic intrusive rocks are quite common. They include thin gneissic units ranging in age from 1178 ± 9 to 1149 ± 8 Ma (Andersen et al. 2004b; Bingen and Viola 2018; Engvik et al. 2016), and also, in Bamble, larger plutons ranging in age from 1152 ± 11 to 1140 ± 13 Ma (Gjeving, Ubergsmoen, Hovdefjell-Vegårshei plutons, Fig. 6) (Bingen and Viola 2018). These metaplutons are characterized by a weakly foliated magmatic charnockite facies in the centre and a garnet-bearing augen gneiss facies at the margin (Touret 1971a, 1971b), and therefore place a maximum age bracket for the high-grade deformation and metamorphism in Bamble.

3.4.3. Sveconorwegian orogeny

The Sveconorwegian overprint in the Bamble and Kongsberg lithotectonic units is typified by a steep to subvertical foliation, isoclinal and highly transposed folds and a penetrative tectonic layering (Bingen and Viola 2018; Slagstad et al. 2020; Starmer 1985, 1991). These features are interpreted as evidence for roughly orthogonal, syn-metamorphic shortening, oriented E–W for Kongsberg and NW–SE for Bamble (Bingen and Viola 2018). A steep stretching lineation on the steep foliation planes suggests a component of near-vertical stretching. Inside the Kongsberg lithotectonic unit, the N–S trending Hokksund-Solumsmo shear zone (Starmer 1985) is characterized by a component of sinistral strike-slip shearing that overprinted and thus postdates the orthogonal shortening (Scheiber et al. 2015).

Metamorphic grade increases across strike, northeastwards in Kongsberg and southeastwards in Bamble. In Kongsberg, it increases from epidote-amphibolite facies to upper amphibolite-facies conditions, with local occurrences of granulite-facies rocks towards the northeast (Fig. 6). In Bamble, the grade increases from amphibolite-facies to granulite-facies conditions towards the southeast, i.e. towards the coast (Tromøy and Hisøy islands; Fig. 6) (Clough and Field 1980; Harlov 2000; Knudsen 1996; Nijland et al. 2014; Nijland and Maijer 1993; Touret 1971a). However, patches of granulite facies rocks are scattered throughout the amphibolite-facies domain of Bamble (Mosleiken granulite; Fig. 6), underscoring the importance of fluid activity on mineral parageneses (Engvik et al. 2016; Nijland et al. 1998). The granulite-facies rocks record peak pressure-temperature values of 1.15 GPa and 850 °C, followed by hydration and decompression to 0.8 GPa – 740 °C (Engvik et al. 2016).

Zircon and monazite U–Pb data constrain the peak of amphibolite- and granulite-facies metamorphism between 1147 ±12 and 1122 ± 8 Ma in both the Bamble and Kongsberg lithotectonic units (Bingen et al. 2008b; Bingen and Viola 2018; Cosca et al. 1998; Engvik et al. 2016; Knudsen et al. 1997). In coastal Bamble, the granulite-facies Tromøy complex (Fig. 6) consists of low-K calc-alkaline enderbitic gneisses depleted in large ion-lithophile elements (LILE) (Cooper and Field 1977; Field et al. 1980; Knudsen and Andersen 1999). Zircon U–Pb data demonstrate that the protoliths formed between 1575 ± 44 and 1544 ± 14 Ma while the granulite facies overprint took place between 1147 ± 12 and 1132 ± 6 Ma (Bingen and Viola 2018). These data show that the volcanic arc magmatism belongs to the Gothian orogenic cycle, while the granulite-facies metamorphism is early-Sveconorwegian in age (Andersen et al. 2004a; Bingen et al. 2008c; Field et al. 1985).

Titanite U–Pb dates and a trail of monazite dates in gneisses range from 1107 ± 9 to 1091 ± 2 Ma (Bingen et al. 2008b; Cosca et al. 1998; deHaas et al. 2002a) while hornblende $^{40}Ar/^{39}Ar$ plateau ages range from 1099 ± 3 to 1079 ± 5 Ma (Cosca et al. 1998; Cosca and O'Nions 1994). These dates are related to regional cooling and exhumation. Monazite, titanite and rutile in albitite record at least two phases of fluid-rock interaction below 550 °C (metasomatism), between 1104 ± 5 and 1078 ± 3 Ma (Engvik et al. 2017; Engvik et al. 2011; Munz et al. 1994), while gadolinite-columbite data in pegmatite record intrusion of a small batches of fluid-rich melt between 1094 ± 11 and 1082 ± 5 Ma (Müller et al. 2017; Scherer et al. 2001). These data imply regional scale fluid mobility after the peak of metamorphism and deformation.

Rare lamprophyre dykes with near vertical attitude and non-foliated chilled margins crosscut at high angle the regional foliation of the host gneiss. One such dyke yields an intrusion age of 1033 ± 12 Ma and thus provides both a minimum bracket for the steep, high-grade fabric of the host gneiss and the age of a batch of ultrapotassic mafic magmatism (Bingen and Viola 2018). The large non-foliated Herefoss granite pluton formed at 920 +16/-27 Ma (Fig. 5) (Andersen et al. 2002a).

3.4.4. Kongsberg–Idefjorden boundary zone

The Kongsberg–Idefjorden boundary zone is marked by a c. 500 m thick amphibolite-facies shear zone made of banded gneiss of mafic composition, characterized by steeply dipping foliation bearing a moderately to steeply plunging lineation (Bingen and Viola 2018). It follows the lithological contact between metagreywackes of the Veme Complex and orthogneisses of the Kongsberg Complex (Viola et al. 2016).

3.4.5. Kongsberg–Telemarkia boundary zone

The Sokna-Saggrenda Shear Zone (Fig. 2) (Starmer 1985) is a N–S trending, east-dipping, up to 2 km thick multiphase shear zone. It is largely hosted within and along the eastern margin of a > 100 km

long belt of foliated granite, dated between 1170 ± 11 and 1146 ± 5 Ma (Fig. 6) (Scheiber et al. 2015). This granite constitutes the footwall of the shear zone and is part of the Telemarkia lithotectonic unit. Three post-1170 Ma ductile deformation phases have been identified in the shear zone (Scheiber et al. 2015). (i) The earliest structures accommodate top-to-the-west kinematics and thrusting of Kongsberg over Telemarkia. (ii) These are selectively reactivated in a sinistral fashion along mylonitic to ultramylonitic shear zones. The sinistral shear zones possibly record the same deformation as the N–S trending, steeply dipping Hokksund-Solumsmo mylonite zones inside the Kongsberg lithotectonic unit, showing evidence for sinistral transpressive shearing. (iii) Extensional top-to-the-east sense of shear. A brittle zone overprinting this long-lived ductile deformation zone and traditionally referred to as the "Great Friction Breccia" (Starmer 1985) probably represents a normal fault of Permian age (Larsen et al. 2008; Scheiber et al. 2015).

3.4.6. Bamble–Telemarkia boundary zone

The Kristiansand–Porsgrunn Shear Zone (Fig. 2) is a c. 1–2 km thick ductile to brittle shear zone juxtaposing the Bamble and Telemarkia lithotectonic units. It dips moderately to the southeast and is possibly connected with an offset of the Moho under the Skagerrak sea (Andersson et al. 1996). The shear zone is interpreted as a top-to-the-northwest thrust, later reactivated coaxially as an extensional shear zone (Henderson and Ihlen 2004; Mulch et al. 2005; Starmer 1991). Upper greenschist- to amphibolite-facies thrust-related structures are invariably northwest vergent. These structures are associated with tabular pegmatite bodies (Henderson and Ihlen 2004). The shear zone overprints the 1132 ± 3 Ma Morkheia monzonite suite exposed in the Telemarkia footwall (Heaman and Smalley 1994; Milne and Starmer 1982), and the 1140 ± 13 Ma Hovdefjell-Vegårshei metapluton exposed on the Bamble hangingwall (Bingen and Viola 2018; Touret 1987), implying that thrusting is younger than 1132 ± 3 Ma. Extension was accommodated by thin greenschist-facies shear zones with syn-kinematic muscovite porphyroblasts constraining the top-to-the-southeast deformation between 891 ± 3 and 880 ± 3 Ma ($^{40}Ar/^{39}Ar$ data) (Mulch et al. 2005). The contrast in titanite U–Pb ages between the Telemarkia footwall (c. 913 to 901 Ma) and Bamble hanging wall (c. 1107 to 1091 Ma) (Bingen et al. 1998; Cosca et al. 1998; deHaas et al. 2002a; Heaman and Smalley 1994) underscores the importance of normal movement along the shear zone. A narrow, fully brittle, Permian, normal fault zone locally reactivates the Sveconorwegian ductile precursors.

3.5. Telemarkia lithotectonic unit

The western part of the Sveconorwegian orogen can be considered as one single lithotectonic unit, c. 230 x 300 km in size, named Telemarkia (Fig. 2) (Bingen et al. 2005). The Telemarkia lithotectonic unit comprises low-grade supracrustal rocks preserved in several syncline structures, structurally overlying amphibolite- to granulite-facies gneiss complexes, and hosts voluminous plutons (Figs. 4-6). The gneiss complexes comprise orthogneisses with subordinate paragneisses. The largest and most complete tract of supracrustal rocks, called the Telemark supracrustal rocks, is exposed in a 60 km wide area in central Telemark (Figs. 4, 6). Original mapping showed that stratigraphic relationships and deposition structures are well preserved in the Telemark supracrustal rocks, and defined three groups or successions separated by unconformities, which are, from bottom to top, the Rjukan, Seljord and Bandak successions (Figs. 11, 12) (Dons 1960; Dons and Jorde 1978; Sigmond 1978). Other supracrustal successsions are described in several other syncline structures, less than 25 km wide, in the Ullensvang, Sauda, Grjotdokki-Nesflaten, Sæsvatn-Valldal and Nissedal areas (Fig. 4).

3.5.1. Telemarkian evolution

Rapid generation of juvenile continental crust is recorded by voluminous magmatism between 1521 ± 6 and 1476 ± 13 Ma, hosted in both the low-grade successions and in the gneiss complexes (Fig. 7) (Bingen et al. 2008a; Bingen et al. 2005; Laajoki and Corfu 2007; Pedersen et al. 2009; Roberts et al. 2013). This event is called the Telemarkian accretionary orogeny and it is geographically zoned.

In the west, in the Suldal area, gneisses and granitoids are characterized by a calc-alkaline geochemical signature, with s supra-chondritic Hf isotopic signature at 1500 Ma (average $\varepsilon_{Hf} = +5.7$; Fig. 8) (Pedersen et al. 2009; Roberts et al. 2013). These are interpreted to reflect volcanic arc magmatism (the Suldal volcanic arc; Roberts et al. 2013).

In the east, in the Telemark area, magmatism is bimodal and typified by the Rjukan bimodal metavolcanic rocks at the base of the Telemark supracrustal rocks (Vemork basalt vs. Tuddal rhyolite dated between 1512 ± 10 and 1495 ± 2 Ma, Fig. 11) and coeval plutonism (Bingen et al. 2005; Laajoki and Corfu 2007). This magmatism is characterized by a within-plate geochemical signature and moderately supra-chondritic Nd isotopic signatures ($+1.1 < \varepsilon_{Nd(1500\ Ma)} < +4.3$) (Fig. 13). It is interpreted to reflect back-arc rifting (the Rjukan rift basin), continentwards of the active volcanic arc (Brewer and Menuge 1998; Köykkä and Lamminen 2011; Lamminen and Köykkä 2010; Roberts et al. 2013).

The Telemarkian orogenic event cannot be demonstrated to be associated with high-grade metamorphism. The Seljord succession overlying the Rjukan succession is a c. 8 km thick, shallow marine sedimentary succession, dominated by quartzite (Figs. 11, 12) (Köykkä and Lamminen 2011). The Seljord succession was deposited during a transgressive cycle, interpreted as reflecting thermal subsidence after magmatism, between 1410 ± 24 Ma (detrital zircon U–Pb data) and 1347 ± 4 Ma (U–Pb age of intrusive dolerite dyke; Corfu and Laajoki 2008; Köykkä and Lamminen 2011; Lamminen and Köykkä 2010).

3.5.2. Pre- to early-Sveconorwegian evolution

The Telemarkia lithotectonic unit hosts several generations of gneissic plutonic rocks in the 1280–1240, 1220–1180 and 1180–1145 Ma time intervals, with frequency maxima at c. 1280, 1260, 1210, 1170 and 1150 Ma (Figs. 6, 7) (Andersen et al. 2007; Bingen et al. 2003; Corfu and Laajoki 2008; Heaman and Smalley 1994; Pedersen et al. 2009; Scheiber et al. 2015).

In the southeast of the Telemarkia lithotectonic unit, a voluminous c. 60 x 120 km gneiss complex consists of amphibolite-facies, NE–SW trending, moderately to weakly foliated granitic gneiss and granitoids, named in different areas Drivheia gneiss (Heaman and Smalley 1994) and Vråvatn complex (Fig. 6) (Andersen et al. 2007). This complex is dominated by c. 1220–1190 Ma plutonic rocks with a within-plate geochemical signature (Andersen et al. 2007; Bingen and Viola 2018; Heaman and Smalley 1994) and a supra-chondritic (radiogenic) Hf isotopic signature ($+9 < \varepsilon_{Hf} < +10$, in zircon from 4 samples, Fig. 8) approaching the depleted mantle reservoir value at 1210 Ma ($\varepsilon_{Hf} = +12$) (Andersen et al. 2007).

The Sæsvatn–Valldal and Nissedal supracrustal complexes are two low-grade basalt-dominated successions (Figs. 6, 11), exposed in two c. 15 km wide syncline. Basalt is interlayered with felsic volcanic and clastic sedimentary rocks and intruded by fine-grained granite sills and dykes (Dons and Jorde 1978; Sigmond 1975). In the Sæsvatn–Valldal area, the basalts are overlying rhyolites and porphyries dated to between 1275 ± 8 and 1259 ± 2 Ma, themselves unconformably overlying the 1520–1480 Ma gneissic basement (Bingen et al. 2002; Brewer et al. 2004). In the Nissedal area, the basalts overly the 1219 ± 8 to 1202 ± 9 Ma Vråvatn complex and host fine-grained granite sheets, one of which yields an intrusion age of 1196 ± 6 Ma (Bingen and Viola 2018). The Nissedal and Sæsvatn-Valldal complexes are interpreted as near-coeval bimodal (mafic dominated) continental successions with an age close to 1210 Ma, coeval with the Drivheia and Vråvatn gneisses

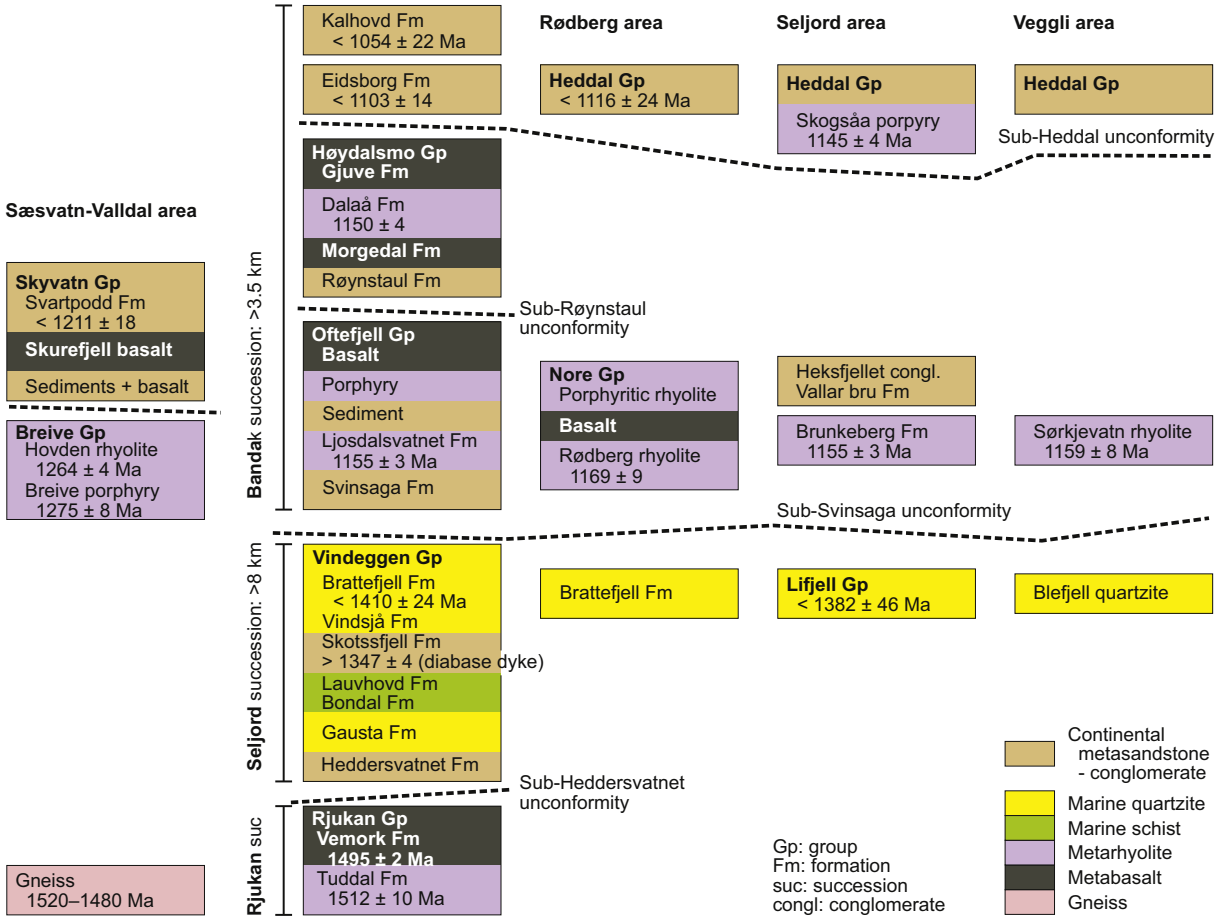

Fig. 11. Simplified stratigraphic columns for the Telemark supracrustal rocks in central Telemark and supracrustal rocks in the Sæsvatn-Valldal area. These columns follow the archetypal subdivision into the Rjukan, Seljord and Bandak successions (Dons 1960; Dons and Jorde 1978; Sigmond 1978), and integrate results of later mapping. Main sources of stratigraphic and geochronological data: Bingen et al. (2002), Bingen et al. (2003), Corfu and Laajoki (2008), Dons (1960; 1978), Laajoki et al. (2002), Laajoki and Corfu (2007), Köykkä and Lammingen (2011), Lamminen and Köykkä (2010), Lamminen (2011), Nordgulen (1999), Sigmond (1975, 1978, 1998), and Spencer et al. (2014).

in the underlying gneiss complex (Andersen et al. 2007; Heaman and Smalley 1994).

In the Telemark supracrustal rocks, the c. 3.5 km thick Bandak succession rests over both the Rjukan and Seljord successions (Köykkä 2011; Laajoki et al. 2002), above a first order unconformity locally decorated by a regolith (Köykkä and Laajoki 2009) (Figs. 6, 11, 12). The succession includes at least two internal unconformities, implying active tectonism during sedimentation (Laajoki 2002; Laajoki et al. 2002). The lower part of the Bandak succession consists of bimodal volcanic rocks interlayered with sediments (Köykkä 2011). The mafic rocks (Morgedal and Gjuve metabasalts) have a within-plate geochemical signature (Brewer et al. 2002; Spencer et al. 2014). The felsic volcanic rocks range in age from 1169 ± 9 to 1145 ± 4 Ma (Bingen et al. 2003; Laajoki et al. 2002). The upper part of the Bandak succession consists of exclusively sedimentary rocks. These are the Heddal Group, Eidsborg Formation and Kalhovd Formation, deposited after 1116 ± 24, 1103 ± 14 and 1054 ± 22 Ma respectively (Figs. 5, 11) (detrital zircon U–Pb data; Bingen et al. 2003; deHaas et al. 1999; Lamminen 2011; Spencer et al. 2014).

The sedimentary rocks of the entire Bandak succession are generally immature, coarse-grained to conglomeratic, and of limited lateral extent. They are interpreted as alluvial fan-, braided fluvial- and locally eolian deposits, accumulated in continental fault-bounded intermontane extensional basins (Bingen et al. 2003; Köykkä 2011; Lamminen 2011; Spencer et al. 2014). Syn-sedimentary normal faults are well documented (Lamminen 2011).

3.5.3. Sveconorwegian magmatism

After 70 Myr of quiescence, magmatism resumed at c. 1065 Ma with the formation of the c. 50 km wide – 170 km long, orogen-parallel, NNW-SSE trending, Sirdal magmatic belt in the Agder area (Fig. 5) (Bingen et al. 2015; Coint et al. 2015; Granseth et al. 2020; Slagstad et al. 2013). This belt is a composite granitoid batholith, comprising mainly elongate and variably foliated plutons of granodiorite, granite and leucogranite. Slivers of heterogeneous gneiss interleaved within granitoid plutons are interpreted as xenoliths or panels of wall-rocks (Coint et al. 2015). The granitoids intruded under pressure conditions of 0.38–0.48 GPa (Coint et al. 2015) between 1066 ± 10 and 1020 ± 15 Ma (Bingen et al. 2015; Bingen and van Breemen 1998a; Coint et al. 2015; Möller et al. 2002; Slagstad et al. 2018; Slagstad et al. 2013). A large portion of the belt comprises silica-rich biotite granite and leucogranite. Foliated plutons of biotite + amphibole K-feldspar-phyric quartz-monzonite to granodiorite are specifically called the Feda suite (1050 ± 8 Ma) and Fennefoss augen gneiss (1031 ± 2 Ma) (Fig. 5) (Bingen and van Breemen 1998a). These are characterized by a magnesian, high-K, high-Sr-Ba, calc-alkaline geochemical signature and locally host ultrapotassic (lamprophyre) mafic layers and enclaves (Fig. 14) (Bingen et al. 1993; Bingen and van Breemen 1998a).

After 985 Ma, large plutons with a distinctly ferroan geochemical signature were emplaced (Figs. 5, 14) (Andersen et al. 2001; Granseth et al. 2020; Vander Auwera et al. 2011). These plutons are weakly- to non-foliated, have sharp contacts to their wall-rock and are well defined on aeromagnetic maps by positive anomalies (Slagstad et al. 2018). Two

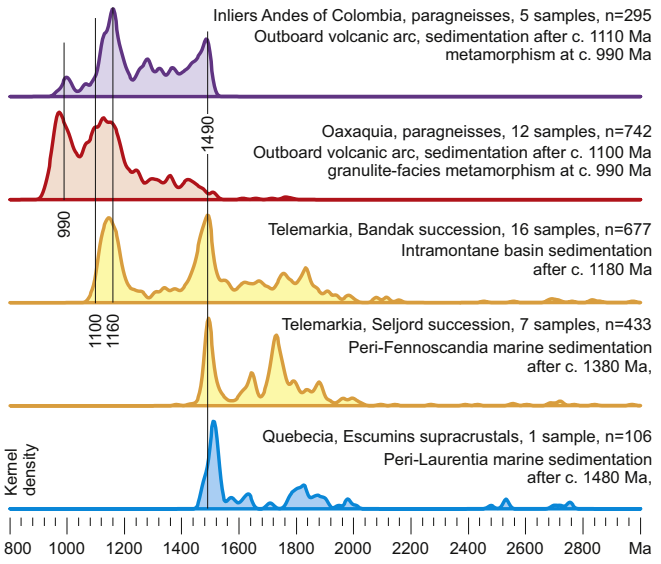

Fig. 12. Kernel density estimators of detrital zircon ages in metasediments of the Telemarkia lithotectonic unit compared with paragneisses and metasediments in Quebecia, Oaxaquia, and inliers in the Andes of Colombia. The Seljord succession in Telemarkia and the Port au Quilles formation in the Escumins supracrustals record marine peri-Baltica (peri-Fennoscandia) and peri-Laurentia sedimentation, respectively, after the 1520–1480 Ma continental generation. The main peak reflects sourcing in the juvenile c. 1520-1480 Ma volcanic arcs, while the diversity of older detrital zircons reflects sourcing from continental sources. The Bandak succession in Telemarkia deposited after c. 1180 Ma (Eidsborg Formation after c. 1100 Ma) and involved important recycling of the Seljord succession and younger magmatic rocks in continental intramontane environment. Contrasting with this situation, the Oaxaquia lithotectonic unit and the Inliers in the Andes of Colombia are interpreted as outboard volcanic arcs formed in the ocean(s) between Laurentia, Amazonia and Baltica after c. 1460 Ma, and isolated almost entirely from continental sediment sources older than c. 1500 Ma. The plots are generated with "DensityPlotter" by (Vermeesch 2012) with a bandwidth of 10 Ma. Data sources: Telemarkia, Bandak and Seljord successions: Bingen et al. (2001), deHaas et al. (1999), Lamminen (2011) and Spencer et al. (2014); Quebecia: Escumins supracrustal rocks, Port aux Quilles formation, Groulier et al. (2018b); Oaxaquia: granulite-facies paragneisses, Solari et al. (2014); inliers in the Andes of Colombia: parageneisses, Cardona et al. (2010) and Ibanez-Mejia et al. (2011).

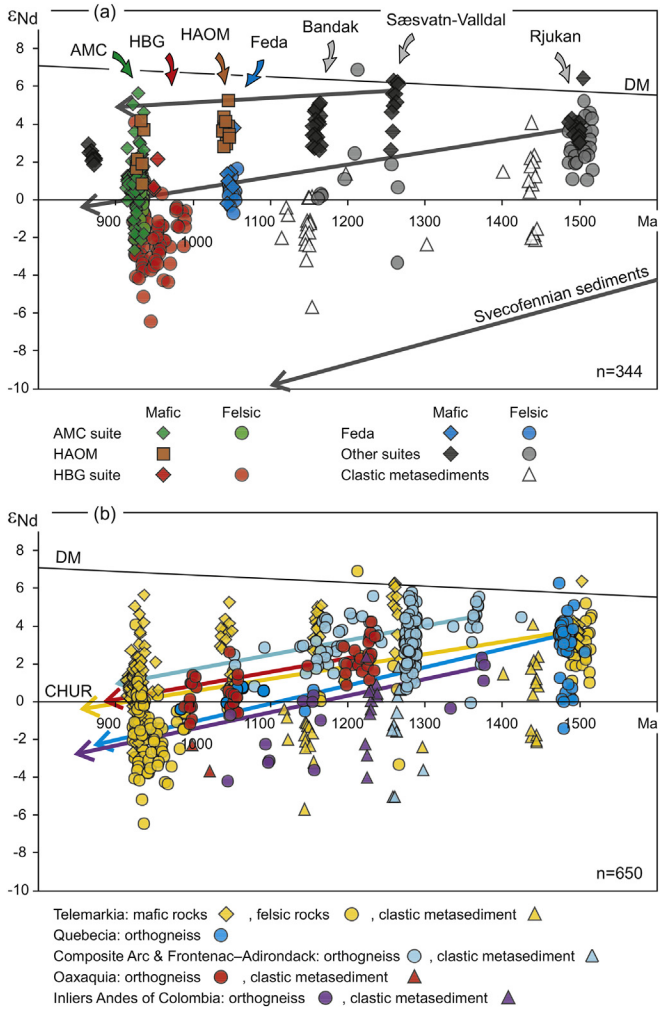

Fig. 13. Neodymium isotopic composition of rock suites in the Telemarkia lithotectonic unit, expressed as ε_{Nd} (initial value) as a function of time. Each symbol represents one sample. Magmatic rocks are represented at their probable time of crystallization and metasedimentary rocks at their probable time of deposition (to improve readability, each symbol is assigned a random scatter lower than ± 8 Ma along the time axis). Interpretations of the distribution of data are discussed in the text. (a) Rock suites in the Telemarkia lithotectonic unit. (b) Comparison between Telemarkia, Quebecia (Grenville orogen, Canada), the Composite Arc and Frontenac–Adirondack belt (Grenville orogen, Canada, USA), the Oaxaquia lithotectonic units (Mexico), and the inliers in the Andes of Colombia. These five lithotectonic units have similar crustal evolution vectors. Compilation of data: Hunnedalen dolerites at c. 870 Ma (Maijer and Verschure 1998); Rogaland AMC suite at 930 Ma (Barling et al. 2000; Bolle et al. 2003a; Demaiffe et al. 1986; Menuge 1988; Nielsen et al. 1996; Robins et al. 1997; Schiellerup et al. 2000); high-alumina orthopyroxene megacrysts (HAOM) in anorthosite plutons, 1040–930 Ma (Bybee et al. 2014; Demaiffe et al. 1986); HBG granitoids, 985–925 Ma (Andersen et al. 2001; Bogaerts et al. 2003; Demaiffe et al. 1990; Menuge 1985, 1988; Vander Auwera et al. 2003; Vander Auwera et al. 2014a); Feda suite at 1050 Ma (Bingen et al. 1993; Menuge 1988; Vander Auwera et al. 2011); other magmatic rocks in Telemarkia (Andersen et al. 2001; Brewer et al. 2002; Brewer et al. 2004; Brewer and Menuge 1998; Menuge 1985, 1988; Vander Auwera et al. 2003); metasedimentary rocks (Andersen and Laajoki 2003; deHaas et al. 1999); Oaxaquia lithotectonic unit (Lawlor et al. 1999; Ruiz et al. 1988; Weber and Köhler 1999); Inliers in the Andes of Colombia (Cordani et al. 2005; Ibanez-Mejia et al. 2015); Quebecia lithotectonic unit (Dickin 2000; Dickin and Higgins 1992; Groulier et al. 2018a; Groulier et al. 2018b); Composite Arc and Frontenac–Adirondack belt (Chiarenzelli et al. 2010; Daly and McLelland 1991; Dickin et al. 2010; Marcantonio et al. 1990; McLelland et al. 1993; Valentino et al. 2019).

main ferroan suites are defined: a ferro-potassic hornblende–biotite–granitoid (HBG) suite and an orthopyroxene-bearing anorthosite–mangerite–charnockite (AMC) suite (Figs. 5, 14) (Bogaerts et al. 2003; Duchesne and Wilmart 1997; Vander Auwera et al. 2003; Vander Auwera et al. 2011; Vander Auwera et al. 2014a). The HBG suite formed between 986 ± 2 and 926 ± 4 Ma and is exposed in the area of the Sirdal magmatic belt and eastwards (Andersen et al. 2001; Andersen et al. 2007; Granseth et al. 2020; Jensen and Corfu 2016; Sigmond 1985; Slagstad et al. 2018; Vander Auwera et al. 2011; Vander Auwera et al. 2014a). The AMC suite formed between 937 ± 1 and 916 ± 9 Ma and is restricted to the southwestern end of the Telemarkia lithotectonic unit (Fig. 5) (Bolle et al. 2018; Schärer et al. 1996; Vander Auwera et al. 2011; Vander Auwera et al. 2014a). A few plutons (Farsund and Kleivan plutons, 931 ± 2 and 936 ± 1 Ma) are composite HBG–AMC plutons, with charnockitic and non-charnockitic facies, reflecting tapping of distinct sources into one pluton (Vander Auwera et al. 2014a).

The Rogaland AMC suite (Fig. 5) consists of three large anorthosite plutons (Egersund-Ogna, Håland-Helleren, Åna-Sira anorthosites), two satellite leuconorite plutons (Hidra and Garsaknatt leuconorites), a layered intrusion (Bjerkreim-Sokndal layered intrusion), and volumetrically minor sills and dykes of jotunite and ilmenite-norite, all emplaced during a short lived magmatic event between c. 932 and 916 Ma (Charlier et al. 2006; Duchesne et al. 1985; Duchesne et al. 1989; Schärer et al. 1996; Vander Auwera et al. 2011).

The Egersund-Ogna anorthosite pluton exhibits an isotropic core and a foliated margin, characterized by a syn-magmatic fabric parallel to the contact. The centre of the pluton is made up of anorthosite and leuconorite with a granulated matrix of plagioclase (An_{40}–An_{50}), hosting 1–3 m large aggregates of plagioclase (up to An_{55}) and high-

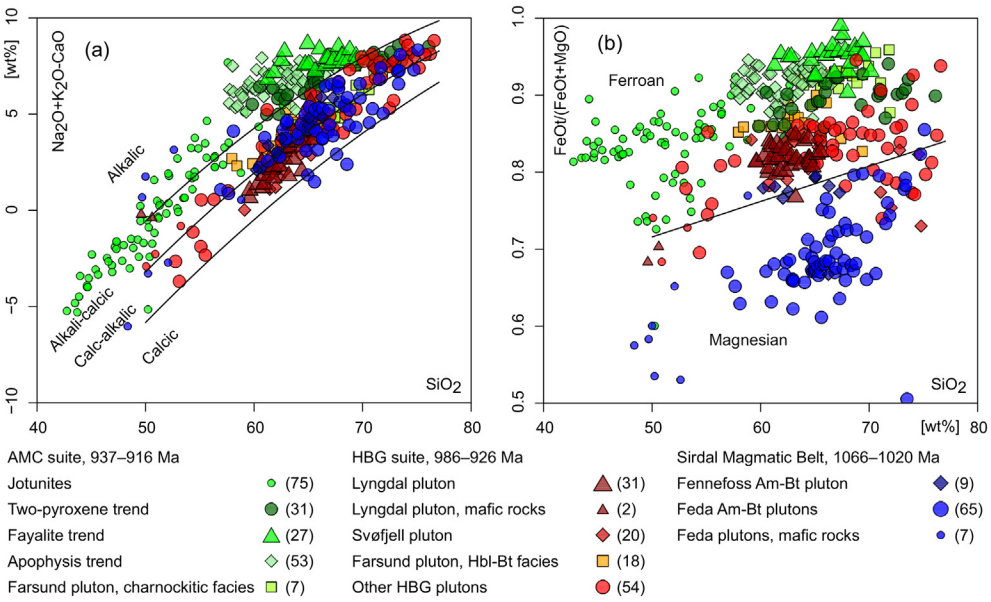

Fig. 14. Comparison of the geochemical signature between three diagnostic magmatic suites intruded between 1066 and 916 Ma in the Telemarkia lithotectonic unit: c. 1050 Ma high-K calc-alkalic Feda plutonic suite of the Sirdal magmatic belt and 1030 Ma Fennefoss pluton (Bingen 1989; Pedersen 1981; Vander Auwera et al. 2011), 986–926 Ma hornblende-biotite granite (HBG) suite with ferro-potassic calc-alkalic to alkali-calcic signature (Bogaerts et al. 2003; Vander Auwera et al. 2003; Vander Auwera et al. 2014a) and the 937–916 Ma anorthosite-mangerite-charnockite (AMC) suite with ferro-potassic alkalic signature (Bolle and Duchesne 2007; Charlier et al. 2010; Duchesne and Wilmart 1997; Vander Auwera et al. 2014a; Vander Auwera et al. 1998; Wilmart et al. 1989). For the AMC suite, 3 different trends are recognized based on the mineralogy (two-pyroxene and fayalite trends) or their belonging to a specific intrusion (apophysis of the Bjerkreim-Sokndal layered intrusion).

alumina orthopyroxene megacrysts (HAOM, En_{75}) (Charlier et al. 2010). The high aluminium and chromium contents (up to 8.5 wt% Al_2O_3 and 1500 ppm Cr) of the orthopyroxene megacrysts indicate a pressure of crystallization of c. 1.1 GPa for the megacrysts, contrasting with the ambient pressure of 0.5 GPa for the matrix minerals (2-3 wt% Al_2O_3 in matrix orthopyroxene). The anorthosite plutons intruded as a plagioclase-dominated crystal mush lubricated by melt, from the base of the crust (1.1 GPa) to the middle of the crust (0.5 GPa) (Barnichon et al. 1999; Charlier et al. 2010; Duchesne et al. 1999). The orthopyroxene megacrysts with the highest aluminum content (> 8 wt% Al_2O_3) define a Sm–Nd isochron with an age of 1041 ± 17 Ma (Bybee et al. 2014), pointing either to inheritance (Vander Auwera et al., 2014b) or protracted ponding of mafic magma at the base of the crust (Bybee et al. 2014).

The Bjerkreim-Sokndal layered intrusion (931 ± 7 Ma) can be subdivided into a layered lower part and a non-layered upper part. The lower part comprises five macrocyclic units of cumulates (Barling et al. 2000; Duchesne 1972; Nielsen et al. 1996; Robins et al. 1997). The upper part comprises, fractionated and wall-rock-contaminated, mangerite and charnockite (Duchesne and Wilmart 1997; Nielsen et al. 1996). The Bjerkreim-Sokndal intrusion intruded at pressure conditions of ≤ 0.5 GPa (Vander Auwera and Longhi 1994). It forms a syncline (lopolith), the formation of which is attributed to gravity-driven subsidence of the central part of the intrusion (Bolle et al. 2000; Bolle et al. 2002; Paludan et al. 1994).

Undeformed pegmatites intruded between c. 914 and 900 Ma. They include the Evje-Iveland rare-mineral pegmatite field (Müller et al. 2017; Pasteels et al. 1979; Scherer et al. 2001; Seydoux-Guillaume et al. 2012).

3.5.4. Sveconorwegian metamorphism

As outlined above, the supracrustal rocks in the centre of the Telemarkia lithotectonic unit were affected by greenschist to epidote-amphibolite facies metamorphism and deformed by open to tight folding. Basalt in the Sæsvatn-Valldal supracrustal complex (Fig. 6) was deformed under epidote-amphibolite facies conditions at c. 1032 ± 2 Ma and faulted at 1017 ± 2 Ma (molybdenite Re-Os data; Stein and Bingen 2002).

In the gneiss complexes, the metamorphic grade typically reached upper amphibolite-facies conditions, with widespread migmatitization between 1026 ± 14 and 1005 ± 7 Ma (zircon and monazite U–Pb data; Bingen et al. 2008b; Coint et al. 2015). Granitoids of the Sirdal magmatic belt (c. 1065–1020 Ma) are commonly moderately deformed (Coint et al. 2015). Locally, they contain zircons with rims recording a hydrothermal to metamorphic overprint at c. 1016 Ma (Knaben Mo district; Bingen et al. 2015).

The metamorphic grade increases southwestwards towards the Rogaland AMC complex, structurally downwards, across to the N–S trending and E-dipping regional fabric (Fig. 5) (Bingen and van Breemen 1998b; Maijer 1987; Slagstad et al. 2018; Tobi et al. 1985). Metamorphism was coeval with the formation of lithological banding, tight to isoclinal folding and migmatitization. Two concentric granulite facies zones are defined: the orthopyroxene zone and the osumilite zone close to the AMC complex (Fig. 5). Osumilite is diagnostic of water poor, low-pressure, ultrahigh temperature (UHT; T > 900 °C) granulite-facies conditions (Harley 2008; Holland et al. 1996).

Zircon and monazite U–Pb geochronology from a diversity of granulite-facies samples gave apparent ages spreading between c. 1045 and 900 Ma (Bingen et al. 2008b; Bingen and van Breemen 1998b; Laurent et al. 2018a; Möller et al. 2002, 2003; Slagstad et al. 2018; Tomkins et al. 2005). Insight into the pressure-temperature-time evolution of this protracted metamorphism requires careful linkage of petrography, phase equilibrium modelling, geochronology and trace-element characterization of zircon and monazite. Typical samples inside the orthopyroxene zone reached peak conditions of 0.5 GPa – 880 °C between c. 1040 and 1010 Ma (Laurent et al. 2018b). Rims of neocrystallized zircon in such samples spread from 1045 to 955 Ma, supporting 90 Myr of melt-present conditions (Laurent et al. 2018a). In the osumilite zone, the onset of migmatitization, associated with biotite and sulfide mineral breakdown, is recorded by sulfate-rich monazite cores in an osumilite-bearing paragneiss at 1034 ± 6 Ma (Laurent et al. 2016). In a (quartz- and garnet-free) sapphirine + orthopyroxene

sample (Fig. 9; Ivesdal locality), a Y-rich monazite (5–7 wt% Y_2O_3) further constrains temperature higher than 900 °C between 1029 ± 9 and 1006 ± 8 Ma (Laurent et al. 2018b), in accordance with zircon data (1010 ± 7 to 1006 ± 4 Ma) (Drüppel et al. 2013). The breakdown of the peak sapphirine + orthopyroxene assemblage into a cordierite + hercynite assemblage implies a clockwise P-T path with a decompression between 0.6 GPa – 920 °C and 4.5 GPa – 900 °C (Fig. 9) (Blereau et al. 2017; Laurent et al. 2018b). This decompression is best captured by a garnet-bearing sample from the osumilite zone that contains Y-rich monazite recording garnet breakdown into cordierite + hercynite + orthopyroxene, pinning a robust P-T-t point at 0.4 GPa – 910 °C – 930 ± 6 Ma (Laurent et al. 2018b). Together, the data give evidence for two events of low-pressure granulite-facies metamorphism peaking at UHT conditions, a first event (M1) between c. 1030 and 1005 Ma, and a second (M2) at c. 930 Ma, associated with formation of osumilite (Blereau et al. 2017; Drüppel et al. 2013; Laurent et al. 2018b; Laurent et al. 2016). Minor exhumation (c. 6 km) took place between the two.

These two events were penecontemporaneous with magmatic activity (Laurent et al. 2018b; Slagstad et al. 2018). The first M1 event started with dehydration melting (c. 1034 Ma) coeval with intrusion of the Sirdal magmatic belt (c. 1065-1020 Ma) and associated underplating (c. 1040 Ma), and peaked at the end and after this magmatic event (1030–1005 Ma). The second M2 event (c. 930 Ma) was coeval with intrusion of the AMC suite. This correlation strongly suggests that magmatism and metamorphism had a common heat source in the mantle. The lag between magmatism and peak metamorphism for M1 may reflect temperature buffering by melt until melt migration effectively took place.

The M2 metamorphic event was followed by regional scale cooling, dated by titanite U–Pb data at 918 ± 2 Ma (Bingen and van Breemen 1998b). Amphibole $^{40}Ar/^{39}Ar$ apparent ages scatter between 1059 ± 8 and 853 ± 3 Ma (Bingen et al. 1998). The main cluster at 871 ± 10 Ma overlaps with biotite Rb–Sr ages (Verschure et al. 1980) and is interpreted as a cooling age.

3.5.5. The Mandal-Ustaoset fault and shear zone

The Mandal-Ustaoset fault and shear zone is a N–S trending structure inside the Telemarkia lithotectonic unit (Fig. 2). It includes a precursor ductile shear zone and a set of later brittle normal faults (Sigmond 1985). In its northern segment, it is an east dipping (c. 45°) normal (extensional) shear zone, juxtaposing the amphibolite-facies Hardangervidda gneiss complex in the west against the low-grade intramontane basin hosting the Kalhovd Formation (≤ 1054 ± 22 Ma) in the east (Sigmond and Ragnhildstveit 2004). Towards the south, the Mandal-Ustaoset fault and shear zone merges into an amphibolite-facies N–S trending banded gneiss unit on the eastern side of an elongate pluton of the Feda suite (1049 ± 8 Ma, Mandal augen gneiss; Bingen and van Breemen 1998a). The Mandal-Ustaoset fault and shear zone still requires detailed kinematic and geochronological characterization.

4. Discussion

4.1. U–Pb and Lu–Hf evidence for continental growth at the margin of Fennoscandia

The continental crust exposed in the Sveconorwegian orogen was formed after 1900 Ma (Åhäll and Connelly 2008; Andersen et al. 2004a; Bingen et al. 2005; Bingen and Viola 2018; Petersson et al. 2015b; Roberts and Slagstad 2015; Roberts et al. 2013). The age of the dominant magmatic suites in the different lithotectonic units decreases towards the west (Fig. 7). The oldest major magmatic suites in each lithotectonic unit are dated between 1710 and 1660 Ma in the Eastern Segment, 1660 and 1520 Ma in the Idefjorden lithotectonic unit, 1575 and 1480 Ma in the Bamble and Kongsberg lithotectonic units, and 1520 and 1480 Ma in the Telemarkia lithotectonic unit. The Lu–Hf isotopic signature of igneous zircon in these magmatic suites (Fig. 8) becomes more radiogenic (more positive ε_{Hf} values) westward in the orogenic belt, with average initial ε_{Hf} values increasing from +3.0 in the Eastern Segment (1700 Ma) to +8.8 in the Bamble-Kongsberg lithotectonic units (1550 Ma), and back to +5.7 in the Telemarkia lithotectonic unit (1500 Ma; Fig. 8) (Andersen et al. 2002b; Pedersen et al. 2009; Petersson et al. 2015a; Petersson et al. 2015b; Roberts et al. 2013). The geochemical signature of these different magmatic suites generally ranges from calc-alkalic to alkali-calcic (references above), suggesting that the continental lithosphere was generated dominantly in a supra-subduction (accretionary) geodynamic setting between 1710 and 1480 Ma (Åhäll and Connelly 2008; Andersen et al. 2004a; Petersson et al. 2015a; Petersson et al. 2015b; Roberts et al. 2013).

The weakly positive initial ε_{Hf} values in the Eastern Segment (Fig. 8) imply significant recycling of older Paleoproterozoic (Svecokarelian) continental crust in the genesis of the 1710–1660 Ma magmatic suites (Petersson et al. 2015a). The more positive initial ε_{Hf} values westwards imply, instead, that the four lithotectonic units to the west of the Mylonite Zone were generated in more juvenile volcanic arc and back arc environment, away from old Paleoproterozoic continental lithosphere (Andersen et al. 2002b; Petersson et al. 2015b; Roberts et al. 2013). The variability within and between these units can be accounted for by a change from an advancing to a retreating subduction system or, alternatively, a variable contribution of metasedimentary components incorporated in the subduction system along the oceanic lower plate (Andersen et al. 2002b; Petersson et al. 2015b; Roberts et al. 2013).

The age and isotopic trends of magmatism in the 1710–1480 Ma interval (Figs. 7, 8) are compatible with incremental westward growth of the continental lithosphere at the margin of Fennoscandia. This is compatible with any orogenic model interpreting the lithotectonic units as endemic to the margin of Fennoscandia (Fig. 3b, d, e, f).

4.2. Significance of high-K calc-alkaline granite plutonism

Tracing past subduction systems largely relies on tracing a subduction-related geochemical signature in magmatic rocks. In the Telemarkia lithotectonic unit, a significant component of the large (50 × 170 km) orogen-parallel Sirdal magmatic belt (c. 1065–1020 Ma) has a calc-alkaline geochemical signature (Bingen et al. 2015; Coint et al. 2015; Granseth et al. 2020; Slagstad et al. 2018; Slagstad et al. 2013). More specifically, the biotite + amphibole K-feldspar-phyric quartz-monzonite–granodiorite foliated plutons of the Feda suite are characterized by a high-K, high-Sr-Ba, magnesian, calc-alkalic geochemical trend (Fig. 14) (Bingen et al. 1993; Bingen and van Breemen 1998a). They are associated with a small volume of ultrapotassic rocks. Calc-alkaline rocks are typically observed in active supra-subduction environment (Bateman and Chappell 1979; Hervé et al. 2007; Pearce et al. 1984). However, high-K calc-alkaline suites are also typically representative of syn- to late-collision plutons and batholiths in collisional orogens (Fig. 15). They are well described in the Caledonian orogen (Bruand et al. 2014; Clemens et al. 2009; Ghani and Atherton 2006; Neilson et al. 2009), the Hercynian orogen (Couzinié et al. 2016; Laurent et al. 2014; Laurent et al. 2017; Moyen et al. 2017) and the Pan-African orogens (Janoušek et al. 2010; Liégeois et al. 1998). These plutons are commonly associated with minor volumes of ultrapotassic rocks such as lamprophyre, appinite or vaugnerite (Fig. 15b). The Sirdal magmatic belt and, more specifically, the Feda suite exhibit a complete overlap in major and trace element geochemical composition with syn- to late-collision high-K calc-alkaline plutons in collisional orogens (Fig. 15). Therefore, the belt can be reasonably interpreted as the product of syn- to late-collision magmatism.

To sum up, the geochemical signature of the Sirdal magmatic belt is not fully diagnostic of a specific geodynamic environment and two

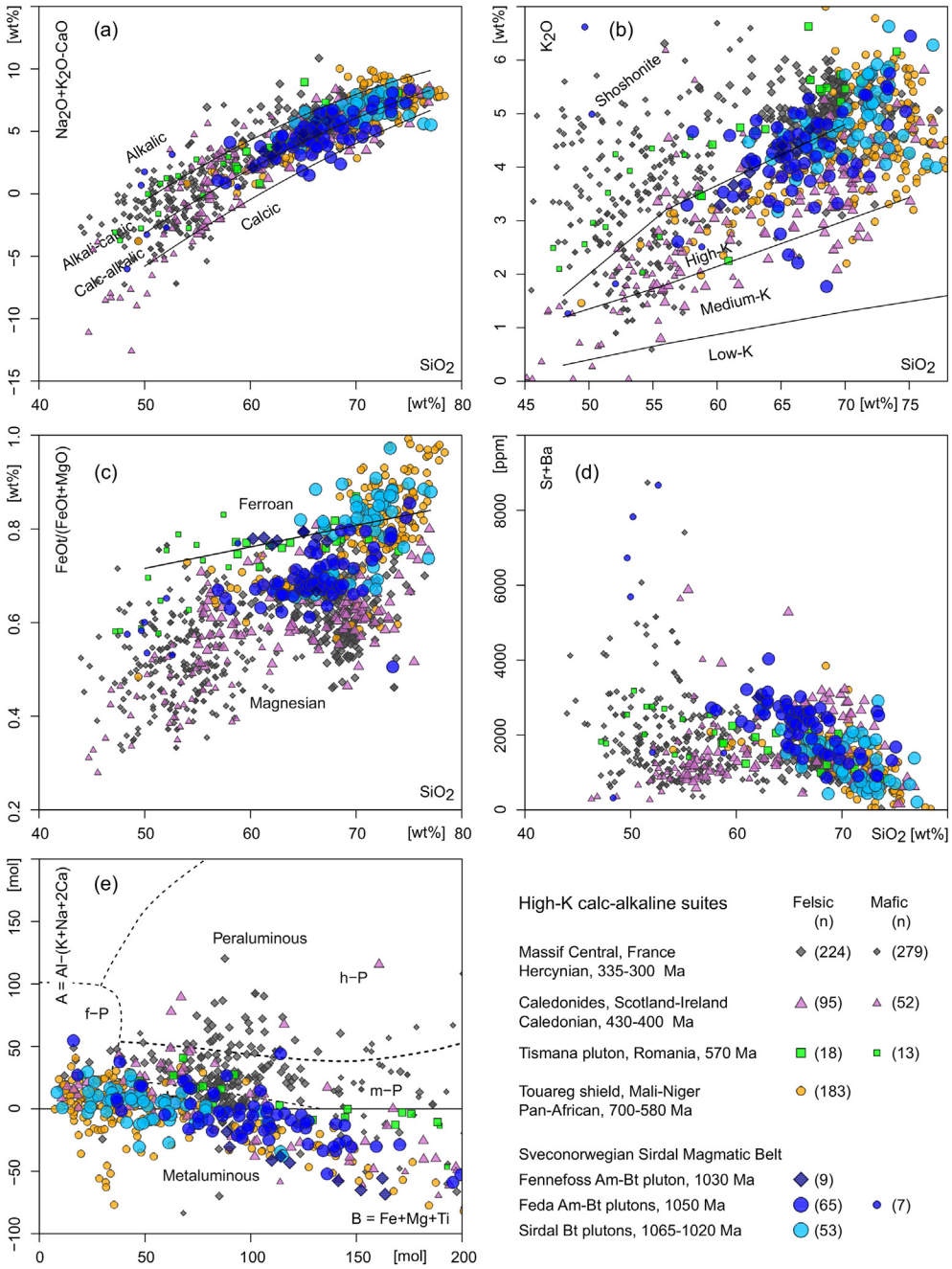

Fig. 15. Comparison of the geochemical signature of the Sirdal magmatic belt (c. 1065–1020 Ma) in the Telemarkia lithotectonic unit with syn-collisional high-K calc-alkaline magmatic suites in younger collision orogenic belts. Large symbols represent granitoids while small symbols represent associated minor mafic sills, dykes and enclaves. The Sirdal magmatic belt is divided into the magnesian amphibole-biotite Feda plutonic suite hosting minor volume of ultrapotassic enclaves, the ferroan amphibole-biotite-bearing Fennefoss pluton and more silica-rich biotite-bearing foliated plutons (Bingen 1989; Pedersen 1981; Slagstad et al. 2013; Vander Auwera et al. 2011). For comparison, the Hercynian high-K calc-alkaline plutons of the Massif Central in France associated with "vaugnerites" (compilation: Moyen et al. 2017), the Caledonian high-K, high Ba-Sr plutons of Scotland and Ireland associated with "appinites" (Clemens et al. 2009; Ghani and Atherton 2006), the Neoproterozoic shoshonitic Tismana pluton in the Carpathians of Romania (Duchesne et al. 1998), and the Neoproterozoic high-K calc-alkalines suites of the Touareg Shield in Mali and Niger (Liégeois et al. 1998). The figure shows a broad overlap of the geochemistry between these different suites. (a) SiO_2 vs. Na_2O+K_2O-CaO diagram (Frost et al. 2001). (b) SiO_2 vs. K_2O diagram (Peccerillo and Taylor 1976). (c) SiO_2 vs. $FeO_{tot}/(FeO_{tot}+MgO)$ (Frost et al. 2001). (d) SiO_2 vs. Sr+Ba diagram showing the high Sr+Ba signature of high-K calc-alkaline suites, including the Feda plutons and their ultrapotassic mafic enclaves. (e) B-A diagram (B = Fe+Mg+Ti, A = Al-(K+Na+2Ca) (expressed in gram-atoms of each element in 100 gr of material) (Debon and Le Fort 1983; Villaseca et al. 1998) (h-P: highly peraluminous, m-P: moderately peraluminous, l-P: low peraluminous, f-P: felsic peraluminous).

alternatives are possible: (i) It records supra-subduction magmatism as part of an active subduction system in the 1065–1020 Ma time interval. This subduction was either dipping eastwards in the context of the models of protracted Andean margin (Fig. 3e, f) (Slagstad et al. 2020; Slagstad et al. 2017; Slagstad et al. 2013) or was dipping westwards in the model of suturing along the Mylonite Zone at c. 990 Ma (Fig. 3 c) (Brueckner 2009; Möller and Andersson 2018; Petersson et al. 2015b). (ii) The Sirdal magmatic belt represents syn-collision magmatism, therefore recording ongoing continent-continent collision between 1065 and 1020 Ma (Fig. 3d).

4.3. Significance of massif-type anorthosite plutonism

Massif-type anorthosite plutons formed on Earth only in the Proterozoic. This peculiarity is inferred to relate directly or indirectly to the secular evolution of the temperature of the asthenosphere (Ashwal 1993). The geodynamic context and petrogenesis of AMC plutonism remain controversial (Ashwal 1993; Bédard 2010; Duchesne et al. 1985; Emslie 1985; Vander Auwera et al. 2011).

Petrologically, the AMC suite of Rogaland (Figs. 5, 14) can be accounted for by differentiation of several parental magmas ranging in composition from high-alumina basalt (anorthosite plutons) to ferrobasalt (Bjerkreim-Sokndal intrusion and jotunites) in anhydrous and reduced (QFM to QFM-1) conditions (Charlier et al. 2010; Duchesne and Wilmart 1997; Duchesne et al. 1989; Robins et al. 1997; Vander Auwera and Longhi 1994).

Here, we draw the attention to the fact that the AMC complex is almost entirely devoid of water-bearing minerals (Duchesne and Charlier 2005; Longhi et al. 1999). Amphibole appears only very locally as a late-stage replacement mineral. The dry nature of the magmas as well as the water-poor to water-absent assemblages of the granulite-facies wall rock of the AMC plutons (Blereau et al. 2017; Drüppel et al. 2013; Laurent et al. 2018b) are objectively irreconcilable with the definition of magmatism in a supra-subduction setting (Grove et al. 2006). Supra-subduction magmatism is induced by fluids released from and fluxing above a subducting oceanic plate. It typically contains 1–6 wt % H_2O (Plank et al. 2013; Sobolev and Chaussidon 1996; Wallace 2005) and produces hornblende-bearing cumulates (Jagoutz and Schmidt 2013). Therefore, in our opinion, models framing AMC magmatism in an active supra-subduction setting (Fig. 3e, f) (Bybee et al. 2014; Slagstad et al. 2013) are not realistic.

4.4. Sveconorwegian orogenic plateau

Evidence for the presence of a past orogenic plateau in Proterozoic orogens is largely indirect (Jamieson and Beaumont 2013; Rey et al. 2001; Rivers 2008, 2012; Vanderhaeghe 2012). Today, following extension (collapse), exhumation and erosion, the Sveconorwegian orogen exposes widespread gneiss complexes characterized by ductile deformation accompanied by partial melting, compressional structures, and protracted upper amphibolite- to granulite-facies metamorphism, structurally overlain by discontinuous exposures of low-grade supracrustal rocks (Fig. 4). The supracrustal rocks are greenschist- to epidote-amphibolite-facies metavolcanic and metasedimentary complexes, exhibiting partially preserved primary structures and stratigraphic relationships. The age distribution of rocks in the supracrustal complexes matches that in the gneiss complexes. Transition between high-grade and low-grade rock occurs over short distances.

We interpret the gneiss complexes and supracrustal complexes as remnants of the infrastructure and superstructure of an orogenic plateau, respectively, now tectonically juxtaposed along extensional shear zones. Characterization of the geometry, kinematics and geochronology of these shear zones is still very fragmentary. However, recent data support diffuse late-Sveconorwegian extensional tectonics (Persson-Nilsson and Lundqvist 2014; Torgersen et al. 2018; Viola et al. 2011).

The sedimentary rocks in the supracrustal complexes offer a window into the surface environment at the time of deposition. As reviewed above, the supracrustal rocks deposited between 1280 and 1050 Ma reflect continental (above sea level) conditions, with evidence for sediment accumulation in fault-bounded intermontane extensional basins (Bingen et al. 2003; Köykkä 2011; Lamminen 2011; Spencer et al. 2014). Gneiss complexes in the Bamble and Kongsberg lithotectonic units were exhumed to upper-crustal level after the early-Sveconorwegian orogenic phase (1150–1120 Ma) and, therefore, they can be regarded as part of the orogenic superstructure during the main Sveconorwegian orogeny (after 1065 Ma).

Plutons, produced by partial melting of the lower and middle crust, can be anticipated to accumulate mainly at the transition between ductile and brittle crust (Brown 2013). In an orogenic plateau, they will accumulate between the infrastructure and superstructure. The Sveconorwegian orogen exposes Sveconorwegian plutons increasing in abundance westwards and mainly hosted in gneiss complexes (Fig. 5). Plutons intruded between 1065 and 920 Ma, define a consistent pressure of intrusion of 0.4–0.5 GPa (Table 1). This suggests a rather constant depth of c. 16 km for the boundary between the infrastructure and superstructure, through time during the main Sveconorwegian orogeny. Additionally, this is consistent with a model of stable orogenic plateau extending over large areas in the orogen.

4.5. End of convergence and collapse of the orogenic plateau

The switch between plate convergence and plate divergence is a fundamental parameter of orogeny. However, it is not trivial to constrain this switch in time, because evidence for compression or extension are distinct in the infrastructure and superstructure of an orogenic plateau. The last undisputable evidence for convergence in the Sveconorwegian orogen corresponds to eclogite facies metamorphism dated at 988 ± 6 Ma in the Eastern Segment (Möller et al. 2015). Several observations, however, indicate that compression continued after this point in the middle crust (infrastructure), probably to at least c. 930 Ma. (i) In the Eastern Segment, the internal section and the eclogite-bearing ductile nappe are folded by east-verging to recumbent folds and later upright folds, recording continued, high-grade E–W contraction (Möller and Andersson 2018; Möller et al. 2015; Piñán-Llamas et al. 2015; Tual et al. 2015). Zircon carries a record of these events between c. 978 and 961 Ma. (ii) In the Telemarkia lithotectonic unit, plutons of the HBG suite exhibit a petrofabric, which is largely controlled by wall-rock ductile deformation during emplacement (Bolle et al. 2018). A study of the anomaly of magnetic susceptibility (AMS) of the Holum, Kleivan, and Sjelset plutons in the Agder area provided evidence for regional E–W contraction during intrusion, at 957 ± 7, 936 ± 1 and 932 ± 1 Ma respectively (Fig. 5) (Bolle et al. 2010; Bolle et al. 2003b; Bolle et al. 2018). (iii) In the frontal wedge of the orogen, dykes attributed to the c. 980–945 Ma Blekinge-Dalarna dolerite swarm (Fig. 5) are known to be displaced along discrete ductile shear zones with top-to-east reverse sense of shear. This suggests that thrusting along the Sveconorwegian front took place as late as after c. 945 Ma (Stephens and Wahlgren 2020a; Wahlgren et al. 1994).

In contrast with this evidence, dykes and sills intruded along brittle structures suggest coeval extension in the upper crust (superstructure). (i) In the Idefjorden lithotectonic unit, WNW–ESE trending mafic to felsic intrusions suggest a phase of NNE-SSW extension between c. 951 and 915 Ma (Fig. 5) (Årebäck et al. 2008; Hellström et al. 2004; Scherstén et al. 2000; Wahlgren et al., 2016). (ii) In the internal section of the Eastern Segment, pegmatite dykes crosscutting the gneiss fabric suggest relaxation between c. 961 and 934 Ma (Andersson et al. 1999; Möller et al. 2007; Möller and Söderlund 1997; Söderlund et al. 2008b; Söderlund et al. 2002) (iii) In the frontal wedge and the foreland of the orogen, the N-S trending Blekinge-Dalarna dolerites document a phase of E–W extension between c. 978 and 946 Ma (Fig. 5) (Gong et al. 2018; Ripa and Stephens 2020d; Söderlund et al. 2005).

Collectively, the data suggest that the Sveconorwegian orogenic plateau was sustained and grew eastwards until c. 930 Ma, in an overall convergent orogen. Evidence of contraction in the ductile middle crust (infrastructure) to c. 930 Ma contrasts with evidence for extension in the same time interval in the brittle upper crust (superstructure), and in the brittle foreland of the orogen.

5. Review of Sveconorwegian orogenic models

In light of the evidence summarised and discussed above, we review and discuss below the orogenic models sketched in Fig. 3.

5.1. Early-Sveconorwegian collision-accretion with suture in Bamble-Kongsberg

The oldest known Sveconorwegian high-grade metamorphism (1150–1120 Ma) is recorded in the Kongsberg and Bamble lithotectonic units, in the centre of the Sveconorwegian orogen. This metamorphism could be interpreted to reflect crustal thickening during an early-Sveconorwegian collision. This interpretation leads to the conceptual model of Fig. 3a involving collision or accretion of an exotic Telemarkia microcontinent to the Idefjorden lithotectonic unit between 1150 and 1120 Ma, closing an intervening ocean and forming the Bamble-Kongsberg orogenic wedge (Bingen et al. 2008c; Bingen et al. 2005). At least two arguments rule out the closure of an oceanic realm. (i) The Mesoproterozoic magmatism exhibits a significant age overlap between the Bamble–Kongsberg, Telemarkia and Idefjorden lithotectonic units. Specifically, the 1520–1480 Ma magmatic suites, which are prominant in the Telemarkia lithotectonic unit, extend well into the Bamble, Kongsberg and Idefjorden lithotectonic units, thus representing a stitching element of these units around c. 1500 Ma (Fig. 7). (ii) The granulite-facies low-K calc-alkaline Tromøy Complex in Bamble was formerly interpreted as an early-Sveconorwegian, c. 1200 Ma old, oceanic volcanic arc (Andersen et al. 2004a; Andersen et al. 2002b; Knudsen and Andersen 1999). However, new data demonstrate that the magmatic protolith of the Tromøy Complex is Gothian (1575 ± 44 to 1544 ± 14 Ma) (Bingen and Viola 2018), meaning that no evidence for remnants of early-Sveconorwegian oceanic lithosphere is known in the Bamble lithotectonic unit. There is therefore no actual geological support for the conceptual model sketched in Fig. 3a.

5.2. Early-Sveconorwegian wrench tectonics

The Bamble and Kongsberg lithotectonic units have been referred to as shear belts in the literature mostly because of widespread, steep shear foliation zones and penetrative lithological banding (Starmer 1991). This intense deformation has inspired tectonic models (Fig. 3b) involving long distance early-Sveconorwegian strike-slip transport of the Telemarkia lithotectonic unit relative to the Idefjorden lithotectonic unit, at the margin of Fennoscandia, generating a Bamble–Kongsberg transpressional shear belt (Andersen et al. 2004a; Bingen et al. 2008c; deHaas et al. 1999; Lamminen and Köykkä 2010). However, recent field data from the tectonic boundaries between the Bamble, Kongsberg, Telemarkia and Idefjorden lithotectonic units, and from the centre of the Bamble and Kongsberg lithotectonic units (Bingen and Viola 2018; Henderson and Ihlen 2004; Scheiber et al. 2015) highlight orthogonal compression and rule out significant wrench tectonics, thus excluding orogen-scale strike-slip transport. A component of sinistral strike-slip shearing is indeed recorded by some of the mylonite zones within the Kongsberg lithotectonic unit (Scheiber et al. 2015). These are, however, compatible with transpressional deformation ensuing only after the peak of orthogonal deformation and high-grade metamorphism (1150–1120 Ma).

5.3. Collisional orogeny with suture along the Mylonite Zone

The Mylonite Zone is a major Sveconorwegian east-southeastward-verging shear zone, juxtaposing the Eastern Segment beneath the Idefjorden lithotectonic unit. The geological records of these two units are significantly distinct and, as a consequence, several authors have argued that the Mylonite Zone may represent a suture zone. An oceanic domain would have closed at c. 990 Ma between the Eastern Segment, representing the Fennoscandia continent as lower plate, and distal terranes formed outboard of the Fennoscandia margin in the west as upper plate (the four western lithotectonic units of the orogen named together 'Sveconorwegia'; Fig. 3c) (Andersson et al. 2002a; Austin Hegardt et al. 2005; Brueckner 2009; Cornell et al. 2000; Möller and Andersson 2018; Möller et al. 2015; Petersson et al. 2015b). This model envisions the pre-990 Ma (pre-collision) magmatism and metamorphism west of the Mylonite Zone as formed in a supra-subduction setting, above a west-dipping subduction zone. At least four arguments support this model. (i) The magmatic records in the Eastern Segment and in the Idefjorden lithotectonic unit are distinct (Fig. 7). Magmatic suites do not extend across the Mylonite Zone. (ii) Hallandian metamorphism between 1465 and 1385 Ma is documented only east of the Mylonite Zone (Fig. 6) (Söderlund et al. 2002; Ulmius et al. 2015). (iii) The Sveconorwegian metamorphism in the Eastern Segment reached eclogite-facies conditions at c. 990 Ma (Möller et al. 2015), significantly after granulite-facies metamorphism in the Idefjorden hanging wall at c. 1050 Ma (Söderlund et al. 2008a). Eclogite-facies metamorphism could record continental burial after closure of an ocean basin (Möller and Andersson 2018; Möller et al. 2015). (iv) The Lu–Hf isotopic signature of magmatic rocks in the 1780–1480 Ma interval are distinct on both sides of the Mylonite Zone, with an average $\varepsilon_{Hf} = +3.0$ in the Eastern Segment at 1700 Ma against +4.8 in the Idefjorden lithotectonic unit at 1570 Ma (Petersson et al. 2015a; Petersson et al. 2015b) (Fig. 8). This difference implies a lower contribution of old continental crust in the genesis of the magmatic rocks in the Idefjorden lithotectonic unit.

These four pro-arguments, however, are balanced by counterarguments. Specifically (i) the Orust dolerites (1457 ± 6 Ma) in the Idefjorden lithotectonic unit (Åhäll and Connelly 1998) overlap in age with 1465–1385 Ma Hallandian granitic to charnockitic plutonism in the Eastern Segment. (ii) The Lu–Hf isotopic signature of early-Sveconorwegian magmatism between 1225 and 1180 Ma is distinctly supra-chondritic in both the Eastern Segment (bimodal magmatism along the Sveconorwegian front; $+1.2 < \varepsilon_{Hf} < +6.6$) and the Telemarkia lithotectonic unit (Vråvatn Complex; $+9 < \varepsilon_{Hf} < +10$; Fig. 8) (Andersen et al. 2007; Petersson et al. 2015a; Söderlund et al. 2005). This signature attests to coeval depleted mantle derived magmatism on both side of the Mylonite Zone before the presumed ocean closure at 990 Ma. (iii) The Mylonite Zone (or geological units in its direct proximity) does not contain any remnants or slivers of pre- to early-Sveconorwegian (1340–1080 Ma) marine sedimentary sequences, oceanic lithosphere, oceanic volcanic arc, or ultramafic rocks, such that no suture zone can be directly constrained.

To conclude, closure of an oceanic basin along the Mylonite Zone at c. 990 Ma represents a plausible model (Fig. 3c) (Möller and Andersson 2018). However, the evidence is not conclusive at this point. In the following text, we do not indicate this model as the most plausible.

5.4. Non-collisional (Andean type) orogeny

In the non-collisional (Andean type) orogenic models (Fig. 3e, f), the Sveconorwegian orogen represents an active margin of Baltica/Fennoscandia, evolving from at least 1280 Ma to after 900 Ma, above an oceanic plate subducting to the east into a trench situated to the west of the exposed orogen (Falkum and Petersen 1980; Slagstad et al. 2013). The geological record in the Sveconorwegian orogen is explained by changes in the conditions of subduction, such as trench position, subduction angle, convergence rate, convergence direction and age of the oceanic lithosphere. This model is an adaptation of the tectonic switching model (Collins 2002; Haschke et al. 2002), which is based on the observation that a retreating or steepening oceanic subduction is associated with an extensional tectonic regime and abundant magmatism in the (supra-subduction) upper plate, while an advancing or flattening subduction is associated with contraction, metamorphism and magmatic quiescence.

Different versions of the non-collisional (Andean type) model have been proposed by Slagstad et al. (2020; 2018; 2017; 2013) and Granseth et al. (2020). These models offer an elegant and flexible conceptual framework for the orogeny. However, we think that they are irreconcilable with a number of key features and concepts. (i) In its simple expression, the tectonic switching model predicts either extension or contraction in the upper (supra-subduction) plate. During the

main Sveconorwegian orogeny, voluminous magmatism (mafic and felsic) in the Telemarkia lithotectonic unit would indicate a retreating subduction trench between 1065 and 1020 Ma, while HP granulite facies metamorphism in the Idefjorden lithotectonic unit (Söderlund et al. 2008a) would indicate an advancing trench in the same time interval, in contradiction with the model. (ii) Conceptually, an eastwards oceanic subduction to the west of the orogen can hardly represent the driving force for westwards underthrusting of the Eastern Segment at c. 990 Ma to eclogite-facies conditions. Considering the presumably weak rheology of the lithosphere in the Telemarkia lithotectonic unit around 990 Ma, it is unlikely that compressive stresses from a plate subducting west of the orogen could be effectively transmitted for at least 400 km to the east to the Eastern Segment. (iii) The Sveconorwegian magmatism (1065–915 Ma) does not represent typical volcanic arc magmatism. The geochemical signature and petrology of magmatic suites can be related to lower crustal sources and partial melting conditions (Granseth et al. 2020; Vander Auwera et al. 2008; Vander Auwera et al. 2011), rather than to an active subduction. The geochemical signature of the Sirdal magmatic belt (1065–1020 Ma) can be interpreted in both a collisional setting or a supra-subduction setting (see above). The magmatism between 985 and 915 Ma lacks a subduction signature and the dry nature of AMC magmatism is not compatible with a supra-subduction setting (see above). The magmatism between 935 and 915 Ma is exposed over a zone at least 350 km wide, much larger than a typical volcanic arc. The geographical polarity of the magmatism in the 935–915 Ma time interval, involving dry plutonism of the AMC suite in the west and water-bearing plutonism of the HBG suite in the east is opposite to what should be expected from an east dipping subduction system.

For these different reasons, we remain sceptical that oceanic subduction in the hinterland of the orogen could have steered tectonic forces and magmatism inside the orogen during the main Sveconorwegian orogeny (1065–900 Ma). The non-collisional models proposed by Slagstad et al. (2020; 2018) omit to propose specific tectonic driving forces, either oceanic subduction or continental subduction-delamination inside the orogen, to explain the high-pressure metamorphism in the Bamble–Kongsberg lithotectonic units (1150–1120 Ma), Idefjorden lithotectonic unit (c. 1050 Ma) and Eastern Segment (c. 990 Ma).

In a recent version of the non-collisional model (Slagstad et al. 2020), the margin of Fennoscandia is proposed to have been fragmented (into micro-continents) by extension before c. 1150 Ma and re-amalgamated during the Sveconorwegian orogeny between c. 1150 and 980 Ma to form the Sveconorwegian orogen. However, as discussed previously in this chapter, there is no evidence between the lithotectonic units for (i) marine sediment sequences that could represent marine basins, (ii) ophiolites or oceanic volcanic arcs that could represent oceanic basins, or (iii) ultramafic bodies that could represent exhumed hyperextended domains. As noted earlier, the low-K calc-alkaline Tromøy Complex in Bamble (Andersen et al. 2004a) should not be interpreted as an early-Sveconorwegian oceanic volcanic arc (Bingen and Viola 2018).

5.5. Collisional orogeny with suture west of the orogen

The Grenville orogen is the archetypal example of a large (> 600 km wide) and hot Mesoproterozoic collisional orogen (Fig. 1) (Gower et al. 2008; Jamieson and Beaumont 2013; Rivers 2008, 2012). The Grenville orogeny was long lived (> 110 Myr). It propagated from a weak Proterozoic lithosphere into the cratonic Archean foreland, with thrusting along two orogen parallel, continuous, crustal-scale shear zones (the Allochthon Boundary Thrust and Grenville Front) and two main phases of orogenic convergence (the Ottawan, 1090–1020 Ma, and Rigolet, 1010–980 Ma, phases; Fig. 1). Protracted high-temperature–low-pressure high-grade metamorphism in the hinterland, associated with both crustal- and mantle-derived magmatism, was coeval with comparatively short-lived high-pressure metamorphism in thick thrust slices towards the foreland (Groulier et al. 2018a; Indares 2020; Rivers 2008). The first order architecture of the Sveconorwegian orogen and its orogenic evolution are comparable to that of the Grenville orogen (Cawood and Pisarevsky 2017; Gower 1985; Gower et al. 2008; Hoffman 1991; Rivers 2008, 2012). An analogy in the geodynamic evolution is therefore natural.

In the collisional models (Fig. 3d), closure of (one or several) oceanic basin(s) to the west of the exposed orogen was followed by the collision of Baltica (Fennoscandia) with (one or several) continental plate(s) at and after 1065 Ma (Bingen et al. 2008c; Bogdanova et al. 2008; Cawood and Pisarevsky 2017; Gower et al. 2008; Ibanez-Mejia et al. 2011; Li et al. 2008; Pisarevsky et al. 2014; Stephens and Wahlgren 2020b; Weber et al. 2010). Consumption of these oceanic basins involved subduction and formation of volcanic arcs, either at the margin of Fennoscandia or in an outboard position prior to final collision. During collision, the Sveconorwegian orogen was situated in the upper plate position, on the Fennoscandia side of the main suture zone.

Here are some key features supporting the collisional model for the main Sveconorwegian orogeny (1065–900 Ma): (i) The Sveconorwegian orogen is c. 550 km wide, i.e. wider than any present-day Andean orogen. It exhibits a c. 550 km wide zone of convergent tectonics (1065–930 Ma) and a c. 350 km wide zone of syn-orogenic magmatism (Fig. 5). (ii) The orogen has the structure of an extended (collapsed) orogenic plateau, with the juxtaposition of high-grade gneiss complexes representing a middle crustal infrastructure, against low-grade supracrustal rocks representing a brittle superstructure, and plutons representing the product of lower- to middle-crustal melting during orogeny (Fig. 4) (Andersen et al. 2001; Granseth et al. 2020; Vander Auwera et al. 2011). The gneiss complexes carry evidence for protracted (> 110 Myr) middle-crustal high-temperature-low-pressure metamorphism (Bingen et al. 2008b; Blereau et al. 2017; Laurent et al. 2018a; Laurent et al. 2018b; Slagstad et al. 2018). (iii) High pressure granulite- and eclogite-facies rocks attest to crustal thickening, up to c. 70 km, between c. 1050 and 990 Ma (Möller and Andersson 2018; Söderlund et al. 2008a). After peak metamorphism, these rocks were incorporated and overprinted into the middle-crustal infrastructure. They were probably more abundant in the orogen than what is apparent from their exposure. (iv) The orogenic zone grew towards the foreland, in a stepwise fashion with time. This process involved thrusting along crustal scale shear zones (Mylonite Zone and Sveconorwegian front). This pattern is typical of collision orogens (Royden et al. 2008). (v) The orogenic zone lacks evidence for syn-orogenic marine sedimentary sequences, in spite of a largely exposed superstructure (Fig. 4), and therefore was above sea-level during the entire orogeny.

5.6. Conjugate margins in Rodinia

In classical Rodinia assembly models, Laurentia and Baltica were probably already contiguous at low latitudes at c. 1260 Ma as part of Nuna (Columbia), facing an ocean, the Mirovoio ocean (Buchan et al. 2000; Evans and Mitchell 2011; Pisarevsky et al. 2014; Zhang et al. 2012). Opening of the Asgard sea (north of Baltica; Fig. 1), clockwise rotation and drift of Baltica relative to Laurentia, and consumption of the Mirovoio ocean (south of Baltica) led to collision of Amazonia with Laurentia and Baltica, involving three sequential tectonic phases (Bogdanova et al. 2008; Cawood and Pisarevsky 2017; Gower et al. 2008; Hynes and Rivers 2010; Ibanez-Mejia et al. 2011; Li et al. 2008; Pisarevsky et al. 2014; Roberts 2013; Tohver et al. 2004a; Weber et al. 2010). (i) Collision between Amazonia and the southwestern part of Laurentia starting at c. 1200 Ma and generating the Llano section of the Grenville orogen and the Sunsás orogen (Fig. 1). (ii) Sinistral transpression between Amazonia and Laurentia, between c. 1150 and 1050 Ma, generating the Grenville orogen. (iii) Collision between Amazonia and Baltica at c. 1060 Ma, following closure of the intervening

oceans, producing the Sveconorwegian and Putumayo orogens (Fig. 1) (Boger et al. 2005; Ibanez-Mejia et al. 2011; Tohver et al. 2004b; Tohver et al. 2005).

Following Cawood et al. (2010), a subduction system was initiated along the northern open margin of Rodinia (Asgard sea; Fig. 1) after the Amazonia–Laurentia–Baltica collision (i.e. after 1000 Ma). In this model, Tonian sediments sequences and volcanic and plutonic rocks hosted in variably far-travelled nappes of the Caledonides of NE Greenland, Scandinavia, Svalbard and Scotland (Augland et al. 2014; Cawood and Pisarevsky 2017; Cawood et al. 2015; Corfu 2019; Cutts et al. 2009; Kalsbeek et al. 2000; Kirkland et al. 2006, 2007) are interpreted as fragments of an accretionary orogen, the Valhalla orogen, at the margin of Rodinia (Fig. 1). An orogenic phase, including magmatism, metamorphism, and deformation (Renlandian) took place between 980 and 910 Ma (Cawood et al. 2010), therefore overlapping with metamorphism in the Sveconorwegian orogen (Table 1).

Several Mesoproterozoic basement inliers in the Andes of Colombia (Garzón, Las Minas) and in Mexico (Oaxaquia lithotectonic unit) are characterized by high-grade metamorphism, dated consistently between 1000 and 980 Ma (Zapotecan-Putumayo orogenies). These lithotectonic units are interpreted as oceanic volcanic arcs formed in the ocean realm between Laurentia, Amazonia and Baltica (after c. 1460 Ma) (Fig. 12 a, b) and involved in the collision zone between these plates (Fig. 1) (Cardona et al. 2010; Cordani et al. 2005; Ibanez-Mejia et al. 2015; Ibanez-Mejia et al. 2011; Jiménez-Mejía et al. 2006; Keppie et al. 2003; Keppie and Ortega-Gutiérrez 2010; Weber and Köhler 1999; Weber et al. 2010).

In archetypal Rodinia reconstructions (Fig. 1), the hinterland of the Sveconorwegian orogen is facing Mesoproterozoic basement inliers in the Andes of Colombia (Garzón, Las Minas) and in Mexico (Oaxaquia lithotectonic unit) and the hinterland of the Grenville orogen. The isotopic signature of these units is compared in a εNd vs. time diagram (Fig. 13b). The Quebecia and Telemarkia lithotectonic units, located in the hinterland of the exposed Grenville and Sveconorwegian orogens respectively, represent coeval continental growth zones generated by volcanic arc and back arc magmatism between c. 1520 and 1480 Ma (Pinwarian and Telemarkian orogenies; Table 1; Fig. 13b) (Dickin and Higgins 1992; Groulier et al. 2018b). These units are characterized by very similar isotopic evolution trends starting from close to the Depleted Mantle reservoir at and after 1520 Ma and decreasing along a continental recycling trend to near-chondritic value at c. 1000 Ma. The basement inliers in the Andes of Colombia (Garzón, Las Minas) and in Mexico (Oaxaquia lithotectonic unit) define evolution trends starting at c. 1380 Ma and 1300 Ma, respectively, that overlap with the Telemarkia trend (Ibanez-Mejia et al. 2015; Lawlor et al. 1999; Weber and Köhler 1999). In the hinterland of the Grenville Belt, the Composite Arc and Frontenac–Adirondack lithotectonic units define the most juvenile trend, starting at c. 1380 Ma (Fig. 13b) (Daly and McLelland 1991; Dickin et al. 2010; Marcantonio et al. 1990). These units are interpreted as marginal or outboard volcanic arcs, back-arcs and microcontinents assembled (or reassembled) to Laurentia before the Grenvillian orogeny (Shawinigan orogeny, 1190–1140 Ma) (Carr et al. 2000; Hanmer et al. 2000; Rivers 2008). Interestingly, the 1280-1200 Ma magmatism in the Composite Arc (Elzevirian orogeny) has a Nd isotopic signature approaching that of the Depleted Mantle reservoir (Carr et al. 2000; Corfu and Easton 1995; Corriveau and van Breemen 2000; Dickin and McNutt 2007), very similar to the one of coeval 1280–1200 Ma continental magmatism in the Sveconorwegian orogen (Sæsvatn–Valldal bimodal volcanism) (Brewer et al. 2004).

In the $^{206}Pb/^{204}Pb$ vs. $^{207}Pb/^{204}Pb$ diagram (Fig. 16), the initial isotopic composition of Sveconorwegian plutonic rocks intruded between 1150 and 930 Ma defines a short trend below the evolution curve of terrestrial common Pb of Stacey and Kramers (1975) ($\mu_{(2)} = 9.74$). Ortho- and paragneisses from the hinterland of the Grenville Belt, including the

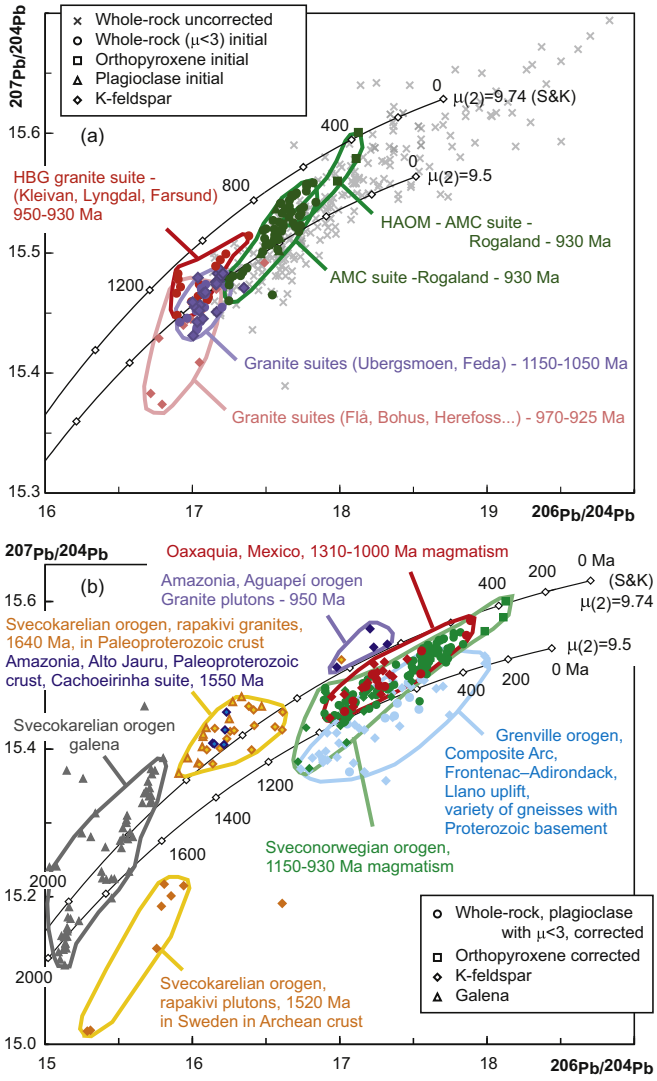

Fig. 16. Common Pb isotopic composition in the $^{206}Pb/^{204}Pb$ vs. $^{207}Pb/^{204}Pb$ diagram, with reference growth curves of terrestrial common Pb ($\mu_{(2)} = 9.74$ (Stacey and Kramers 1975) and $\mu_{(2)} = 9.5$, with $\mu = {}^{238}U/^{204}Pb$). (a) Compilation of data from the Sveconorwegian orogen. Highlighted symbols represent initial ratio of plutonic suites dated between 1150 and 930 Ma. Initial ratio (ratio corrected for U decay since intrusion) is calculated for analyses of K-feldspar, plagioclase, orthopyroxene and whole-rock with $\mu < 3$. The initial ratio of plutonic rocks defines a short trend below the reference growth curve of Stacey and Kramers (1975). High alumina orthopyroxene megacrysts (HAOM) hosted in the anorthosite plutons are situated at the radiogenic (upper-right) end of the trend. They are interpreted to represent a mafic, mantle-derived, underplate, formed at c. 1040 Ma and remelted at c. 930 Ma. The granite plutons partly sourced from metasedimentary protoliths, like the Flå and Bohus muscovite-bearing plutons, are situated at the less radiogenic (lower-left) end of the trend. The hornblende-biotite granite plutons, ranging from c. 1150 to 930 Ma, sourced from metaigneous protoliths, cluster in the centre of the trend (Andersen 1997; Andersen et al. 2001; Andersen et al. 1994; Andersen and Munz 1995; Bingen et al. 1993; Vander Auwera et al. 2014a; Weis 1986). (b) Compilation of initial isotopic compositions for Baltica (Fennoscandia) and selected late-Mesoproterozoic orogenic belts. Data for the Sveconorwegian orogen are copied from panel (a). A variety of ortho- and paragneisses from the hinterland of the Grenville orogen, including the Composite Arc (Ontario), Frontenac-Adirondack (Ontario) and Llano uplift (Texas) overlap with the data of the Sveconorwegian orogen, as well as orthogneisses from the Oaxaquia lithotectonic unit (Mexico) (Cameron et al. 2004; DeWolf and Mezger 1994). Granite plutons (950 Ma) in the Aguapei Belt in Amazonia are characterized by a more radiogenic ^{207}Pb signature than coeval rocks in the Sveconorwegian orogen, consistent with involvement of an older Paleoproterozoic basement in this orogen (Geraldes et al. 2001). Data for rapakivi granite plutons from Fennoscandia on Paleoproterozoic and Archean basement, as well as Paleoproterozoic galena deposits from the Svecokarelian orogen are shown for reference (Andersson et al. 2002b; Rämö 1991; Vaasjoki 1981).

Composite Arc (Ontario), Frontenac-Adirondack (Ontario) and Llano uplift (Texas) and orthogneisses from the Oaxaquia lithotectonic unit (Mexico) overlap with the data of the Sveconorwegian orogen (Cameron et al. 2004; DeWolf and Mezger 1994).

To summarize, Nd and Pb isotopic data (Figs. 13; 16) and detrital zircon data (Fig. 12) underscore the existence of juvenile lithotectonic units generated at and after c. 1520 Ma exposed in the hinterland of the Grenville and Sveconorwegian orogens and the basement inliers in the Andes of Colombia (Garzón, Las Minas) and in Mexico (Oaxaquia lithotectonic unit). These isotopic data therefore support to join these lithotectonic units in the core of the collision zone between Laurentia, Amazonia and Baltica, in a classical Rodinia reconstruction (Fig. 1). These data also suggest that, in the collision model of Fig. 3d, the continental margin colliding with the Sveconorwegian orogen possessed a weak lithosphere similar to the one of the Telemarkia lithotectonic unit (as opposed to a stronger cratonic lithosphere).

6. Model of large, hot and long-duration continental collision

The previous discussion argues for a collisional model for the main Sveconorwegian orogeny. Here, we further develop a model of large, hot and long-duration continent-continent collision starting at c. 1065 Ma, wherein the five lithotectonic units of the orogen are endemic to Fennoscandia (Fig. 3d). The plate tectonic interpretation of the pre-collision evolution between 1280 and 1080 Ma is still largely speculative. The model is fitted into a classical Rodinia assembly framework (Fig. 1), involving an Amazonia-Laurentia-Baltica collision, as discussed previously. However, the model is based upon evidence from within the exposed Sveconorwegian orogen (and its foreland) and therefore independent of Rodinia models.

6.1. 1280–1080 Ma, pre-collision: lithospheric mantle delamination

The geological record for the pre- to early-Sveconorwegian 1280-1080 Ma time interval is very distinct in the Telemarkia, Kongsberg–Bamble and Idefjorden lithotectonic units. Abundant bimodal magmatism between 1280 and 1145 Ma, and protracted (upper) crustal extension in Telemarkia between 1280 and 1080 Ma (Figs. 17; 18) contrast with amphibolite- to granulite-facies metamorphism and shortening in the Kongsberg–Bamble lithotectonic units between 1150 and 1120 Ma (Fig. 18). Except for a few dolerite dykes, the Idefjorden lithotectonic unit is lacking evidence for magmatism,

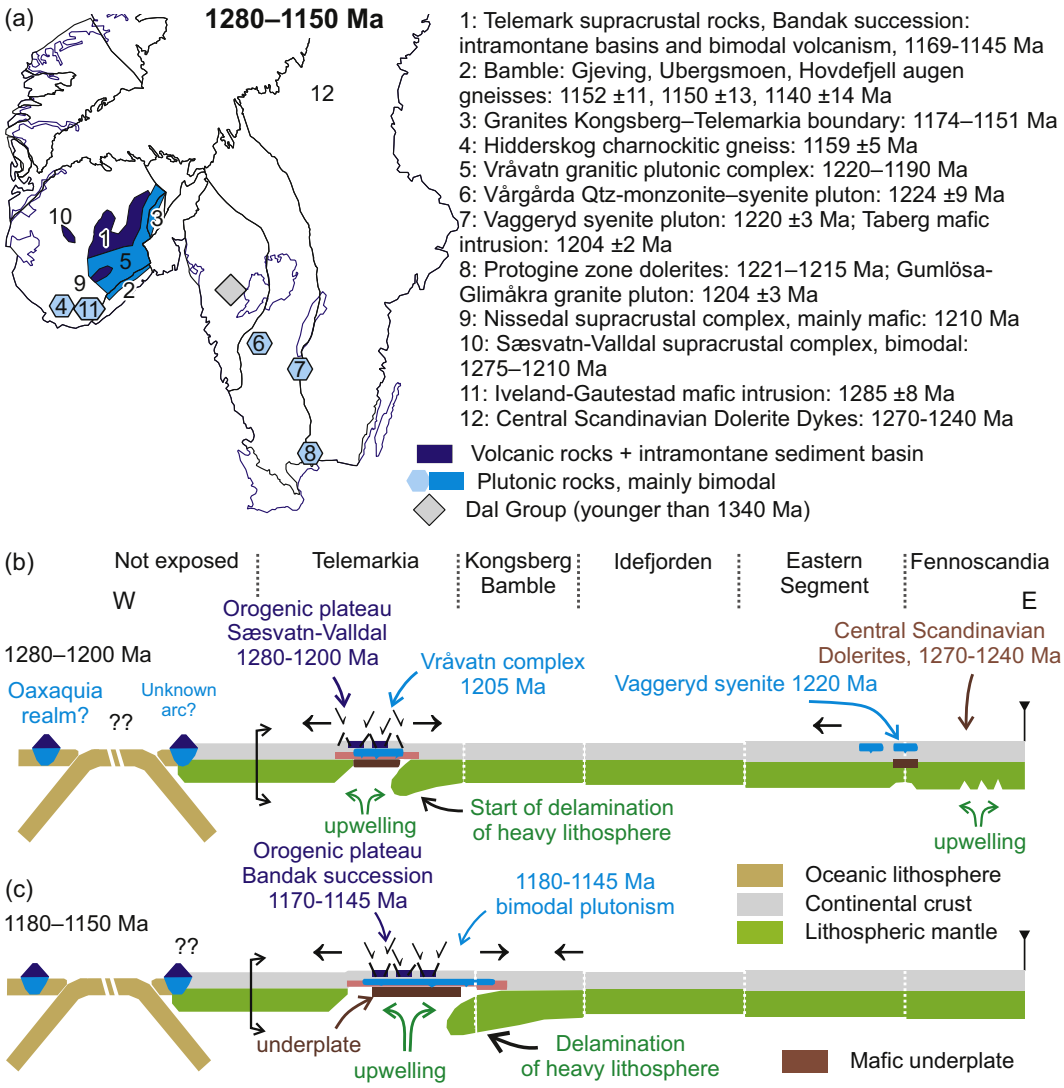

Fig. 17. Schematic geodynamic model for the 1280–1150 Ma time interval. (a) Sketch map of the Sveconorwegian orogen, with position and list of plutonic and supracrustal complexes. (b, c) Interpretative E-W cross sections of the Sveconorwegian orogen and speculative linkage westwards. The exposed part of the orogen is limited by an arrowed bracket. The limit between lithotectonic units is schematically represented by a white vertical dashed line. References and explanations in the text.

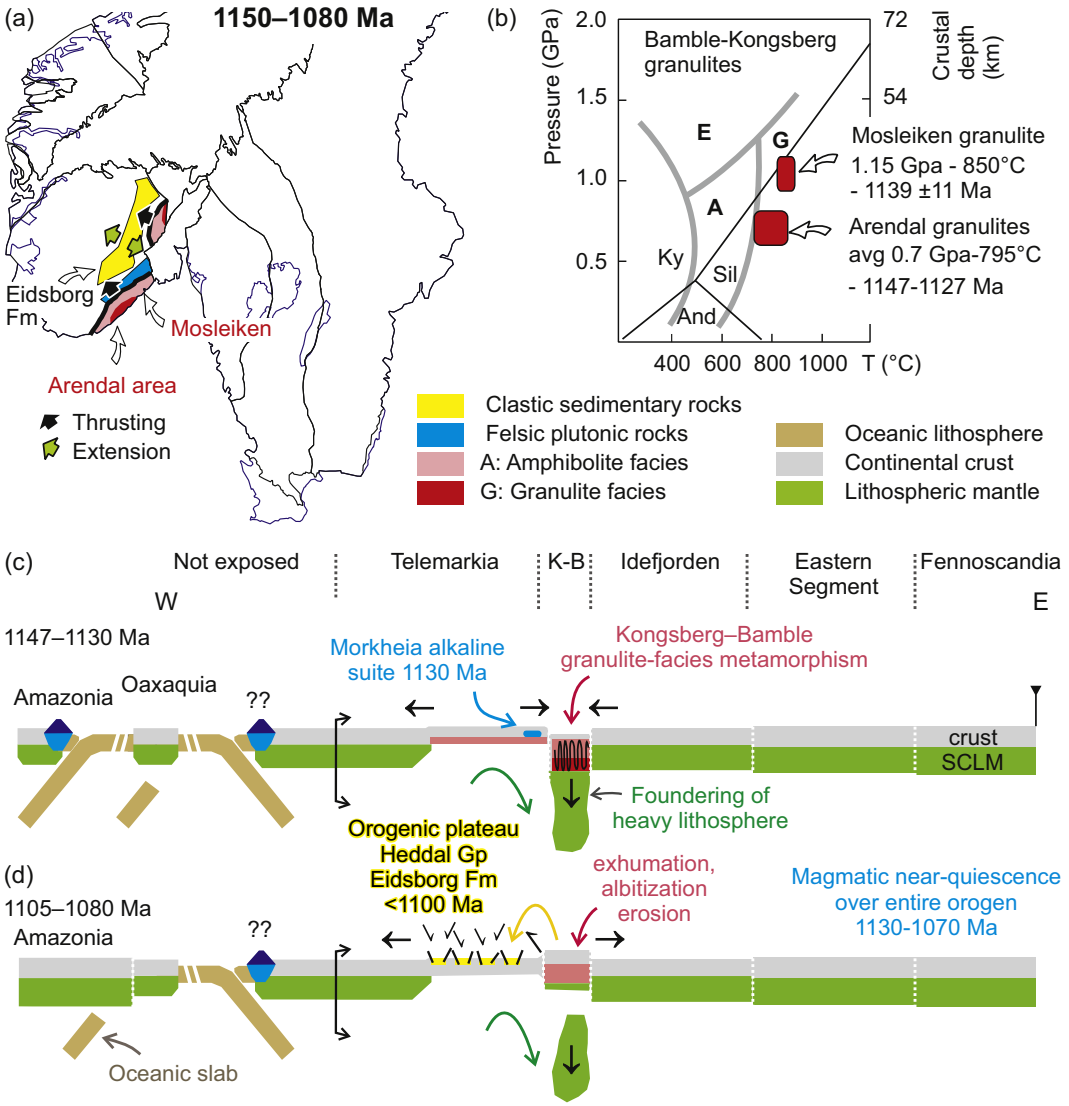

Fig. 18. Schematic geodynamic model for the 1150–1080 Ma time interval. (a) Sketch map of the Sveconorwegian orogen, with distribution of metamorphism, magmatism and clastic sediment basins. (b) Pressure-temperature diagram for metamorphism with fields of the main metamorphic facies following Spear (1993): E: eclogite facies, G: granulite facies, A: amphibolite facies. (c, d) Interpretative E-W cross sections of the Sveconorwegian orogen and speculative linkage westwards.

metamorphism and deformation between 1280 and 1080 Ma, and therefore it is regarded as having played the role of a passive buttress during this time interval. There is no evidence for closure of marine or oceanic basins between the Telemarkia, Kongsberg–Bamble and Idefjorden lithotectonic units (Scheiber et al. 2015). These different features cannot be explained by a simple model of regional scale inversion from extension to compression at c. 1150 Ma, as one would anticipate contraction structures to be located in the weakest Telemarkia lithosphere, or distributed evenly throughout the Telemarkia, Bamble and Kongsberg lithotectonic units.

In Fig. 17, we propose that upwelling of asthenosphere and development of an orogenic plateau started at c. 1280 Ma in the Telemarkia lithotectonic unit. Repeated pulses of bimodal magmatism between 1280 and 1145 Ma provide evidence for upwelling and decompression melting of asthenospheric mantle (Fig. 7). The most prominent mafic volcanic rocks (Fig. 11; Sæsvatn–Valldal, Nissedal, Morgedal and Gjuve metabasalts) exhibit a within-plate geochemical signature and suprachondritic Nd isotopic signature ($+2.6 < \varepsilon_{Nd} < +6.3$) implying sourcing in the asthenosphere (Fig. 13a) (Brewer et al. 2002; Brewer et al. 2004; Spencer et al. 2014). The voluminous felsic gneisses of the Vråvatn Complex (1220–1190 Ma) have Hf isotopic signature of zircon ($+9 < \varepsilon_{Hf} < +10$) also close to the depleted mantle reservoir at 1210 Ma ($\varepsilon_{Hf} = +12$) (Fig. 8) (Andersen et al. 2007). These values indicate that the Vråvatn complex was not produced principally by partial melting of the Telemarkian (1520–1480 Ma) crust. Rather, it was probably produced by partial melting of a mafic lower crust or mafic underplate, itself produced shortly before in the depleted mantle (a maximum of some 50 Mys before 1210 Ma; Andersen et al. 2007). The earliest magmatism between 1280 and 1190 Ma occurred in the centre of the Telemarkia lithotectonic unit (Vråvatn, Nissedal, Sæsvatn–Valldal, Iveland-Gautestdad complexes; Figs. 6; 17) while younger magmatism between 1170 and 1140 Ma is more abundant towards the periphery of the lithotectonic unit (mainly eastwards and southwards) and is well recorded into the Kongsberg and Bamble lithotectonic units. This geographic distribution suggests that mantle upwelling affected progressively a larger area between c. 1280 and 1145 Ma (Fig. 17).

Upwelling of hot asthenosphere at c. 1280 Ma induced partial melting at the base of the crust. This weakening of the lower crust possibly initiated decoupling between the crust and the lithospheric mantle and progressive delamination of the lithospheric mantle between c.

1280 and 1145 Ma. Alternatively, protracted upwelling of asthenosphere between 1280 and 1145 Ma progressively induced convective removal (or displacement) of the continental lithospheric mantle. Both interpretations resulted in uplift, formation of a plateau and extension in the crust (Dewey 1988; Li et al. 2016).

Evidence for an orogenic plateau involving uplift and extension in the upper crust is provided by the sedimentology of low-grade sedimentary rocks deposited between 1260 and 1080 Ma in Telemarkia. The sediments of the Bandak succession are high-energy immature deposits, accumulated in continental (above sea level) intermontane basins (Bingen et al. 2003; Köykkä 2011; Lamminen 2011; Spencer et al. 2014). The limited lateral extent of the basin infills, the existence of at least two major internal unconformities in the Bandak succession, and the direct evidence for normal syn-sedimentary growth faults, suggest active extension during accumulation (Figs. 11; 12) (Laajoki 2002; Laajoki et al. 2002; Lamminen 2011). This orogenic plateau does not satisfy to the definition of a Tibetan orogenic plateau, as evidence for crustal thickening and protracted metamorphism is lacking in the 1280–1080 Ma time interval inside the Telemarkia lithotectonic unit.

Compression in the Kongsberg–Bamble lithotectonic units in the interval between 1150 and 1120 Ma can be explained by compression at the margin of the plateau and foundering (subduction) below the Kongsberg–Bamble lithotectonic units of the lithospheric mantle slab delaminated below Telemarkia (Fig. 18). We suggest that the pull effect of foundering generated subsidence in the crust, high-grade metamorphism (up to 1.15 GPa) and deformation with lithological banding and commonly steep lineation in Kongsberg–Bamble between 1150 and 1120 Ma.

Eventual break-off of the mantle slab triggered exhumation of the Bamble and Kongsberg lithotectonic units after 1120 Ma (Fig. 18d). The volumetrically minor alkaline Morkheia monzonite suite, located just north of the Bamble–Telemarkia boundary zone, may record this event with local melting of a sliver of lithospheric mantle at c. 1134–1130 Ma (Fig. 18c) (Heaman and Smalley 1994). Exhumation to upper crustal levels (1105–1080 Ma) was associated with northwestwards thrusting of Bamble and westwards thrusting of the Kongsberg onto Telemarkia and reworking of plutons emplaced shortly before the foundering process (Henderson and Ihlen 2004; Scheiber et al. 2015). Exhumation of the Bamble and Kongsberg lithotectonic units after 1105 Ma was associated with fluid-rock interaction, albitization and scapolitization (Engvik et al. 2017). Erosion provided the clastic material stored in the Heddal Group and Eidsborg Formation in Telemarkia (Figs. 6; 11; 12; 18).

The plate tectonic configuration and paleogeographic setting of this pre- to early-Sveconorwegian asthenosphere upwelling, orogenic plateau development and sub-continental lithospheric mantle delamination model is difficult to assess. The asthenosphere upwelling could be related to a deep mantle plume, similar to the ones that generated the four mafic dyke swarms of the Central Scandinavian dolerites in the cratonic center of Fennoscandia between c. 1271 and 1246 Ma (Brander et al. 2011; Söderlund et al. 2006), and dolerites along the Sveconorwegian front (Protogine zone dolerites) between 1221 and 1215 Ma (Söderlund et al. 2005) (Fig. 17). Alternatively, in recent paleogeographic models (Cawood and Pisarevsky 2017), the Sveconorwegian orogen (Telemarkia–Bamble–Kongsberg lithotectonic units) is located in a continent back-arc position on the Fennoscandia side of an active volcanic arc, in the 1280–1080 Ma interval, during consumption of the oceans between Baltica, Amazonia and Laurentia (Figs. 17; 18) (Bingen et al. 2003; Brewer et al. 2002; Roberts and Slagstad 2015; Slagstad et al. 2017; Spencer et al. 2014). This arc would be located to the west of the exposed orogenic belt and possibly disappeared by tectonic erosion (Spencer et al. 2014). A Cenozoic analogue to this Mesoproterozoic evolution would be plateau building and lithospheric delamination in the Colorado Plateau and the North American Cordillera (Bao et al. 2014; Levander et al. 2011).

6.2. 1065–1000 Ma: main Sveconorwegian continental collision

After a period of quiescence, the orogenic zone widened substantially around 1065 Ma, both eastwards (continentwards) and westwards, to include the entire Idefjorden and Telemarkia lithotectonic units (Figs. 19; 20). Widespread contractional deformation, high-grade metamorphism, partial melting and magmatism are recorded in these units between 1065 and 1000 Ma (Agder phase). Little is recorded in the Kongsberg–Bamble lithotectonic units, which were exhumed to high crustal levels (superstructure) and juxtaposed as reflected by their current position before 1080 Ma. High-pressure granulite facies metamorphism in the Idefjorden lithotectonic unit, dated to c. 1050 Ma, contrasts with the voluminous granite magmatism of the Sirdal magmatic belt (1065–1020 Ma) and low-pressure granulite-facies metamorphism (1045–990 Ma) culminating at UHT conditions (1030–1005 Ma) in the west of the Telemarkia lithotectonic unit (Figs. 5; 19; 20). The width of the orogenic zone (minimum of 460 km), the large volume of magmatism with syn- to late-collision geochemical signature (Sirdal magmatic belt), the paired belts of high-pressure (towards the foreland) vs. high-temperature (towards the hinterland) metamorphism, and the structural evidence for contraction suggests that the Sveconorwegian orogeny entered the main phase of continent-continent collision around 1065 Ma.

In Fig. 19, we propose that collision resulted in the formation of a Tibetan-style orogenic plateau (Jamieson and Beaumont 2013) extending from the Telemarkia to the Idefjorden lithotectonic units. The infrastructure of this orogenic plateau is defined by widespread gneiss complexes characterized by partial melting, contractional ductile deformation and amphibolite- to granulite-facies metamorphism between 1050 and 1000 Ma. Evidence from the superstructure of this plateau is scanty, simply because little upper crustal rocks younger than 1050 Ma are preserved. The N–S trending Kalhovd Formation consists of unconformable conglomerate and immature sandstone, deposited after c. 1054 Ma, in a continental (above sea level) intermontane basin (Figs. 5; 11; 19; 20). This basin was downfaulted along the Mandal-Ustaoset fault zone, possibly during deposition, recording extension after c. 1054 Ma in the upper crust in the centre of the Telemarkia lithotectonic unit.

The dynamics of the mantle in the collision zone would be simulated by a “pro-plate” (upper-plate) Tibetan-style delamination numerical models by Li et al. (2016). In Fig. 19, we propose that mantle upwelling under the Telemarkia lithotectonic unit was counterbalanced by mantle downwelling and lithospheric mantle delamination and foundering under the Idefjorden lithotectonic unit. In the Idefjorden lithotectonic unit, the crust was pulled down by a lithospheric mantle slab to reach peak high-pressure low-temperature granulite facies conditions (c. 1.2–1.5 GPa, 740–780 °C) between c. 1052 and 1046 Ma (Fig. 19) (Bingen et al. 2008b; Söderlund et al. 2008a). The crust in the Idefjorden lithotectonic unit was not affected by orogenic processes before 1050 Ma and therefore could reach high-pressure conditions before melting. Decoupling between the mantle slab and the crust (breakoff) probably took place when partial melting reactions were activated in the lower crust. During exhumation, widespread migmatitization (including muscovite-, biotite- and amphibole-dehydration melting) is observed at regional scale between c. 1040 and 1000 Ma in the Idefjorden lithotectonic unit (Figs. 10; 20; Table 2). Migmatitization took place in convergent setting; east of the Oslo rift, it is associated with a well-defined top-to-west direction of transport (Viola et al. 2011). Lamprophyre dykes, close to the boundary between the Kongsberg and Idefjorden lithotectonic units, attests to local melting of lithospheric mantle material at c. 1030 Ma (Bingen and Viola 2018), and is consistent with a model of foundering of the lithospheric mantle around 1030 Ma.

In the Telemarkia lithotectonic unit (Agder area), the NNW-SSE trending Sirdal magmatic belt attests to voluminous crustal melting between c. 1065 and 1020 Ma (Figs. 5; 19) (Bingen et al. 2015; Coint et al.

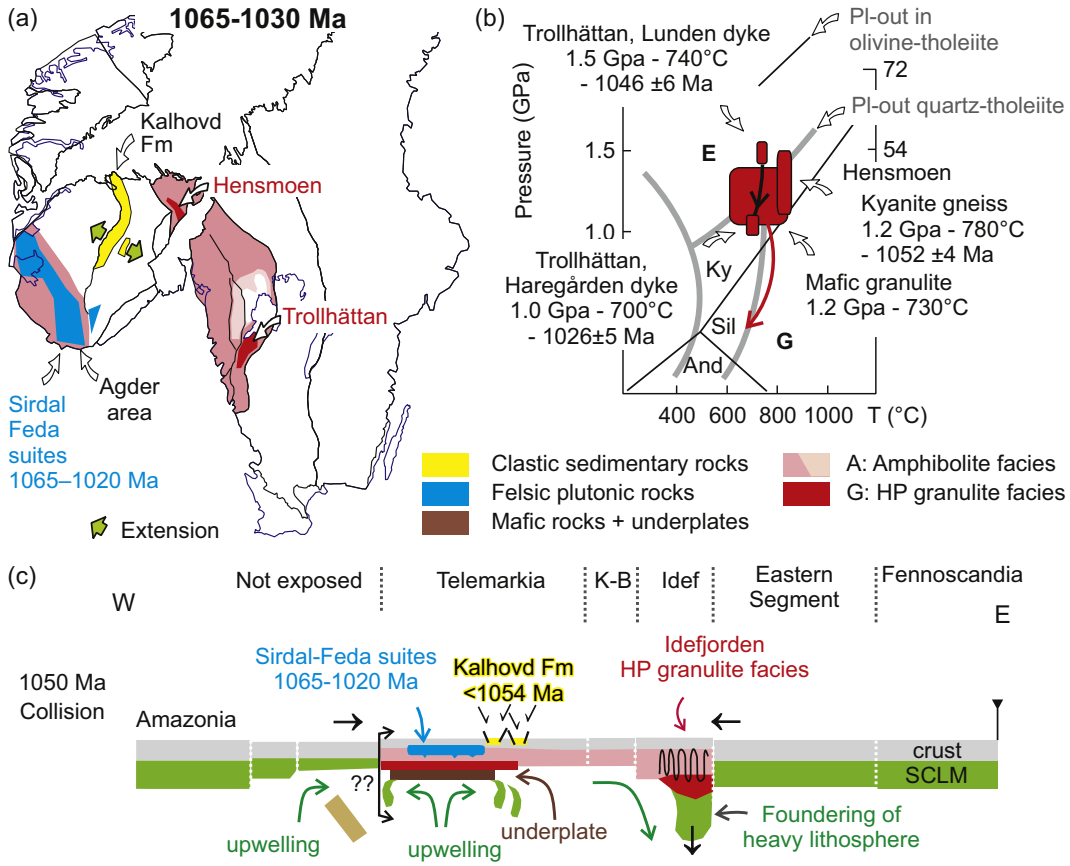

Fig. 19. Schematic geodynamic model for the 1065–1030 Ma time interval. (a) Sketch map of the Sveconorwegian orogen, with distribution of metamorphism, magmatism and clastic sediment basins. (b) Pressure-temperature diagram. (c) Interpretative E-W cross section.

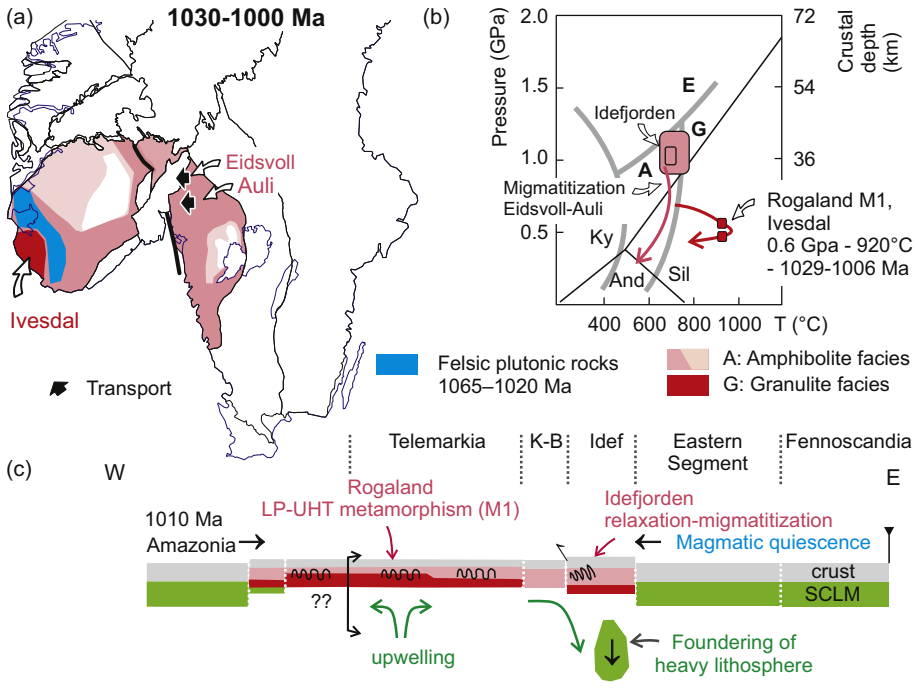

Fig. 20. Schematic geodynamic model for the 1030–1000 Ma interval. (a) Sketch map of the Sveconorwegian orogen, with distribution of metamorphism and magmatism. (b) Pressure-temperature diagram. (c) Interpretative E-W cross section.

2015; Granseth et al. 2020; Slagstad et al. 2013). As discussed earlier, it contains high-K calc-alkaline quartz-monzonite–granodiorite plutons associated with minor ultrapotassic rocks (Figs. 7; 15) (Bingen et al. 1993; Bingen and van Breemen 1998a). Such calc-alkaline granitoids can be derived by partial melting of lower crustal mafic metaigneous rocks. Enrichment in K and other large ion lithophile elements (LILE) implies either that this crustal source was previously enriched in LILE or that the melts were mixed with ultrapotassic lamprophyric melts, themselves generated from lithospheric mantle previously enriched in LILE. The most straightforward interpretation is that this lithospheric mantle source was part of a mantle wedge enriched in LILE by supra-subduction fluids between 1520 and 1480 Ma. It would then become part of a subcontinental lithospheric mantle after 1480 Ma, and finally, it would melt during collision between 1065 and 1020 Ma, heated during orogeny. Two observations support this three stage model: i) the 1065–1020 Ma Sirdal magmatic belt overlaps geographically with the 1520-1480 Ma Suldal volcanic arc (Roberts et al. 2013); ii) the near-chondritic Nd isotopic signature of the Feda suite granitoids ($-1 < \varepsilon_{Nd} < +1.5$) and ultrapotassic enclaves ($+1 < \varepsilon_{Nd} < +1.5$) are lying on the evolution vector of the crust generated at 1520-1480 Ma (Fig. 13a). A similar interpretation is provided for near-coeval (1063 ± 3 Ma) high-Sr-Ba quartz-monzonite plutons in the Quebecia lithotectonic unit of the Grenville orogen (Michaud pluton hosted in the c. 1500 Ma Escumins supracrustal rocks) (Groulier et al. 2018a).

Voluminous melting of the crust clearly requires an appropriate heat source. The high-alumina orthopyroxene megacrysts (HAOM) and plagioclase megacrysts hosted in the c. 930 Ma anorthosite plutons constrain mafic magmatism at the base of the crust at 1041 ± 17 Ma coeval with formation of the Sirdal magmatic belt (Bybee et al. 2014; Slagstad et al. 2018; Vander Auwera et al., 2014b). The supra-chondritic Nd isotopic values for the megacrysts ($+2.8 < \varepsilon_{Nd(1041\ Ma)} < +5.3$) trace the source of this magmatism to the asthenosphere (Fig. 13a). Here we suggest that upwelling of hot asthenosphere in the collision zone generated asthenospheric melts, produced underplates (with HAOM), reheated and destabilized the lithospheric mantle, and generated minor lamprophyre melts (from this lithospheric mantle) (Figs. 19; 20). Heating of the crust produced granitoids of the Sirdal magmatic belt. After extraction of these melts, protracted heating in the crust resulted in a first phase of granulite-facies metamorphism (M1), reaching ultra-high temperature conditions (0.7–0.5 GPa, 900–950 °C) between c. 1030 and 1005 Ma (Fig. 20) (Blereau et al. 2017; Drüppel et al. 2013; Laurent et al. 2018b).

The HAOM hosted in the anorthosites record a pressure of crystallization of 1.1 GPa and an age of 1041 ± 17 Ma (Bybee et al. 2014; Charlier et al. 2010). These numbers imply a crustal thickness of at least 42 km around 1040 Ma, corresponding to a moderate crustal overthickening relative to the standard 30 km. The regional folding observed at various scales in the Telemarkia lithotectonic unit, also requires at least one phase of compression between 1030 and 1000 Ma.

In Figs. 17-20, the Oaxaquia lithotectonic unit and inliers in the Andes of Columbia, which contain evidence of high-grade metamorphism between 1050 and 980 Ma, are represented speculatively as volcanic arcs in the ocean between, Amazonia Laurentia and Baltica (Figs. 8, 12, 13, 16). They were first accreted to Amazonia (Putumayo) before colliding with Baltica around 1050 Ma (Figs. 19; 20) (Ibanez-Mejia et al. 2011; Lawlor et al. 1999; Weber et al. 2010). In this framework, the Telemarkia–Kongsberg–Bamble units are indeed situated in a back-arc domain, in the time interval between 1280 and 1080 Ma, before closure of all oceans, and they ended-up in upper plate position at c. 1065 Ma during collision with Amazonia (Figs. 18-20). Upwelling of hot asthenosphere in the collision zone was possibly promoted by break-off all oceanic lithospheric plates to the west of the orogen when subductions ceased (Fig. 19).

6.3. 1000–920 Ma: long-duration collision

At c. 1000 Ma, orogeny propagated to the east, all the way into the Eastern Segment. Continued high-temperature low-pressure metamorphism in the west of the collision zone and voluminous magmatism contrast with high pressure metamorphism in the east, suggesting that the western part was characterized by protracted mantle upwelling while the eastern part by underthrusting and mantle downwelling. In Figs. 21-23, we propose that the Tibetan-style orogenic plateau widened towards the foreland to includes the Eastern Segment and covered the entire orogen. The Eastern Segment offers a nice example of how crust underthrust to high-pressure conditions is incorporated into a melt-lubricated middle-crustal infrastructure of an orogenic plateau. We suggest that the orogenic plateau was sustained to c. 930 Ma before it collapsed.

6.3.1. Eastward widening of the orogenic plateau

The Eastern Segment was a cold lithospheric segment of Fennoscandia foreland affinity, unaffected by Sveconorwegian orogenic processes before 1000 Ma. At this point in time, it was underthrust as a slab towards the west beneath the Mylonite Zone during convergence (Fig. 21) (Möller and Andersson 2018; Möller et al. 2015). The deepest underthrust western part of the slab reached eclogite-facies conditions corresponding to a depth of c. 70 km (1.65–1.9 GPa, 850–900 °C) at c. 990 Ma (Figs. 5; 21b), while the adjacent part of the slab (now the internal section) reached high-pressure granulite-facies conditions (1.1 GPa, 850 °C; Fig. 21b) (Möller et al. 2015; Piñán-Llamas et al. 2015; Tual et al. 2017). Preservation of prograde zoning in garnet in eclogites attests to faster-than-equilibration prograde metamorphism (Möller 1998; Tual et al. 2017). In Fig. 21, we propose that this underthrust crustal slab was pulled down by foundering of the dense subcontinental lithospheric mantle. Breakoff of the lithospheric mantle slab triggered exhumation after c. 980 Ma and widening of the orogenic plateau towards the east (Fig. 22). Exhumation took place in two steps (Fig. 22): (i) During the first step, the eclogitized westernmost part of the Eastern Segment was detached from the deepest part of the segment and exhumed with an overall eastward vergence, as a single and coherent (eclogite-bearing) ductile nappe to an intermediate depth of c. 35–40 km (1.1 GPa), where it was juxtaposed to the granulite-facies internal section. This process is interpreted as eastwards extrusion during overall E-W convergence (Möller and Andersson 2018; Möller et al. 2015; Piñán-Llamas et al. 2015; Tual et al. 2015). (ii) During the second step, the eclogite-bearing nappe and the granulite-facies internal section were exhumed together, also with an overall eastwards vergence. Accurate geochronology of these two steps remains difficult to establish. Breakoff of the lithospheric mantle slab was probably facilitated by partial melting in the crust. East vergent exhumation was clearly lubricated by abundant partial melting. The crystallization of these leucosome melts is dated between c. 978 and 961 Ma inside the eclogite-bearing nappe (Andersson et al. 2002a; Möller et al. 2015) and between c. 976 and 965 Ma, i.e. in a coeval time interval, in the granulite-facies internal section (Andersson et al. 2002a; Hansen et al. 2015; Möller et al. 2007; Piñán-Llamas et al. 2015; Söderlund et al. 2002).

The Blekinge-Dalarna dolerite dyke swarm intruded in the upper crust in the foreland of the orogen between c. 978 and 946 Ma (Gong et al. 2018; Ripa and Stephens 2020d; Söderlund et al. 2005). This mafic magmatism is characterized by a within-plate geochemical signature and supra-chondritic Hf isotopic signature ($+1 < \varepsilon_{Hf} < +5$). It is evidence for asthenosphere upwelling and decompression melting under the cratonic lithosphere of the foreland (Gong et al. 2018; Ripa and Stephens 2020d; Söderlund et al. 2005). The upwelling may represent a dynamic response in the asthenosphere of the breakoff and foundering of the lithospheric mantle slab under the Eastern Segment at and after c. 980 Ma (Fig. 22).

Eastwards thrusting in the frontal wedge and along the Sveconorwegian front represents a final spasm of the orogeny. Both

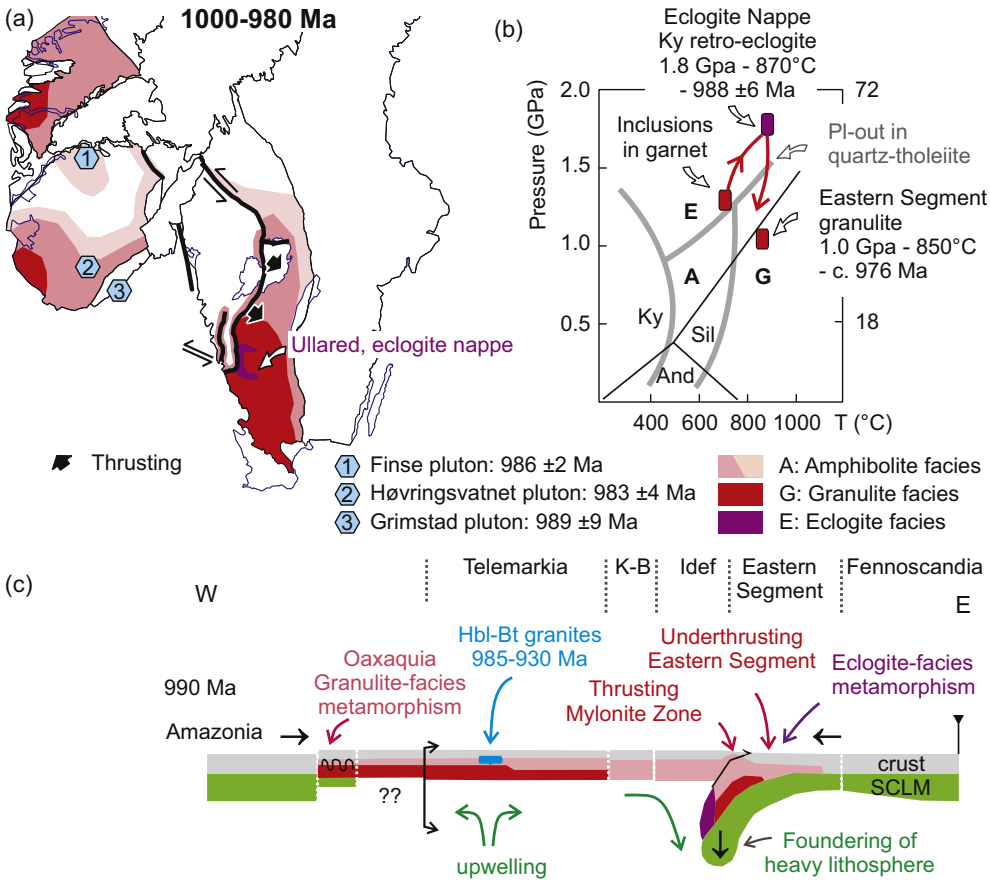

Fig. 21. Schematic geodynamic model for the 1000–980 Ma time interval. (a) Sketch map of the Sveconorwegian orogen, with distribution of metamorphism and magmatism. (b) Pressure-temperature diagram. (c) Interpretative E-W cross section.

$^{40}Ar/^{39}Ar$ data and the observation that Blekinge-Dalarna dolerite dykes are sheared in the frontal wedge suggest that it took place after c. 945 Ma (Andréasson and Dallmeyer 1995; Page et al. 1996a; Stephens and Wahlgren 2020a; Ulmius et al. 2018).

6.3.2. Sustained orogenic plateau west of the Mylonite Zone

Little tectonic activity or metamorphism is dated in the central part of the orogen (western part of the Idefjorden lithotectonic unit, Kongsberg and Bamble lithotectonic units and eastern part of the Telemarkia lithotectonic unit) between c. 980 and 930 Ma, suggesting that this part of the orogen behaved passively during this time interval. In the west, in the orthopyroxene zone of Rogaland, a scatter of zircon rim U–Pb ages between 1045 and 955 Ma is interpreted as evidence for protracted high-grade metamorphism with melt-present conditions in the middle crust (0.45–0.55 GPa) (Fig. 22) (Blereau et al. 2017; Laurent et al. 2018a; Slagstad et al. 2018). In Fig. 22, we propose that the orogenic plateau formed between 1050 and 1000 Ma west of the Mylonite Zone was sustained throughout the orogeny to c. 930 Ma.

6.3.3. Late-Sveconorwegian magmatism and associated metamorphism

The volume of late-Sveconorwegian magmatism increases dramatically westwards in the orogen (Figs. 5; 7; 22; 23). In the Eastern Segment, minor pegmatite and granite bodies formed between c. 961 and 935 Ma during regional cooling (Möller et al. 2007; Söderlund et al. 2008b). In the Idefjorden lithotectonic unit, the large biotite + muscovite-bearing Flå and Bohus granite plutons (c. 932–922 Ma) (Eliasson et al. 2003; Eliasson and Schöberg 1991; Lamminen et al. 2011) carry a distinctly peraluminous signature (S-type) and sub-chondritic epsilon Nd values ($-8.4 < \varepsilon_{Ndi} < -2.7$) (Andersen et al. 2001). These properties imply a metasedimentary source, most probably in the hosting Stora Le-Marstrand complex ($-8.0 < \varepsilon_{Nd930} < -3.0$) (Åhäll and Daly 1989). In the Telemarkia lithotectonic unit, large plutons of the HBG granite suite emplaced between c. 985 and 926 Ma (Figs. 22; 23). There is a significant spread in geochemical and isotopic composition, reflecting a diversity of sources and petrogenesis (Andersen et al. 2001; Granseth et al. 2020; Vander Auwera et al. 2011). The HBG suite is characterized by a distinctly ferroan geochemical signature (Fig. 14). Experimental petrology and geochemical modelling of the representative Lyngdal pluton in Vest Agder (Bogaerts et al. 2006; Vander Auwera et al. 2008), suggest that this granodiorite crystallized at shallow conditions corresponding to pressures between 0.2 and 0.4 GPa from a wet (5–6 wt% H_2O), oxydized (QFM +1) and hot (c. 975 °C) magma. This magma can be generated by partial melting of an amphibole-rich mafic source (with c. 1.5 wt% H_2O). The near-chondritic to sub-chondritic Nd isotopic signature of the HBG plutons ($-6.4 < \varepsilon_{Ndi} < +1.9$, $n = 7$; $-2.0 < \varepsilon_{Hfi} < +1.7$, $n = 10$) overlaps with the evolution trend of the crust generated at 1520-1480 Ma (Figs. 8; 13). This implies sources isotopically similar to those of the Sirdal magmatic belt. However, the geographical overlap between the HBG suite and the Sirdal magmatic belt suggests that more refractory lower crustal sources were exploited at higher temperature after 985 Ma for the HBG suite (Granseth et al. 2020; Vander Auwera et al. 2008).

To the west of the Sirdal magmatic belt, the AMC suite formed between 932 and 915 Ma in a crust previously metamorphosed to granulite facies conditions (1030–1005 Ma). The AMC suite is ferroan and alkalic (Fig. 14). Constraints from experimental petrology indicate that the high alumina basalt parental to the anorthosite plutons is

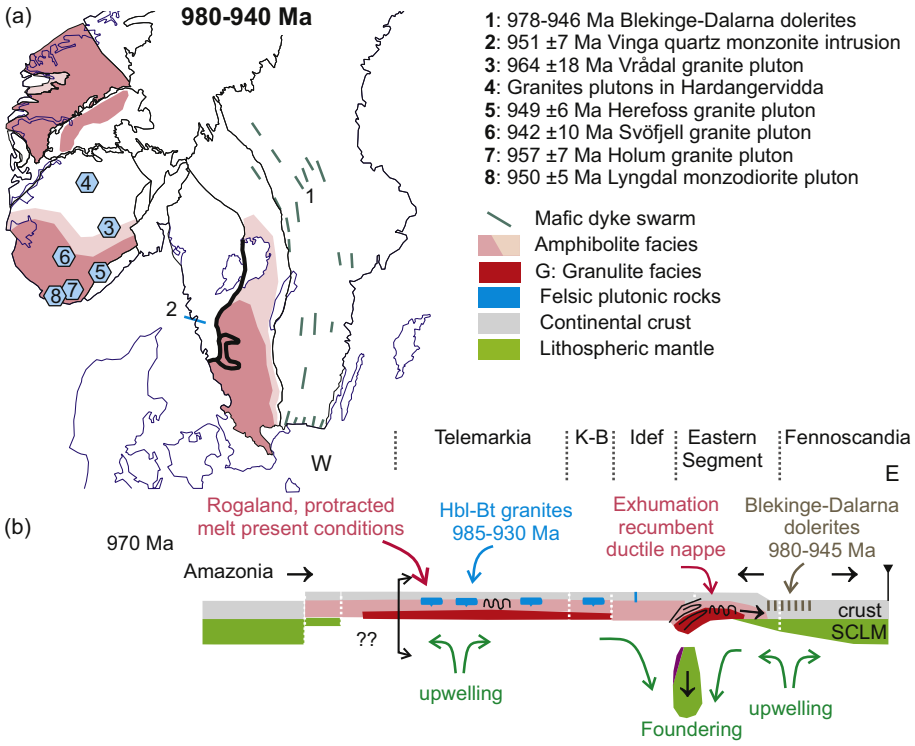

Fig. 22. Schematic geodynamic model for the 980–940 Ma time interval. (a) Sketch map of the Sveconorwegian orogen, with distribution of metamorphism and magmatism. (b) Interpretative E-W cross section. WGR: Western Gneiss Region.

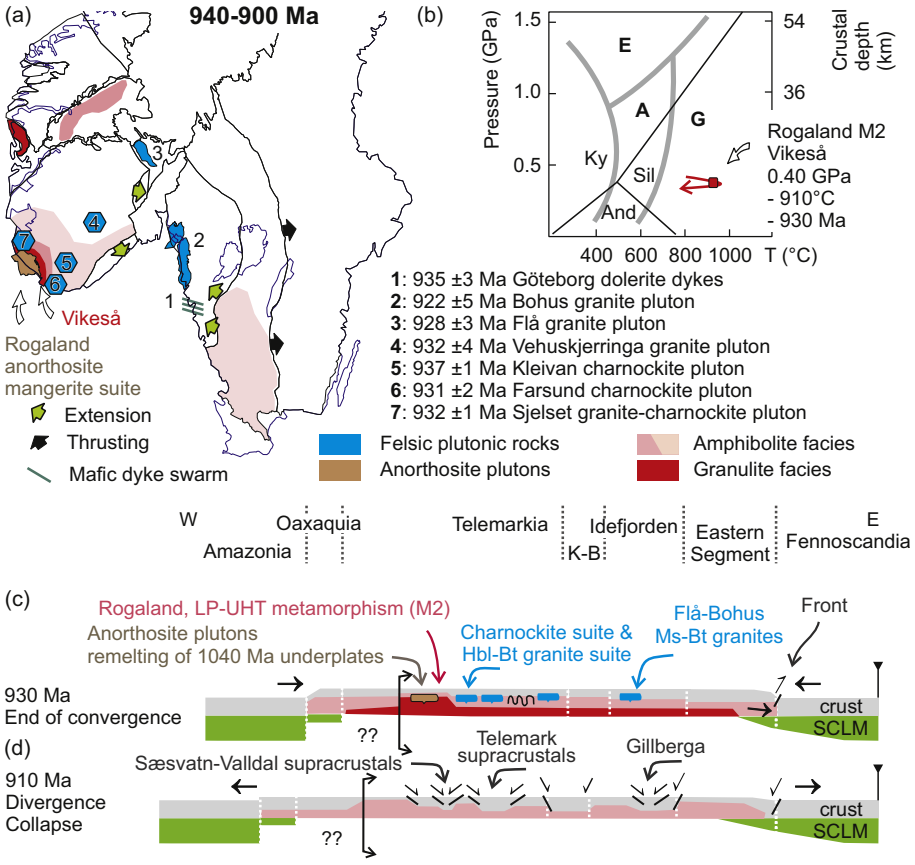

Fig. 23. Schematic geodynamic model for the 940–900 Ma time interval. (a) Sketch map of the Sveconorwegian orogen, with distribution of metamorphism and magmatism. (b) Pressure-temperature diagram. (c, d) Interpretative E-W cross sections.

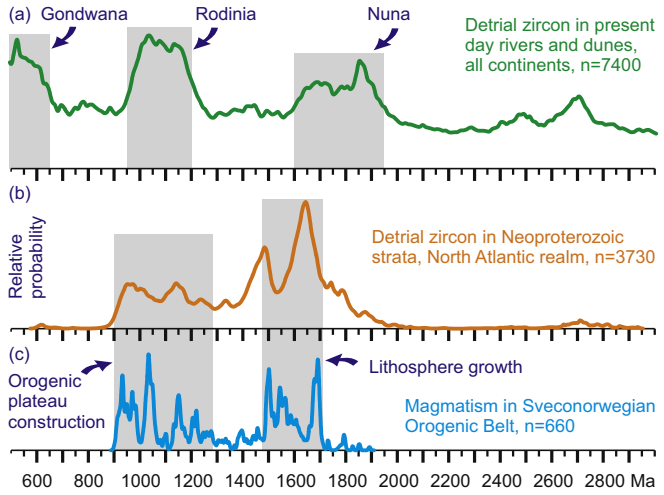

Fig. 24. Erosion of the Sveconorwegian orogen. (a) Relative probability diagrams of detrital zircons in present day river sediments and dunes. Peaks in this distribution are attributed to formation of supercontinents Nuna, Rodinia and Gondwana. Compilation of Campbell and Allen (2008). (b) Relative probability diagrams of detrital zircons in Neoproterozoic clastic sediments in the North Atlantic realm, deposited in marine and continental environment mainly during the Tonian and Cryogenian. The compilation includes 3730 detrital zircons from the Moine Supergroup in Scotland (Kirkland et al. 2008b), Caledonian Lower and Middle Allochthons in Norway and Sweden (Be'eri-Shlevin et al. 2011; Bingen et al. 2011; Gee et al. 2015; Kirkland et al. 2007, 2008a; Lamminen et al. 2015; Zhang et al. 2015, 2016), Timanides in N Norway (Zhang et al. 2015), Northwestern terrane in Svalbard (Pettersson et al. 2009) and Eleonore Bay Supergroup in E Greenland (Sláma et al. 2011). Only analyses with discordance < 5% are selected; the $^{206}Pb/^{238}U$ age is selected for zircon younger than 1500 Ma and the $^{206}Pb/^{207}Pb$ age for older zircons. (c) Relative probability diagram for magmatic events in the entire Sveconorwegian orogen. The time intervals for continental lithosphere generation and orogenic plateau development are highlighted. The similitude in the age distribution between magmatic events in the Sveconorwegian orogen and the Neoproterozoic strata argues for sourcing in the Sveconorwegian orogen for these sediments and important transport of detritus northwards and westwards.

characterized by a too low Mg# (molar Mg/(Mg+Fe) = 0.52) and crystallizes too sodic plagioclase (An55) to be generated by melting of a mantle peridotite (HLCA and TJ compositions; Duchesne et al. 1999; Longhi 2005; Longhi et al. 1999). Instead, its composition is situated on the thermal divide of the plagioclase + pyroxene liquidus surface at 1.0 to 1.3 GPa, imposing that it was produced by partial melting of a gabbronoritic source (Longhi 2005; Longhi et al. 1999). Experiments show that compositionally adequate melts in equilibrium with plagioclase and orthopyroxene are found in a temperature range between c. 1180 and 1250 °C at c. 1.1 GPa (Fram and Longhi 1992; Longhi et al. 1999; Vander Auwera and Longhi 1994). The Sm–Nd isochron of 1041 ± 17 Ma defined by the high-aluminium orthopyroxene megacrysts (HAOM) hosted in the anorthosite plutons (Bybee et al. 2014) suggests that these megacrysts are restitic crystals from a lower crustal source (Vander Auwera et al., 2014b). The isochron implies that the gabbronoritic source formed at c. 1040 Ma as an underplate (1.1 GPa) and was remelted at c. 930 Ma to form the parental magmas of the AMC suite (Vander Auwera et al., 2014b). Isotopically, this two stage model is realistic, with overlapping positive epsilon Nd values for the megacrysts ($+3.1 < \varepsilon_{Nd(930\ Ma)} < +5.9$) and mafic rocks in the AMC suite ($\varepsilon_{Nd(930\ Ma)} < +5.8$) (Fig. 13). However, the wide range of Nd isotopic composition of differentiated rocks in the AMC suite ($-2.8 < \varepsilon_{Nd(930\ Ma)} < +5.8$), implies a variety of lower crustal sources and crustal contaminants in the suite, all of them characterized by low water content (Barling et al. 2000; Duchesne and Wilmart 1997). This two-stage model requires that hot asthenosphere was upwelling just under the crust around 930 Ma in order to extensively remelt (high degree of partial melting) gabbronoritic layers of the 1040 Ma underplate. Heat transfer from the mantle and the anorthosite plutons to the crust resulted in a second phase of ultra-high temperature granulite-facies metamorphism (M2; 0.35–0.5 GPa, 900–950 °C, c. 930 Ma) (Laurent et al. 2018b). Using a conservative geothermal gradient of 20 °C/km, extrapolation of a 900 °C temperature at 0.4 GPa (15 km depth; M2) to the base of the crust at 1.1 GPa (41.5 km depth) indeed yield a temperature of 1420 °C, compatible with the presence of asthenosphere at the base of the crust at c. 930 Ma.

6.4. After 930 Ma: late- to post-Sveconorwegian collapse and sedimentation

The orogenic plateau developed during the Sveconorwegian orogeny (Fig. 17 to Fig. 23) could not be sustained when convergence came to a halt sometime after c. 930 Ma, and it collapsed. As noted earlier, syn- to late-Sveconorwegian plutons (1066–920 Ma) exposed today define a rather uniform depth of intrusion of c. 16 km (0.4–0.5 GPa, Table 1) (Charlier et al. 2010; Coint et al. 2015; Eliasson et al. 2003; Vander Auwera et al. 2014a; Vander Auwera and Longhi 1994). Removal of this c. 16 km thick overburden took place by a combination of late- to post-Sveconorwegian erosion and extensional tectonics.

Mapping and characterization of extensional shear zones that could explain exhumation of amphibolite-facies gneiss complexes (infrastructure of the orogenic plateau) relative to low-grade supracrustal rocks (superstructure) are still in their infancy (Persson-Nilsson and Lundqvist 2014; Torgersen et al. 2018; Viola et al. 2011). Extensional reactivation of the main shear zones in the orogen, including the Sveconorwegian front, the Mylonite Zone and the Bamble-Telemarkia boundary zone, are documented between c. 930 and 860 Ma by muscovite and biotite $^{40}Ar/^{39}Ar$ data (Andréasson and Dallmeyer 1995; Mulch et al. 2005; Page et al. 1996b; Viola et al. 2011). Extension was associated with regional cooling, as documented by regional scale titanite U–Pb and amphibole, muscovite and biotite $^{40}Ar/^{39}Ar$ data (Bingen et al. 1998; Connelly et al. 1996; Johansson et al. 2001; Page et al. 1996a; Page et al. 1996b; Söderlund et al. 1999; Ulmius et al. 2018; Verschure et al. 1980; Wang et al. 1998).

Pegmatite bodies represent the youngest magmatism of regional significance in the orogen between c. 914 and 900 Ma (Hetherington and Harlov 2008; Müller et al. 2015; Müller et al. 2017; Pasteels et al. 1979; Scherer et al. 2001; Seydoux-Guillaume et al. 2012). Pegmatites are locally abundant in the gneiss complexes of the Telemarkia and Idefjorden lithotectonic units. In the Telemarkia lithotectonic unit, they formed shortly after the regional scale titanite U–Pb age of c. 918 Ma, interpreted to record regional cooling below c. 600 °C. The pegmatites are not genetically related to any exposed granite pluton and therefore they represent small individual batches of fluid-rich melt sourced locally in the gneiss complexes (Müller et al. 2015; Müller et al. 2017). Their relation to the extensional collapse of the orogen and the source (s) of fluids necessary to generate the fluid-rich melts remain enigmatic.

Absence of widespread late-Sveconorwegian sedimentation inside the orogen is suggested by a lack of post-Sveconorwegian sedimentary cover below the sub-Cambrian peneplain in southern Norway and Sweden (Gabrielsen et al. 2015). The Neoproterozoic Visingsö Group deposited between c. 885 and 740 Ma along the Sveconorwegian Front is directly and unconformably overlying Paleoproterozoic basement (Loron and Moczydłowska 2018; Moczydłowska et al. 2018; Pulsipher and Dehler 2019). These observations suggest that the Sveconorwegian orogen was erodible, i.e. above sea level, at the end of the Sveconorwegian orogeny.

The rock record supportive for clastic transport towards the Fennoscandia foreland is only local (Almesåkra Group) (Ripa and Stephens 2020d). However, thermochronological data suggest heating of the foreland up to c. 220 °C some 150 km east of the Sveconorwegian Front between 944 Ma and 851 Ma, which corresponds to burial of the present day surface to c. 7 km (Guenthner et al. 2017). Clastic transport towards the north and west of the Sveconorwegian orogen is, instead, quite well established, as Neoproterozoic continental and marine sediments abound in Caledonian parautochthons and allochthons, Svalbard,

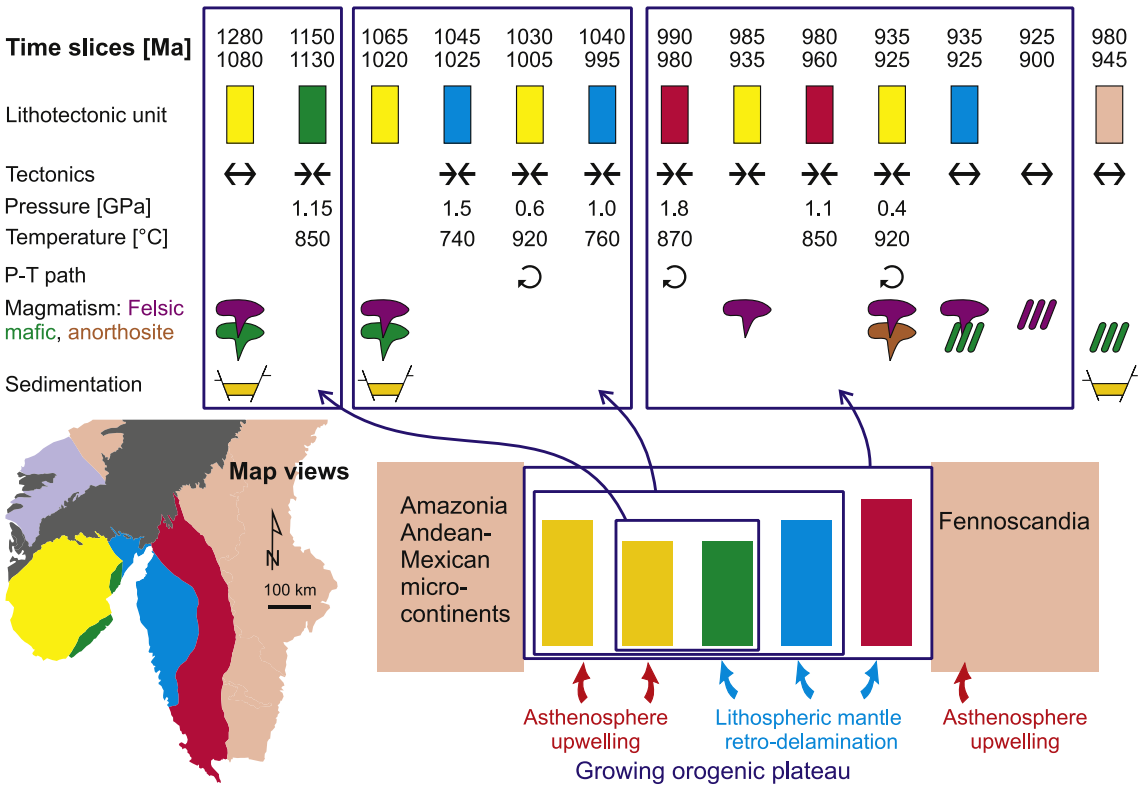

Fig. 25. Summary matrix of the Sveconorwegian orogeny. The first line provides the time slices of the recognised events. Line 2 represents the involved lithotectonic units, colour coded according to the inset map at the bottom. Line 3 (Tectonics) indicates if the tectonic regime is contractional or extensional in the specific time interval and geographic location. Note that for the time interval between 1280 and 1080 Ma, the tectonic regime is extensional in Telemarkia while it is contractional in the Bamble and Kongsberg Lithotectonic Units. Lines 4-5 (Pressure-Temperature) provides the conditions of peak metamorphism and line 6 (P-T path) indicates where this metamorphism follows a clockwise P-T path. Line 7 (magmatism) records plutonic events, with color coding for felsic (purple), mafic (green) or anorthositic (brown) magmatism. Line 9 records known episodes of sedimentation in intermontane basins or foreland basins. The bottom-right figure is a interpretative transect in map view through the orogen between the Amazonia hinterland and Fennoscandia foreland, showing the three-step growth of the orogenic plateau from the centre of the orogen. This three-step growth is associated with three phases of retro-delamination of the sub-continental lithospheric mantle (SCLM) towards the foreland, as recorded by metamorphism with a high-pressure signature. The western part of the orogen is characterized by upwelling and shallow asthenosphere during the entire orogenic period.

and the Timanides (Nystuen et al. 2008). These sediment sequences contain detrital zircons with age between 1700 and 1500 Ma and 1280 and 900 Ma (Bingen et al. 2011; Gee et al. 2015; Kirkland et al. 2007; Kirkland et al. 2008b; Pettersson et al. 2009; Sláma et al. 2011; Strachan et al. 1995; Strachan et al. 2013; Zhang et al. 2015). These sequences can, at least partly, be sourced directly from within the Sveconorwegian orogen (Fig. 24).

7. Conclusions

Published models attempting to explain the tectonic evolution of the Sveconorwegian orogeny vary widely even with respect to their first-order features and boundary conditions. They range from end-members involving continental collision between Baltica/Fennoscandia and another continent to accretion in the absence of collision (Fig. 3). This diversity reflects the difficulty to translate the observed geological record and the analytical data into geodynamic processes in the Proterozoic.

Based on a review of data and concepts, we favour a model of large, hot and long-duration continental collision at the margin of Fennoscandia between c. 1065 and 920 Ma, as synthesized in Figs. 17-23, and by a matrix in Fig. 25. The plate tectonic configuration of the pre-collision events, between 1280 and 1080 Ma, remains uncertain, although it was possibly that of a continental back arc setting (Figs. 17; 18). Although not strictly necessary, the model is adjusted into a classical Rodinia assembly framework, involving a Baltica–Laurentia–Amazonia collision (Figs. 1; 8, 12; 13; 16).

The width of the orogenic zone, the evidence for protracted and widespread crustal melting and high-temperature metamorphism reaching UHT conditions, the evidence for high-pressure metamorphism recording crustal thickening, the growth of the orogenic zone towards the foreland, the juxtaposition of low-grade supracrustal rocks and high-grade gneiss complexes, and the lack of syn-orogenic marine sedimentary sequence, argue for a collisional orogeny. We suggest that an orogenic plateau started to form around 1280 Ma in the Telemarkia lithotectonic unit, first as a Cordillera-style (back-arc) orogenic plateau, and that it widened stepwise towards both the orogenic hinterland and foreland, as a Tibetan-style (collisional) orogenic plateau. Shallow asthenosphere conditions were maintained in the western part of the orogenic belt at least up to c. 930 Ma, when the formation of anorthosite plutons took place by remelting of mafic underplates themselves formed at c. 1040 Ma. Formation of the orogenic plateau was paired with retro-delamination and foundering of the sub-continental lithospheric mantle. This process is recorded by contraction tectonics and regional metamorphism with an increasingly higher pressure signature towards the foreland followed by exhumation. Three stages of lithosphere foundering are inferred, one at c. 1150–1120 Ma under the Bamble and Kongsberg Lithotectonic units, one at c. 1050 Ma under the Idefjorden lithotectonic unit and one at c. 990 Ma under the Eastern Segment. In the Eastern Segment, peak conditions reached eclogite facies conditions (1.8 GPa-870 °C) and exhumation of eclogite-bearing units was aided by extrusion of a ductile nappe lubricated by partial melting, within an overall compressional setting. The increasing peak pressure recorded in time and space reflects

increasing mechanical coupling between the lower crust and colder lithospheric mantle, as the delamination process progressed toward the Fennoscandia craton.

After c. 930 Ma, convergence came to a halt, the orogenic plateau collapsed, and 16 km of overburden was removed by extension and erosion.

Supplementary data to this article can be found online at https://doi.org/10.1016/j.gr.2020.10.014.

Declaration of Competing Interest

The authors declare that they have no known competing financial interests or personal relationships that could have appeared to influence the work reported in this paper.

The following are the supplementary data related to this article.

Acknowledgements

The Geological Survey of Norway provided project time to perform this research. T. Horscroft and M. Santosh are thanked for handling this publication. Mike Stephens and Aphrodite Indares provided very constructive review of the manuscript.

References

Åhäll, K.I., Connelly, J.N., 1998. Intermittent 1.53-1.13 Ga magmatism in western Baltica; age constraints and correlations within a postulated supercontinent. Precambrian Res. 92, 1–20.

Åhäll, K.I., Connelly, J.N., 2008. Long-term convergence along SW Fennoscandia: 330 m.y. of Proterozoic crustal growth. Precambrian Res. 161, 452–474.

Åhäll, K.I., Daly, J.S., 1989. Age, tectonic setting and provenance of Östfold-Marstrand Belt supracrustals: westward crustal growth of the Baltic Shield at 1760 Ma. Precambrian Res. 45, 45–61.

Åhäll, K.I., Gower, C.F., 1997. The Gothian and Labradorian orogens: variations in accretionary tectonism along a late Paleoproterozoic Laurentia–Baltica margin. GFF 119, 181–191.

Åhäll, K.I., Larson, Å., 2000. Growth-related 1.85-1.55 Ga magmatism in the Baltic Shield; a review addressing the tectonic characteristics of Svecofennian, TIB 1 -related, and Gothian events. GFF 122, 193–206.

Åhäll, K.I., Samuelsson, L., Persson, P.O., 1997. Geochronology and stuctural setting of the 1.38 Ga Torpa granite; implications for charnockite formation in SW Sweden. Geol. Fören. Stockh. Förh. 119, 37–43.

Åhäll, K.I., Cornell, D.H., Armstrong, R., 1998. Ion probe zircon dating of metasedimentary units across the Skagerrak: new constraints for early Mesoproterozoic growth of the Baltic Shield. Precambrian Res. 87, 117–134.

Ahlin, S., Austin Hegardt, E., Cornell, D., 2006. Nature and stratigraphic position of the 1614 Ma Delsjön augen granite-gneiss in the Median Segment of south-west Sweden. GFF 128, 21–32.

Andersen, T., 1997. Radiogenic isotope systematics of the Herefoss granite, South Norway: an indicator of Sveconorwegian (Grenvillian) crustal evolution in the Baltic shield. Chem. Geol. 135, 139–158.

Andersen, T., Laajoki, K., 2003. Provenance characteristics of Mesoproterozoic metasedimentary rocks from Telemark, South Norway: a Nd-isotope mass-balance model. Precambrian Res. 126, 95–122.

Andersen, T., Munz, I.A., 1995. Radiogenic whole-rock lead in Precambrian metasedimentary gneisses from South Norway: evidence of Sveconorwegian LILE mobility. Nor. Geol. Tidsskr. 75, 156–168.

Andersen, T., Hagelia, P., Whitehouse, M.J., 1994. Precambrian multi-stage crustal evolution in the Bamble sector of south Norway: Pb isotopic evidence from a Sveconorwegian deep-seated intrusion. Chem. Geol. (Isotope Geosci. Sec.) 116, 327–343.

Andersen, T., Andresen, A., Sylvester, A.G., 2001. Nature and distribution of deep crustal reservoirs in the southwestern part of the Baltic Shield: evidence from Nd, Sr and Pb isotope data on late Sveconorwegian granites. J. Geol. Soc. Lond. 158, 253–267.

Andersen, T., Andresen, A., Sylvester, A.G., 2002a. Timing of late- to post-tectonic Sveconorwegian granitic magmatism in South Norway. Norges Geol. Unders. Bull. 440, 5–18.

Andersen, T., Griffin, W.L., Pearson, N.J., 2002b. Crustal evolution in the SW part of the Baltic Shield: the Hf isotope evidence. J. Petrol. 43, 1725–1747.

Andersen, T., Griffin, W.L., Jackson, S.E., Knudsen, T.L., Pearson, N.J., 2004a. Mid-Proterozoic magmatic arc evolution at the southwest margin of the Baltic shield. Lithos 73, 289–318.

Andersen, T., Laajoki, K., Saeed, A., 2004b. Age, provenance and tectonostratigraphic status of the Mesoproterozoic Blefjell quartzite, Telemark sector, southern Norway. Precambrian Res. 135, 217–244.

Andersen, T., Griffin, W.L., Sylvester, A.G., 2007. Sveconorwegian crustal underplating in southwestern Fennoscandia: LAM-ICPMS U-Pb and Lu-Hf isotope evidence from granites and gneisses in Telemark, southern Norway. Lithos 93, 273–287.

Andersen, T., Andersson, U.B., Graham, S., Åberg, G., Simonsen, S.L., 2009. Granitic magmatism by melting of juvenile continental crust: new constraints on the source of Palaeoproterozoic granitoids in Fennoscandia from Hf isotopes in zircon. J. Geol. Soc. Lond. 166, 233–247.

Andersson, M., Lie, J.E., Husebye, E.S., 1996. Tectonic setting of post-orogenic granites within SW Fennoscandia based on deep seismic and gravity data. Terra Nova 8, 558–566.

Andersson, J., Söderlund, U., Cornell, D., Johansson, L., Möller, C., 1999. Sveconorwegian (-Grenvillian) deformation, metamorphism and leucosome formation in SW Sweden, SW Baltic Shield: constraints from a Mesoproterozoic granite intrusion. Precambrian Res. 98, 151–171.

Andersson, J., Möller, C., Johansson, L., 2002a. Zircon chronology of migmatite gneisses along the Mylonite Zone (S Sweden): a major Sveconorwegian terrane boundary in the Baltic Shield. Precambrian Res. 114, 121–147.

Andersson, U.B., Neymark, L.A., Billström, K., 2002b. Petrogenesis of Mesoproterozoic (Subjotnian) rapakivi complexes of central Sweden: implications for U-Pb zircon ages, Nd, Sr and Pb isotopes. Trans. R. Soc. Edinb. Earth Sci. 92, 201–228.

Andréasson, P.G., Dallmeyer, R.D., 1995. Tectonothermal evolution of high-alumina rocks within the Protogine Zone, southern Sweden. J. Metamorph. Geol. 13, 461–474.

Andréasson, P.G., Rodhe, A., 1994. Ductile and brittle deformation within the Protogine Zone, southern Sweden: a discussion. Geol. Fören. Stockh. Förh. 116, 115–117.

Appelquist, K., Cornell, D., Brander, L., 2008. Age, tectonic setting and petrogenesis of the Habo Volcanic Suite: evidence for an active continental margin setting for the Transscandinavian Igneous Belt. GFF 130, 123–138.

Appelquist, K., Brander, L., Johansson, Å., Andersson, U.B., Cornell, D., 2011. Character and origin of variably deformed granitoids in central southern Sweden: implications from geochemistry and Nd isotopes. Geol. J. 46, 597–618.

Årebäck, H., Stigh, J., 2000. The nature and origin of an anorthosite associated ilmenite-rich leuconorite, Hakefjorden Complex, south-west Sweden. Lithos 21, 247–267.

Årebäck, H., Andersson, U.B., Petersson, J., 2008. Petrological evidence for crustal melting, unmixing, and undercooling in an alkali-calcic, high-level intrusion: the late Sveconorwegian Vinga intrusion, SW Sweden. Mineral. Petrol. 93, 1–46.

Ashwal, L.D., 1993. Anorthosites. Springer-Verlag, Berlin.

Augland, L.E., Andresen, A., Corfu, F., Agyei-Dwarko, N.Y., Larionov, A.N., 2014. The Bratten-Landegode gneiss complex: a fragment of Laurentian continental crust in the Uppermost Allochthon of the Scandinavian Caledonides. In: Corfu, F., Gasser, D., Chew, D.M. (Eds.), New Perspectives on the Caledonides of Scandinavia and Related Areas. Geological Society, Special Publications, London, pp. 633–654.

Austin Hegardt, E., 2010. Pressure, Temperature and Time Constraints on Tectonic Models for Southwestern Sweden. Ph.D. thesis, Department of Earth Science, University of Gothenburg, pp. 1–91.

Austin Hegardt, E., Cornell, D.H., Claesson, L., Simakov, S., Stein, H.J., Hannah, J.L., 2005. Eclogites in the central part of the Sveconorwegian Eastern Segment of the Baltic Shield: support for an extensive eclogite terrane. GFF 127, 221–232.

Austin Hegardt, E., Cornell, D.H., Hellström, F.A., Lundqvist, I., 2007. Emplacement age of the mid-Proterozoic Kungsbacka Bimodal Suite, SW Sweden. GFF 129, 227–234.

Bao, X.W., Eaton, D.W., Guest, B., 2014. Plateau uplift in western Canada caused by lithospheric delamination along a craton edge. Nat. Geosci. 7, 830–833.

Barling, J., Weis, D., Demaiffe, D., 2000. A Sr-, Nd- and Pb-isotopic investigation of the transition between two megacyclic units of the Bjerkreim–Sokndal layered intrusion, south Norway. Chem. Geol. 165, 47–65.

Barnichon, J.D., Havenith, H., Hoffer, B., Charlier, R., Jongmans, D., Duchesne, J.C., 1999. The deformation of the Egersund-Ogna anorthosite massif, south Norway: finite-element modelling of diapirism. Tectonophysics 303, 109–130.

Bateman, P.C., Chappell, B.W., 1979. Crystallization, fractionation, and solidification of the Tuolumne Intrusive Series, Yosemite National Park, California. Geol. Soc. Am. Bull. 90, 465–482.

Beaumont, C., Nguyen, M.H., Jamieson, R.A., Ellis, S., 2006. Crustal flow modes in large hot orogens. Geol. Soc. Lond., Spec. Publ. 268, 91–145.

Beckman, V., Möller, C., Söderlund, U., Andersson, J., 2017. Zircon growth during progressive recrystallization of gabbro to garnet amphibolite, Eastern Segment, Sveconorwegian orogen. J. Petrol. 58, 167–187.

Bédard, J., 2010. Parental magmas of Grenville Province massif-type anorthosites, and conjectures about why massif anorthosites are restricted to the Proterozoic. Earth Environ. Sci. Trans. Roy. Soc. Edinburgh - Earth Sci. 100, 77–103.

Be'eri-Shlevin, Y., Gee, D.G., Claesson, S., Ladenberger, A., Majka, J., Kirkland, C.L., Robinson, P., Frei, D., 2011. Provenance of Neoproterozoic sediments in the Särv nappes (Middle Allochthon) of the Scandinavian Caledonides: LA-ICP-MS and SIMS U-Pb dating of detrital zircons. Precambrian Res. 187, 181–200.

Bergerat, F., Angelier, J., Andreasson, P.G., 2007. Evolution of paleostress fields and brittle deformation of the Tornquist Zone in Scania (Sweden) during Permo-Mesozoic and Cenozoic times. Tectonophysics 444, 93–110.

Bergman, S., Högdahl, K., Nironen, M., Ogenhall, E., Sjöström, H., Lundqvist, L., Lahtinen, R., 2008. Timing of Palaeoproterozoic intra-orogenic sedimentation in the central Fennoscandian Shield; evidence from detrital zircon in metasandstone. Precambrian Res. 161, 231–249.

Bergström, U., Stephens, M.B., Wahlgren, C.H., 2020. Chapter 16 - Polyphase (1.6–1.5 and 1.1–1.0 Ga) deformation and metamorphism of Proterozoic (1.7–1.1 Ga) continental crust, Idefjorden terrane, Sveconorwegian orogen. Geol. Soc. Lond. Mem. 50, 397–434.

Berthelsen, A., 1980. Towards a palinspastic tectonic analysis of the Baltic Shield. In: Cogne, J., Slansky, M. (Eds.), Geology of Europe, from Precambrian to the post-Hercyninan sedimentary basins. Mémoires du B.R.G.M, Paris, pp. 5–21.

Bingen, B., 1989. Geochemistry of Sveconorwegian augen gneisses from SW Norway at the amphibolite-granulite facies transition. Nor. Geol. Tidsskr. 69, 177–189.

Bingen, B., van Breemen, O., 1998a. Tectonic regimes and terrane boundaries in the high-grade Sveconorwegian belt of SW Norway, inferred from U-Pb zircon geochronology and geochemical signature of augen gneiss suites. J. Geol. Soc. Lond. 155, 143–154.

Bingen, B., van Breemen, O., 1998b. U-Pb monazite ages in amphibolite- to granulite-facies orthogneisses reflect hydrous mineral breakdown reactions: Sveconorwegian Province of SW Norway. Contrib. Mineral. Petrol. 132, 336–353.

Bingen, B., Viola, G., 2018. The early-Sveconorwegian orogeny in southern Norway: tectonic model involving delamination of the sub-continental lithospheric mantle. Precambrian Res. 313, 170–204.

Bingen, B., Demaiffe, D., Hertogen, J., Weis, D., Michot, J., 1993. K-rich calc-alkaline augen gneisses of Grenvillian age in SW Norway: mingling of mantle-derived and crustal components. J. Geol. 101, 763–778.

Bingen, B., Boven, A., Punzalan, L., Wijbrans, J., Demaiffe, D., 1998. Hornblende $^{40}Ar/^{39}Ar$ geochronology across terrane boundaries in the Sveconorwegian province of S Norway. Precambrian Res. 90, 159–185.

Bingen, B., Birkeland, A., Nordgulen, Ø., Sigmond, E.M.O., 2001. Correlation of supracrustal sequences and origin of terranes in the Sveconorwegian orogen of SW Scandinavia: SIMS data on zircon in clastic metasediments. Precambrian Res. 108, 293–318.

Bingen, B., Mansfeld, J., Sigmond, E.M.O., Stein, H.J., 2002. Baltica-Laurentia link during the Mesoproterozoic: 1.27 Ga development of continental basins in the Sveconorwegian Orogen, southern Norway. Can. J. Earth Sci. 39, 1425–1440.

Bingen, B., Nordgulen, Ø., Sigmond, E.M.O., Tucker, R.D., Mansfeld, J., Högdahl, K., 2003. Relations between 1.19-1.13 Ga continental magmatism, sedimentation and metamorphism, Sveconorwegian province, S Norway. Precambrian Res. 124, 215–241.

Bingen, B., Skår, Ø., Marker, M., Sigmond, E.M.O., Nordgulen, Ø., Ragnhildstveit, J., Mansfeld, J., Tucker, R.D., Liégeois, J.P., 2005. Timing of continental building in the Sveconorwegian orogen, SW Scandinavia. Nor. J. Geol. 85, 87–116.

Bingen, B., Andersson, J., Söderlund, U., Möller, C., 2008a. The Mesoproterozoic in the Nordic countries. Episodes 31, 29–34.

Bingen, B., Davis, W.J., Hamilton, M.A., Engvik, A., Stein, H.J., Skår, Ø., Nordgulen, Ø., 2008b. Geochronology of high-grade metamorphism in the Sveconorwegian belt, S Norway: U-Pb, Th-Pb and Re-Os data. Nor. J. Geol. 88, 13–42.

Bingen, B., Nordgulen, Ø., Viola, G., 2008c. A four-phase model for the Sveconorwegian orogeny, SW Scandinavia. Nor. J. Geol. 88, 43–72.

Bingen, B., Belousova, E.A., Griffin, W.L., 2011. Neoproterozoic recycling of the Sveconorwegian orogenic belt: detrital-zircon data from the Sparagmite basins in the Scandinavian Caledonides. Precambrian Res. 189, 347–367.

Bingen, B., Corfu, F., Stein, H.J., Whitehouse, M.J., 2015. U-Pb geochronology of the syn-orogenic Knaben molybdenum deposits, Sveconorwegian orogen, Norway. Geol. Mag. 152, 537–556.

Bird, P., 1979. Continental delamination and the Colorado Plateau. J. Geophys. Res. Solid Earth 84, 7561–7571.

Blereau, E., Johnson, T.E., Clark, C., Taylor, R.J.M., Kinny, P.D., Hand, M., 2017. Reappraising the P–T evolution of the Rogaland–Vest Agder Sector, southwestern Norway. Geosci. Front. 8, 1–14.

Bogaerts, M., Scaillet, B., Liégeois, J.P., Vander Auwera, J., 2003. Petrology and geochemistry of the Lyngdal granodiorite (Southern Norway) and the role of fractional crystallization in the genesis of Proterozoic ferro-potassic A-type granites. Precambrian Res. 124, 149–184.

Bogaerts, M., Scaillet, B., Vander Auwera, J., 2006. Phase equilibria of the Lyngdal granodiorite (Norway): implications for the origin of metaluminous ferroan granitoids. J. Petrol. 47, 2405–2431.

Bogdanova, S., Bingen, B., Gorbatschev, R., Kheraskova, T., Kozlov, V., Puchkov, V., Volozh, Y., 2008. The East European Craton (Baltica) before and during the assembly of Rodinia. Precambrian Res. 160, 23–45.

Boger, S.D., Raetz, M., Giles, D., Etchart, E., Fanning, C.M., 2005. U–Pb age data from the Sunsas region of Eastern Bolivia, evidence for the allochthonous origin of the Paragua Block. Precambrian Res. 139, 121–146.

Bolle, O., Duchesne, J.C., 2007. The Apophysis of the Bjerkreim-Sokndal layered intrusion (Rogaland anorthosite province, SW Norway): a composite pluton build up by tectonically-driven emplacement of magmas along the margin of an AMC igneous complex. Lithos 98, 292–312.

Bolle, O., Diot, H., Duchesne, J.C., 2000. Magnetic fabric and deformation in charnockitic igneous rocks of the Bjerkreim–Sokndal layered intrusion (Rogaland, Southwest Norway). J. Struct. Geol. 22, 647–667.

Bolle, O., Trindade, R.I.F., Bouchez, J.L., Duchesne, J.C., 2002. Imaging downward granitic magma transport in the Rogaland Igneous Complex, SW Norway. Terra Nova 14, 87–92.

Bolle, O., Demaiffe, D., Duchesne, J.C., 2003a. Petrogenesis of jotunitic and acidic members of an AMC suite (Rogaland anorthosite province, SW Norway): a Sr and Nd isotopic assessment. Precambrian Res. 124, 185–214.

Bolle, O., Diot, H., Trindade, R.I.F., 2003b. Magnetic fabrics in the Holum granite (Vest-Agder, southernmost Norway): implications for the late evolution of the Sveconorwegian (Grenvillian) orogen of SW Scandinavia. Precambrian Res. 121, 221–249.

Bolle, O., Diot, H., Liégeois, J.P., Vander Auwera, J., 2010. The Farsund intrusion (SW Norway): a marker of late-Sveconorwegian (Grenvillian) tectonism emplaced along a newly defined major shear zone. J. Struct. Geol. 32, 1500–1518.

Bolle, O., Diot, H., Vander Auwera, J., Dembele, A., Schittekat, J., Spassov, S., Ovtcharova, M., Schaltegger, U., 2018. Pluton construction and deformation in the Sveconorwegian crust of SW Norway: magnetic fabric and U-Pb geochronology of the Kleivan and Sjelset granitic complexes. Precambrian Res. 305, 247–267.

Bouvier, A., Vervoort, J.D., Patchett, P.J., 2008. The Lu-Hf and Sm-Nd isotopic composition of CHUR: constraints from unequilibrated chondrites and implications for the bulk composition of terrestrial planets. Earth Planet. Sci. Lett. 273, 48–57.

Brander, L., Söderlund, U., 2009. Mesoproterozoic (1.47-1.44 Ga) orogenic magmatism in Fennoscandia; baddeleyite U-Pb dating of a suite of massif-type anorthosite in S Sweden. Int. J. Earth Sci. 98, 499–516.

Brander, L., Söderlund, U., Bingen, B., 2011. Tracing the 1271-1246 Ma Central Scandinavian Dolerite Group mafic magmatism in Fennoscandia: U-Pb baddeleyite and Hf isotope data on the Moslätt and Børgefjell dolerites. Geol. Mag. 148, 632–643.

Brander, L., Appelquist, K., Cornell, D., Andersson, U.B., 2012. Igneous and metamorphic geochronologic evolution of granitoids in the central Eastern Segment, southern Sweden. Int. Geol. Rev. 54, 509–546.

Brewer, T.S., Menuge, J.F., 1998. Metamorphic overprinting of Sm-Nd isotopic systems in volcanic rocks: the Telemark Supergroup, southern Norway. Chem. Geol. 145, 1–16.

Brewer, T.S., Daly, J.S., Åhäll, K.I., 1998. Contrasting magmatic arcs in the Palaeoproterozoic of the south-western Baltic Shield. Precambrian Res. 92, 297–315.

Brewer, T.S., Åhäll, K.I., Darbyshire, D.P.F., Menuge, J.F., 2002. Geochemistry of late Mesoproterozoic volcanism in southwestern Scandinavia: implications for Sveconorwegian/Grenvillian plate tectonic models. J. Geol. Soc. Lond. 159, 129–144.

Brewer, T.S., Åhäll, K.I., Menuge, J.F., Storey, C.D., Parrish, R.R., 2004. Mesoproterozoic bimodal volcanism in SW Norway, evidence for recurring pre-Sveconorwegian continental margin tectonism. Precambrian Res. 134, 249–273.

Broekmans, M.A., Nijland, T.G., Jansen, J.B.H., 1994. Are stable isotopic trends in amphibolite to granulite facies transitions metamorphic of diagenetic? - An answer for the Arendal area (Bamble sector, S.E. Norway) from mid-Proterozoic carbon bearing rocks. Am. J. Sci. 294, 1135–1165.

Brown, M., 2006. Duality of thermal regimes is the distinctive characteristic of plate tectonics since the Neoarchean. Geology 34, 961–964.

Brown, M., 2013. Granite: from genesis to emplacement. Geol. Soc. Am. Bull. 125, 1079–1113.

Bruand, E., Storey, C., Fowler, M., 2014. Accessory mineral chemistry of high Ba–Sr granites from northern Scotland: constraints on petrogenesis and records of whole-rock signature. J. Petrol. 55, 1619–1651.

Brueckner, H.K., 2009. Subduction of continental crust, the origin of post-orogenic granitoids (and anorthosites?) and the evolution of Fennoscandia. J. Geol. Soc. Lond. 166, 753–762.

Buchan, K.L., Mertanen, S., Park, R.G., Pesonen, L.J., Elming, S.-Å., Abrahamsen, N., Bylund, G., 2000. Comparing the drift of Laurentia and Baltica in the Proterozoic: the importance of key palaeomagnetic poles. Tectonophysics 319, 167–198.

Bybee, G.M., Ashwal, L.D., Shirey, S.B., Horan, M., Mock, T., Andersen, T.B., 2014. Pyroxene megacrysts in Proterozoic anorthosites: Implications for tectonic setting, magma source and magmatic processes at the Moho. Earth Planet. Sci. Lett. 389, 74–85.

Cagnard, F., Barbey, P., Gapais, D., 2011. Transition between "Archaean-type" and "modern-type" tectonics: Insights from the Finnish Lapland Granulite Belt. Precambrian Res. 187, 127–142.

Cameron, K.L., Lopez, R., Ortega-Gutiérrez, F., Solari, Luigi A., Keppie, J. Duncan, Schulze, Carlos, 2004. U-Pb geochronology and Pb isotopic compositions of leached feldspars: constraints on the origin and evolution of Grenville rocks from eastern and southern Mexico. Geol. Soc. Am. Mem. 197, 755–769.

Campbell, I.H., Allen, C.M., 2008. Formation of supercontinents linked to increases in atmospheric oxygen. Nat. Geosci. 1, 554–558.

Cardona, A., Chew, D., Valencia, V.A., Bayona, G., Miskovic, A., Ibañez-Mejía, M., 2010. Grenvillian remnants in the Northern Andes: Rodinian and Phanerozoic paleogeographic perspectives. J. S. Am. Earth Sci. 29, 92–104.

Carr, S.D., Easton, R.M., Jamieson, R.A., Culshaw, N.G., 2000. Geologic transect across the Grenville orogen of Ontario and New York. Can. J. Earth Sci. 37, 193–216.

Cawood, P.A., Pisarevsky, S.A., 2017. Laurentia-Baltica-Amazonia relations during Rodinia assembly. Precambrian Res. 292, 386–397.

Cawood, P.A., Strachan, R., Cutts, K., Kinny, P.D., Hand, M., Pisarevsky, S., 2010. Neoproterozoic orogeny along the margin of Rodinia: Valhalla orogen, North Atlantic. Geology 38, 99–102.

Cawood, P.A., Strachan, R.A., Merle, R.E., Millar, I.L., Loewy, S.L., Dalziel, I.W.D., Kinny, P.D., Jourdan, F., Nemchin, A.A., Connelly, J.N., 2015. Neoproterozoic to early Paleozoic extensional and compressional history of East Laurentian margin sequences: the Moine Supergroup, Scottish Caledonides. Geol. Soc. Am. Bull. 127, 349–371.

Cecys, A., Benn, K., 2007. Emplacement and deformation of the ca. 1.45 Ga Karlshamn granitoid pluton, southeastern Sweden, during ENE-WSW Danopolonian shortening. Int. J. Earth Sci. 96, 397–414.

Cecys, A., Bogdanova, S., Janson, C., Bibikova, E., Kornfält, K.A., 2002. The Stenshuvud and Tåghusa granitoids: new representative of Mesoproterozoic magmatism in southern Sweden. GFF 124, 149–162.

Chardon, D., Gapais, D., Cagnard, F., 2009. Flow of ultra-hot orogens: a view from the Precambrian, clues for the Phanerozoic. Tectonophysics 477, 105–118.

Charlier, B., Duchesne, J.C., Vander Auwera, J., 2006. Magma chamber processes in the Tellnes ilmenite deposit (Rogaland Anorthosite Province, SW Norway) and the formation of Fe-Ti ores in massif-type anorthosites. Chem. Geol. 234, 264–290.

Charlier, B., Duchesne, J.C., Vander Auwera, J., Storme, J.Y., Maquil, R., Longhi, J., 2010. Polybaric fractional crystallization of high-alumina basalt parental magmas in the Egersund-Ogna massif-type anorthosite (Rogaland, SW Norway) constrained by plagioclase and high-alumina orthopyroxene megacrysts. J. Petrol. 51, 2515–2546.

Chen, M., Niu, F., Tromp, J., Lenardic, A., Lee, C.T.A., Cao, W., Ribeiro, J., 2017. Lithospheric foundering and underthrusting imaged beneath Tibet. Nat. Commun. 8, 15659.

Chiarenzelli, J., Lupulescu, M., Cousens, B., Thern, E., Coffin, L., Regan, S., 2010. Enriched Grenvillian lithospheric mantle as a consequence of long-lived subduction beneath Laurentia. Geology 38, 151–154.

Christoffel, C.A., Connelly, J.N., Åhäll, K.I., 1999. Timing and characterization of recurrent pre-Sveconorwegian metamorphism and deformation in the Varberg-Halmstad region of SW Sweden. Precambrian Res. 98, 173–195.
Clemens, J.D., Darbyshire, D.P.F., Flinders, J., 2009. Sources of post-orogenic calcalkaline magmas: The Arrochar and Garabal Hill–Glen Fyne complexes, Scotland. Lithos 112, 524–542.
Clough, P.W., Field, D., 1980. Chemical variation in metabasites from a Proterozoic amphibolite-granulite transition zone, S Norway. Contrib. Mineral. Petrol. 73, 277–286.
Coint, N., Slagstad, T., Roberts, N.M.W., Marker, M., Røhr, T., Sørensen, B.E., 2015. The Late Mesoproterozoic Sirdal Magmatic Belt, SW Norway:Relationships between magmatism and metamorphism and implications for Sveconorwegian orogenesis. Precambrian Res. 265, 57–77.
Collins, W.J., 2002. Hot orogens, tectonic switching, and creation of continental crust. Geology 30, 535–538.
Connelly, J.N., Åhäll, K.I., 1996. The Mesoproterozoic cratonization of Baltica – new age constraints from SW Sweden. In: Brewer, T.S. (Ed.), Precambrian crustal evolution in the North Atlantic Region. Geological Society, Special Publications, London, pp. 261–273.
Connelly, J.N., Berglund, J., Larson, S.Å., 1996. Thermotectonic evolution of the Eastern Segment of southwestern Sweden: tectonic constraints from U-Pb geochronology. In: Brewer, T.S. (Ed.), Precambrian crustal evolution in the North Atlantic Region. Geological Society, Special Publications, London, pp. 297–313.
Cooper, D.C., Field, D., 1977. The chemistry and origins of Proterozoic low-potash, high-iron, charnockitic gneisses from Tromøy, South Norway. Earth Planet. Sci. Lett. 35, 105–115.
Cordani, U.G., Cardona, A., Jimenez, D.M., Liu, D., Nutman, A.P., 2005. Geochronology of Proterozoic basement inliers in the Colombian Andes: Tectonic history of remnants of a fragmented Grenville belt. Geol. Soc. Lond., Spec. Publ. 246, 329–346.
Corfu, F., 2019. The Sognefjell volcanic-subvolcanic complex – A late Sveconorwegian arc imbricated in the central Norwegian Caledonides. Precambrian Res. 331, 105353.
Corfu, F., Easton, R.M., 1995. U-Pb geochronology of the Mazinaw terrane, an imbricate segment of the Central Metasedimentary Belt, Grenville Province, Ontario. Can. J. Earth Sci. 32, 959–976.
Corfu, F., Laajoki, K., 2008. An uncommon episode of mafic magmatism at 1347 Ma in the Mesoproterozoic Telemark supracrustals, Sveconorwegian orogen - Implications for stratigraphy and tectonic evolution. Precambrian Res. 160, 299–307.
Cornell, D., Årebäck, H., Scherstén, A., 2000. Ion microprobe discovery of Archaean and Early Proterozoic zircon xenocrysts in southwest Sweden. GFF 122, 377–383.
Corriveau, L., van Breemen, O., 2000. Docking of the Central Metasedimentary Belt to Laurentia in geon 12: evidence from the 1.17–1.16 Chevreuil intrusive suite and host gneisses, Quebec. Can. J. Earth Sci. 37, 253–269.
Cosca, M.A., O'Nions, R.K., 1994. A re-examination of the influence of composition on argon retentivity in metamorphic calcic amphiboles. Chem. Geol. 112, 39–56.
Cosca, M.A., Mezger, K., Essene, E.J., 1998. The Baltica-Laurentia connection: Sveconorwegian (Grenvillian) metamorphism, cooling, and unroofing in the Bamble Sector, Norway. J. Geol. 106, 539–552.
Couzinié, S., Laurent, O., Moyen, J.F., Zeh, A., Bouilhol, P., Villaros, A., 2016. Post-collisional magmatism: crustal growth not identified by zircon Hf-O isotopes. Earth Planet. Sci. Lett. 456, 182–195.
Cutts, K.A., Hand, M., Kelsey, D.E., Wade, B., Strachan, R.A., Clark, C., Netting, A., 2009. Evidence for 930 Ma metamorphism in the Shetland Islands, Scottish Caledonides: implications for Neoproterozoic tectonics in the Laurentia-Baltica sector of Rodinia. J. Geol. Soc. Lond. 166, 1033–1047.
Dahlgren, S., Bogoch, R., Magaritz, M., Michard, A., 1993. Hydrothermal dolomite marbles associated with charnockitic magmatism in the Proterozoic Bamble Shear Belt, south Norway. Contrib. Mineral. Petrol. 113, 394–409.
Daly, J.S., McLelland, J.M., 1991. Juvenile Middle Proterozoic crust in the Adirondack Highlands, Grenville province, northeastern North America. Geology 19, 119–122.
Dalziel, I.W.D., 1997. Neoproterozoic-Paleozoic geography and tectonics: reviews, hypothesis, environmental speculations. Geol. Soc. Am. Bull. 109, 16–42.
Debon, F., Le Fort, P., 1983. A chemical-mineralogical classification of common plutonic rocks and associations. Trans. R. Soc. Edinb. Earth Sci. 73, 135–149.
deHaas, G.J.L.M., Andersen, T., Vestin, J., 1999. Detrital zircon geochronology: new evidence for an old model for accretion of the SW Baltic Shield. J. Geol. 107, 569–586.
deHaas, G.J.L.M., Nijland, T.G., Andersen, T., Corfu, F., 2002a. New constraints on the timing of deposition and metamorphism in the Bamble sector, south Norway: zircon and titanite U-Pb data from the Nelaug area. GFF 124, 73–78.
deHaas, G.J.L.M., Nijland, T.G., Valbracht, P.J., Maijer, C., Verschure, R., Andersen, T., 2002b. Magmatic versus metamorphic origin of olivine-plagioclase coronas. Contrib. Mineral. Petrol. 143, 537–550.
Demaiffe, D., Michot, J., 1985. Isotope geochronology of the Proterozoic crustal segment of southern Norway: a review. In: Tobi, A.C., Touret, J.L. (Eds.), The Deep Proterozoic Crust in the North Atlantic provinces. Reidel, Dordrecht, pp. 411–433.
Demaiffe, D., Weis, D., Michot, J., Duchesne, J.C., 1986. Isotopic constraints on the genesis of the Rogaland anorthositic suite (SW Norway). Chem. Geol. 57, 167–179.
Demaiffe, D., Bingen, B., Wertz, P., Hertogen, J., 1990. Geochemistry of the Lyngdal hyperites (SW Norway): comparison with the monzonorites associated with the Rogaland anorthosite complex. Lithos 24, 237–250.
Dewey, J.F., 1988. Extensional collapse of orogens. Tectonics 7, 1123–1139.
DeWolf, C.P., Mezger, K., 1994. Lead isotope analyses of leached feldspars: constraints on the early crustal history of the Grenville Orogen. Geochim. Cosmochim. Acta 58, 5537–5550.
Dhuime, B., Hawkesworth, C., Cawood, P., 2011. When continents formed. Science 331, 154–155.
Dickin, A.P., 2000. Crustal formation in the Grenville Province: Nd-isotope evidence. Can. J. Earth Sci. 37, 165–181.
Dickin, A.P., Higgins, M.D., 1992. Sm/Nd evidence for a major 1.5 Ga crust-forming event in the Central Grenville Province. Geology 20, 137–140.
Dickin, A.P., McNutt, R.H., 2007. The Central Metasedimentary Belt (Grenville Province) as a failed backarc rift zone: Nd isotope evidence. Earth Planet. Sci. Lett. 259, 97–106.
Dickin, A.P., McNutt, R.H., Martin, C., Guo, A., 2010. The extent of juvenile crust in the Grenville Province: Nd isotope evidence. Geol. Soc. Am. Bull. 122, 870–883.
Dons, J.A., 1960. The stratigraphy of Supracrustal Rocks, Granitization and Tectonics in the Precambrian Telemark area, Southern Norway. 212h. Norges Geologiske Undersøkelse, pp. 1–30.
Dons, J.A., Jorde, K., 1978. Geologisk kart over Norge, berggrunnskart Skien, 1:250000. Norges Geologiske Undersøkelse.
Drüppel, K., Elsässer, L., Brandt, S., Gerdes, A., 2013. Sveconorwegian mid-crustal ultrahigh-temperature metamorphism in Rogaland, Norway: U-Pb LA-ICP-MS geochronology and pseudosections of sapphirine granulites and associated paragneisses. J. Petrol. 54, 305–350.
Duchesne, J.C., 1972. Iron-titanium oxide minerals in the Bjerkrem-Sogndal massif, southwestern Norway. J. Petrol. 13, 57–81.
Duchesne, J.C., Charlier, B., 2005. Geochemistry of cumulates from the Bjerkreim-Sokndal layered intrusion (S. Norway). Part I: constraints from major elements on the mechanism of cumulate formation and on the jotunite liquid line of descent. Lithos 83, 229–254.
Duchesne, J.C., Wilmart, E., 1997. Igneous charnockites and related rocks from the Bjerkreim-Sokndal layered intrusion (SW Norway): a jotunite (hypersthene monzodiorite)-derived A-type granitoid suite. J. Petrol. 38, 337–369.
Duchesne, J.C., Maquil, R., Demaiffe, D., 1985. The Rogaland anorthosites: facts and speculations. In: Tobi, A.C., Touret, J.L. (Eds.), The Deep Proterozoic Crust in the North Atlantic provinces. Reidel, Dordrecht, pp. 449–476.
Duchesne, J.C., Wilmart, E., Demaiffe, D., Hertogen, J., 1989. Monzonorites from Rogaland (southwest Norway): a series of rocks coeval but not comagmatic with massif-type anorthosites. Precambrian Res. 45, 111–128.
Duchesne, J.C., Berza, T., Liégeois, J.P., Vander Auwera, J., 1998. Shoshonitic liquid line of descent from diorite to granite: the Late Precambrian post-collisional Tismana pluton (South Carpathians, Romania). Lithos 45, 281–303.
Duchesne, J.C., Liégeois, J.P., Vander Auwera, J., Longhi, J., 1999. The crustal tongue melting model and the origin of massive anorthosites. Terra Nova 11, 100–105.
Eliasson, T., Schöberg, H., 1991. U-Pb dating of the post-kinematic Sveconorwegian (Grenvillian) Bohus granite, SW Sweden: evidence of restitic zircon. Precambrian Res. 51, 337–350.
Eliasson, T., Ahlin, S., Petersson, J., 2003. Emplacement mechanism and thermobarometry of the Sveconorwegian Bohus granite, SW Sweden. GFF 125, 113–130.
Elminen, T., Zwingmann, H., Kaakinen, A., 2018. Constraining the timing of brittle deformation and sedimentation in southern Finland: Implications for Neoproterozoic evolution of the eastern Fennoscandian shield. Precambrian Res. 304, 110–124.
Emslie, R.F., 1985. Proterozoic anorthosite massifs. In: Tobi, A.C., Touret, J.L. (Eds.), The deep Proterozoic crust in the north Atlantic provinces. Reidel, Dordrecht, pp. 39–60.
Engvik, A.K., Mezger, K., Wortelkamp, S., Bast, R., Corfu, F., Korneliussen, A., Ihlen, P.M., Bingen, B., Austrheim, H., 2011. Metasomatism of gabbro - mineral replacement and element mobilization during the Sveconorwegian metamorphic event. J. Metamorph. Geol. 29, 399–423.
Engvik, A.K., Ihlen, P.M., Austrheim, H., 2014. Characterisation of Na-metasomatism in the Sveconorwegian Bamble Sector of South Norway. Geosci. Front. 5, 659–672.
Engvik, A.K., Bingen, B., Solli, A., 2016. Localized occurrences of granulite: P-T modeling, U-Pb geochronology and distribution of early-Sveconorwegian high-grade metamorphism in Bamble, South Norway. Lithos 240-243, 84–103.
Engvik, A.K., Corfu, F., Solli, A., Austrheim, H., 2017. Sequence and timing of mineral replacement reactions during albitisation in the high-grade Bamble lithotectonic domain, S-Norway. Precambrian Res. 291, 1–16.
Erlström, M., 2020. Chapter 24 - Carboniferous–Neogene tectonic evolution of the Fennoscandian transition zone, southern Sweden. Geol. Soc. Lond. Mem. 50, 603–620.
EUGENO-S-working-group, 1988. Crustal structure and tectonic evolution of the transition between the Baltic Shield and the North German Caledonides (the EUGENO-S Project). Tectonophysics 150, 253–348.
Evans, D.A.D., Mitchell, R.N., 2011. Assembly and breakup of the core of Paleoproterozoic-Mesoproterozoic supercontinent Nuna. Geology 39, 443–446.
Falkum, T., 1985. Geotectonic evolution of southern Scandinavia in light of a late-Proterozoic plate-collision. In: Tobi, A.C., Touret, J.L. (Eds.), The Deep Proterozoic Crust in the North Atlantic proVinces. Reidel, Dordrecht, pp. 309–322.
Falkum, T., Petersen, J.S., 1980. The Sveconorwegian orogenic belt, a case of late-Proterozoic plate collision. Geol. Rundsch. 69, 622–647.
Field, D., Drury, S.A., Cooper, D.C., 1980. Rare-earth and LIL element fractionation in high-grade charnockitic gneisses, south Norway. Lithos 13, 281–289.
Field, D., Smalley, P.C., Lamb, R.C., Råheim, A., 1985. Geochemical evolution of the 1.6-1.5 Ga-old amphibolite- granulite facies terrain, Bamble sector, Norway: dispelling the myth of grenvillian high-grade reworking. In: Tobi, A.C., Touret, J.L. (Eds.), The Deep Proterozoic Crust in the North Atlantic Provinces. Reidel, Dordrecht, pp. 567–578.
Fram, M.S., Longhi, J., 1992. Phase equilibria of dikes associated with Proterozoic anorthosite complexes. Am. Mineral. 77, 605–616.
Frost, B.R., Barnes, C.G., Collins, W.J., Arculus, R.J., Ellis, W.J., Frost, D.J., 2001. A geochemical classification for granitic rocks. J. Petrol. 42, 2033–2048.
Gabrielsen, R.H., Nystuen, J.P., Jarsve, E.M., Lundmark, A.M., 2015. The Sub-Cambrian Peneplain in southern Norway: its geological significance and its implications for post-Caledonian faulting, uplift and denudation. J. Geol. Soc. Lond. 172, 777–791.
Gammon, J.B., 1966. Fahlbands in the Precambrian of southern Norway. Econ. Geol. 61, 174–188.

Gee, D.G., Andréasson, P.G., Lorenz, H., Frei, D., Majka, J., 2015. Detrital zircon signatures of the Baltoscandian margin along the Arctic Circle Caledonides in Sweden: the Sveconorwegian connection. Precambrian Res. 265, 40–56.
Geraldes, M.C., Van Schmus, W.R., Condie, K.C., Bell, S., Teixeira, W., Babinski, M., 2001. Proterozoic geologic evolution of the SW part of the Amazonian Craton in Mato Grosso state, Brazil. Precambrian Res. 111, 91–128.
Gerya, T., 2014. Precambrian geodynamics: concepts and models. Gondwana Res. 25, 442–463.
Ghani, A.A., Atherton, M.P., 2006. The chemical character of the Late Caledonian Donegal granites, Ireland, with comments on their genesis. Trans. Roy. Soci. Edinburgh-Earth Sci. 97, 437–454.
Godin, L., Grujic, D., Law, R.D., Searle, M.P., 2006. Channel flow, ductile extrusion and exhumation in continental collision zones: an introduction. Geol. Soc. Lond., Spec. Publ. 268, 1–23.
Gong, Z., Evans, D.A.D., Elming, S.Å., Söderlund, U., Salminen, J.M., 2018. Paleomagnetism, magnetic anisotropy and U-Pb baddeleyite geochronology of the early Neoproterozoic Blekinge-Dalarna dolerite dykes, Sweden. Precambrian Res. 317, 14–32.
Gorbatschev, R., Bogdanova, S., 2006. Aspects of the Proterozoic boundary between SE and SW Sweden. Report, Department of Geology, Lund University, Sweden, pp. 1–50.
Gower, C.F., 1985. Correlations between the Grenville Province and Sveconorwegian orogenic belt - implications for Proterozoic evolution of the southern margins of the Canadian and Baltic Shields. In: Tobi, A.C., Touret, J.L. (Eds.), The Deep Proterozoic Crust in the North Atlantic Provinces. Reidel, Dordrecht, pp. 247–258.
Gower, C.F., Kamo, S., Krogh, T.E., 2008. Indentor tectonism in the eastern Grenville Province. Precambrian Res. 167, 201–212.
Granseth, A., Slagstad, T., Coint, N., Roberts, N.M.W., Røhr, T.S., Sørensen, B.E., 2020. Tectonomagmatic evolution of the Sveconorwegian orogen recorded in the chemical and isotopic compositions of 1070–920 Ma granitoids. Precambrian Res. 340, 105527.
Graversen, O., Pedersen, S., 1999. Timing of Gothian structural evolution in SE Norway: a Rb-Sr whole-rock age study. Nor. Geol. Tidsskr. 79, 47–56.
Griffin, W.L., Pearson, N.J., Belousova, E.A., Jackson, S.E., van Achterbergh, E., O'Reilly, S.Y., Shee, S.R., 2000. The Hf isotope composition of cratonic mantle: LAM-MC-ICPMS analysis of zircon megacrysts in kimberlites. Geochim. Cosmochim. Acta 64, 133–147.
Griffin, W.L., O'Reilly, S.Y., Afonso, J.C., Begg, G.C., 2009. The composition and evolution of lithospheric mantle: a re-evaluation and its tectonic implications. J. Petrol. 50, 1185–1204.
Groulier, P.A., Indares, A., Dunning, G., Moukhsil, A., Jenner, G., 2018a. Syn-orogenic magmatism over 100 m.y. in high crustal levels of the central Grenville Province: Characteristics, age and tectonic significance. Lithos 312-313, 128–152.
Groulier, P.A., Indares, A., Dunning, G., Moukhsil, A., Wälle, M., 2018b. Peri-Laurentian, Pinwarian-age oceanic arc crust preserved in the Grenville Province: Insights from the Escoumins supracrustal belt. Precambrian Res. 311, 37–64.
Grove, T.L., Chatterjee, N., Parman, S.W., Médard, E., 2006. The influence of H2O on mantle wedge melting. Earth Planet. Sci. Lett. 249, 74–89.
Guenthner, W.R., Reiners, P.W., Drake, H., Tillberg, M., 2017. Zircon, titanite, and apatite (U-Th)/He ages and age-eU correlations from the Fennoscandian Shield, southern Sweden. Tectonics 36, 1254–1274.
Hanmer, S., Corrigan, D., Pehrsson, S., Nadeau, L., 2000. SW Grenville Province, Canada: the case against post-1.4 Ga accretionary tectonics. Tectonophysics 319, 33–51.
Hansen, E., Johansson, L., Andersson, J., LaBarge, L., Harlov, D., Möller, C., Vincent, S., 2015. Partial melting in amphibolites in a deep section of the Sveconorwegian Orogen, SW Sweden. Lithos 236–237, 27–45.
Harley, S.L., 2008. Refining the P–T records of UHT crustal metamorphism. J. Metamorph. Geol. 26, 125–154.
Harley, S., Kelly, N.M., Möller, A., 2007. Zircon behaviour and the thermal histories of mountain chains. Elements 3, 25–30.
Harlov, D.E., 2000. Pressure-temperature estimation in orthopyroxene-garnet bearing granulite facies rocks, Bamble Sector, Norway. Mineral. Petrol. 69, 11–33.
Harlov, D.E., Van Den Kerkhof, A., Johansson, L., 2013. The Varberg-Torpa charnockite-granite association, SW Sweden: Mineralogy, petrology, and fluid inclusion chemistry. J. Petrol. 54, 3–40.
Hartz, E.H., Torsvik, T.H., 2002. Baltica upside down: a new plate tectonic model for Rodinia and the Iapetus Ocean. Geology 30, 255–258.
Haschke, M.R., Scheuber, E., Günther, A., Reutter, K.J., 2002. Evolutionary cycles during the Andean orogeny: repeated slab breakoff and flat subduction. Terra Nova 14, 49–55.
Hawkesworth, C., Cawood, P., Kemp, T., Storey, C., Dhuime, B., 2009. A Matter of preservation. Science 232, 49–50.
He, Z.Y., Klemd, R., Yan, L.L., Zhang, Z.M., 2018. The origin and crustal evolution of microcontinents in the Beishan orogen of the southern Central Asian Orogenic Belt. Earth Sci. Rev. 185, 1–14.
Heaman, L.M., Smalley, P.C., 1994. A U–Pb study of the Morkheia Complex and associated gneisses, south Norway: implications for disturbed Rb–Sr systems and for the temporal evolution of Mesoproterozoic magmatism in Laurentia. Geochim. Cosmochim. Acta 58, 1899–1911.
Hellström, F.A., Johansson, Å., Larson, S.Å., 2004. Age emplacement of late Sveconorwegian monzogabbroic dykes, SW Sweden. Precambrian Res. 128, 39–55.
Henderson, I.H.C., Ihlen, P.M., 2004. Emplacement of polygeneration pegmatites in relation to Sveconorwegian contractional tectonics: examples from southern Norway. Precambrian Res. 133, 207–222.
Hervé, F., Pankhurst, R.J., Fanning, C.M., Calderon, M., Yaxley, G.M., 2007. The South Patagonian batholith: 150 my of granite magmatism on a plate margin. Lithos 97, 373–394.
Herzberg, C., Condie, K., Korenaga, J., 2010. Thermal history of the Earth and its petrological expression. Earth Planet. Sci. Lett. 292, 79–88.
Hetherington, C.J., Harlov, D.E., 2008. Metasomatic thorite and uraninite inclusions in xenotime and monazite from granitic pegmatites, Hidra anorthosite massif, southwestern Norway: mechanics and fluid chemistry. Am. Mineral. 93, 806–820.
Hoffman, P.F., 1991. Did the breakout of Laurentia turn Gondwanaland inside-out? Science 252, 1409–1412.
Högdahl, K., Andersson, U.B., Eklund, O., 2004. The Transcandinavian Igneous Belt (TIB) in Sweden: A Review of Its Character and Evolution. Geological Survey of Finland, pp. 1–123 Special Paper 37.
Holland, T.J., Babu, E.V., Waters, D.J., 1996. Phase relations of osumilite and dehydration melting in pelitic rocks: a simple thermodynamic model for the KFMASH system. Contrib. Mineral. Petrol. 124, 383–394.
INSPIRE_Directive, 2007. INSPIRE Knowledge Base, Infrastructure for Spatial Information in Europe, Registry. European Commission http://inspire.ec.europa.eu/registry.
Hynes, A., Rivers, T., 2010. Protracted continental collision - evidence from the Grenville Orogen. Can. J. Earth Sci. 47, 591–620.
Ibanez-Mejia, M., Ruiz, J., Valencia, V.A., Cardona, A., Gehrels, G.E., Mora, A.R., 2011. The Putumayo Orogen of Amazonia and its implications for Rodinia reconstructions: new U-Pb geochronological insights into the Proterozoic tectonic evolution of northwestern South America. Precambrian Res. 191, 58–77.
Ibanez-Mejia, M., Pullen, A., Arenstein, J., Gehrels, G.E., Valley, J., Ducea, M.N., Mora, A.R., Pecha, M., Ruiz, J., 2015. Unraveling crustal growth and reworking processes in complex zircons from orogenic lower-crust: the Proterozoic Putumayo Orogen of Amazonia. Precambrian Res. 267, 285–310.
Indares, A., 2020. Deciphering the metamorphic architecture and magmatic patterns of large hot orogens: Insights from the central Grenville Province. Gondwana Res. 80, 385–409.
Jagoutz, O., Schmidt, M.W., 2013. The composition of the foundered complement to the continental crust and a re-evaluation of fluxes in arcs. Earth Planet. Sci. Lett. 371-372, 177–190.
Jamieson, R.A., Beaumont, C., 2013. On the origin of orogens. Geol. Soc. Am. Bull. 125, 1671–1702.
Janoušek, V., Konopásek, J., Ulrich, S., Erban, V., Tajčmanová, L., Jeřábek, P., 2010. Geochemical character and petrogenesis of Pan-African Amspoort suite of the Boundary Igneous Complex in the Kaoko Belt (NW Namibia). Gondwana Res. 18, 688–707.
Jensen, E., Corfu, F., 2016. The U–Pb age of the Finse batholith, a composite bimodal Sveconorwegian intrusion. Nor. J. Geol. 96, 171–178.
Jiménez-Mejía, D.M., Juliani, C., Cordani, U.G., 2006. P–T–t conditions of high-grade metamorphic rocks of the Garzon Massif, Andean basement, SE Colombia. J. S. Am. Earth Sci. 21, 322–336.
Johansson, Å., 2009. Baltica, Amazonia and the SAMBA connection - 1000 million years of neighbourhood during the Proterozoic? Precambrian Res. 175, 221–234.
Johansson, Å, 2014. From Rodinia to Gondwana with the 'SAMBA' model—A distant view from Baltica towards Amazonia and beyond. Precambrian Res. 244, 226–235.
Johansson, L., Lindh, A., Möller, C., 1991. Late Sveconorwegian (Grenville) high-pressure granulite facies metamorphism in southwest Sweden. J. Metamorph. Geol. 9, 283–292.
Johansson, L., Möller, C., Söderlund, U., 2001. Geochronology of eclogite facies metamorphism in the Sveconorwegian Province of SW Sweden. Precambrian Res. 106, 261–275.
Johansson, Å., Waight, T., Andersen, T., Simonsen, S.L., 2016. Geochemistry and petrogenesis of Mesoproterozoic A-type granitoids from the Danish island of Bornholm, southern Fennoscandia. Lithos 244, 94–108.
Johnson, T.E., Brown, M., Kaus, B.J.P., VanTongeren, J.A., 2013. Delamination and recycling of Archaean crust caused by gravitational instabilities. Nat. Geosci. 7, 47.
Kalsbeek, F., Thrane, K., Nutman, A.P., Jepsen, H., 2000. Late Mesoproterozoic to early Neoproterozoic history of the East Greenland Caledonides: evidence for Grenvillian orogenesis? J. Geol. Soc. Lond. 157, 1215–1225.
Kelsey, D.E., Clark, C., Hand, M., 2008. Thermobarometric modelling of zircon and monazite growth in melt-bearing systems: examples using model metapelitic and metapsammitic granulites. J. Metamorph. Geol. 26, 199–212.
Keppie, J.D., Ortega-Gutiérrez, F., 2010. 1.3-0.9 Ga Oaxaquia (Mexico): Remnant of an arc/backarc on the northern margin of Amazonia. J. S. Am. Earth Sci. 29, 21–27.
Keppie, J.D., Dostal, J., Cameron, K.L., Solari, L.A., Ortega-Gutiérrez, F., Lopez, R., 2003. Geochronology and geochemistry of Grenvillian igneous suites in the northern Oaxacan Complex, southern Mexico: tectonic implications. Precambrian Res. 120, 365–389.
Kirkland, C.L., Daly, J.S., Whitehouse, M.J., 2006. Granitic magmatism of Grenvillian and late Neoproterozoic age in Finnmark, Arctic Norway – Constraining pre-Scandian deformation in the Kalak Nappe Complex. Precambrian Res. 145, 24–52.
Kirkland, C.L., Daly, J.S., Whitehouse, M.J., 2007. Provenance and terrane evolution of the Kalak Nappe Complex, Norwegian Caledonides: Implications for Neoproterozoic paleogeography and tectonics. J. Geol. 115, 21–41.
Kirkland, C.L., Daly, J.S., Whitehouse, M.J., 2008a. Basement-cover relationships of the Kalak Nappe Complex, Arctic Norwegian Caledonides and constraints on Neoproterozoic terrane assembly in the North Atlantic region. Precambrian Res. 160, 245–276.
Kirkland, C.L., Strachan, R.A., Prave, A.R., 2008b. Detrital zircon signature of the Moine Supergroup, Scotland: contrasts and comparisons with other Neoproterozoic successions within the circum-North Atlantic region. Precambrian Res. 163, 332–350.
Knudsen, T.L., 1996. Petrology and geothermobarometry of granulite facies metapelites from the Hisøy-Torungen area, south Norway: new data on the Sveconorwegian P-T-t path of the Bamble sector. J. Metamorph. Geol. 14, 267–287.
Knudsen, T.L., Andersen, T., 1999. Petrology and geochemistry of the Tromøy gneiss complex, South Norway, an alleged example of Proterozoic depleted lower continental crust. J. Petrol. 40, 909–933.

Knudsen, T.L., Andersen, T., Whitehouse, M.J., Vestin, J., 1997. Detrital zircon ages from southern Norway - implications for the Proterozoic evolution of the southwestern Baltic Shield. Contrib. Mineral. Petrol. 130, 47–58.
Koistinen, T., Stephens, M.B., Bogatchev, V., Nordgulen, Ø., Wennerström, M., Korhonen, J., 2001. Geological Map of the Fennoscandian Shield, Scale 1:2000000. Geological Surveys of Finland Norway and Sweden and the North-West Department of Natural Resources of Russia.
Korenaga, J., 2008. Urey ratio and the structure and evolution of Earth's mantle. Rev. Geophys. 46, RG2007.
Korja, A., Lahtinen, R., Nironen, M., 2006. The Svecofennian orogen: a collage of microcontinents and island arcs. In: Gee, D.G., Stephenson, R.A. (Eds.), European Lithosphere Dynamics. Geological Society, London, Memoirs, pp. 561–578.
Köykkä, J., 2011. The sedimentation and paleohydrology of the Mesoproterozoic stream deposits in a strike-slip basin (Svinsaga Formation), Telemark, southern Norway. Sediment. Geol. 236, 239–255.
Köykkä, J., Laajoki, K., 2009. Mesoproterozoic frost action at the base of the Svinsaga Formation, central Telemark, South Norway. Nor. J. Geol. 89, 291–303.
Köykkä, J., Lamminen, J., 2011. Tidally influenced clastic epeiric sea at a Mesoproterozoic continental margin, Rjukan Rift Basin, southern Norway. Precambrian Res. 185, 164–182.
Krystopowicz, N.J., Currie, C.A., 2013. Crustal eclogitization and lithosphere delamination in orogens. Earth Planet. Sci. Lett. 361, 195–207.
Laajoki, K., 2002. The Mesoproterozoic sub-Heddal unconformity, Sauland, central Telemark, Norway. Nor. J. Geol. 82, 139–152.
Laajoki, K., Corfu, F., 2007. Lithostratigraphy of the Mesoproterozoic Vemork formation, central Telemark, Norway. Bull. Geol. Soc. Finl. 79, 41–67.
Laajoki, K., Corfu, F., Andersen, T., 2002. Lithostratigraphy and U-Pb geochronology of the Telemark supracrustals in the Bandak-Sauland area, Telemark, South Norway. Nor. J. Geol. 82, 119–138.
Lahtinen, R., Korja, A., Nironen, M., Heikkinen, P., 2009. Palaeoproterozoic accretionary processes in Fennoscandia. Geol. Soc. Lond., Spec. Publ. 318, 237–256.
Lamminen, J., 2011. Provenance and correlation of sediments in Telemark, South Norway: status of the Lifjell Group and implications for early Sveconorwegian fault tectonics. Nor. J. Geol. 91, 57–75.
Lamminen, J., Köykkä, J., 2010. The provenance and evolution of the Rjukan Rift Basin, Telemark, south Norway: The shift from a rift basin to an epicontinental sea along a Mesoproterozoic supercontinent. Precambrian Res. 181, 129–149.
Lamminen, J., Andersen, T., Nystuen, J.P., 2011. Zircon U-Pb ages and Lu-Hf isotopes from basement rocks associated with Neoproterozoic sedimentary successions in the Sparagmite Region and adjacent areas, South Norway: the crustal architecture of western Baltica. Nor. J. Geol. 91, 35–55.
Lamminen, J., Andersen, T., Nystuen, J.P., 2015. Provenance and rift basin architecture of the Neoproterozoic Hedmark Basin, South Norway inferred from U-Pb ages and Lu-Hf isotopes of conglomerate clasts and detrital zircons. Geol. Mag. 152, 80–105.
Larsen, B.T., Olaussen, S., Sundvoll, B., Heeremans, M., 2008. The Permo-Carboniferous Oslo Rift through six stages and 65 million years. Episodes 31, 52–58.
Larsson, D., Söderlund, U., 2005. Lu-Hf apatite geochronology of mafic cumulates: an example from a Fe-Ti mineralization at Smålands Taberg, southern Sweden. Chem. Geol. 224, 201–211.
Lassen, A., Thybo, H., 2012. Neoproterozoic and Palaeozoic evolution of SW Scandinavia based on integrated seismic interpretation. Precambrian Res. 204, 75–104.
Laurent, A., Janoušek, V., Magna, T., Schulmann, K., Míková, J., 2014. Petrogenesis and geochronology of a post-orogenic calc-alkaline magmatic association: the Žulová Pluton, Bohemian Massif. J. Geosci. 59, 415–440.
Laurent, A.T., Seydoux-Guillaume, A.M., Duchene, S., Bingen, B., Bosse, V., Datas, L., 2016. Sulphate incorporation in monazite lattice and dating the cycle of sulphur in metamorphic belts. Contrib. Mineral. Petrol. 171, 1–19.
Laurent, O., Couzinié, S., Zeh, A., Vanderhaeghe, O., Moyen, J.F., Villaros, A., Gardien, V., Chelle-Michou, C., 2017. Protracted, coeval crust and mantle melting during Variscan late-orogenic evolution: U–Pb dating in the eastern French Massif Central. Intern. J. Earth Sci. 106, 421–451.
Laurent, A.T., Bingen, B., Duchene, S., Whitehouse, M.J., Seydoux-Guillaume, A.M., Bosse, V., 2018a. Decoding protracted zircon geochronological record in ultra-high temperature granulite, and persistence of partial melting in the crust, Rogaland, Norway. Contrib. Mineral. Petrol. 173, 29.
Laurent, A.T., Duchene, S., Bingen, B., Bosse, V., Seydoux-Guillaume, A.M., 2018b. Two successive phases of ultrahigh temperature metamorphism in Rogaland, S. Norway: evidence from Y-in-monazite thermometry. J. Metamorp. Geol. 36, 1009–1037.
Lawlor, P.J., Ortega-Gutiérrez, F., Cameron, K.L., Ochoa-Camarillo, H., Lopez, R., Sampson, D.E., 1999. U-Pb geochronology, geochemistry, and provenance of the Grenvillian Huiznopala Gneiss of Eastern Mexico. Precambrian Res. 94, 73–99.
Levander, A., Schmandt, B., Miller, M.S., Liu, K., Karlstrom, K.E., Crow, R.S., Lee, C.T.A., Humphreys, E.D., 2011. Continuing Colorado plateau uplift by delamination-style convective lithospheric downwelling. Nature 472, 461–465.
Li, Z.X., Bogdanova, S.V., Collins, A.S., Davidson, A., De Waele, B., Ernst, R.E., Fitzsimons, I.C.W., Fuck, R.A., Gladkochub, D.P., Jacobs, J., Karlstrom, K.E., Lu, S., Natapov, L.M., Pease, V., Pisarevsky, S.A., Thrane, K., Vernikovsky, V., 2008. Assembly, configuration, and break-up history of Rodinia: a synthesis. Precambrian Res. 160, 179–210.
Li, Z.-H., Liu, M., Gerya, T., 2016. Lithosphere delamination in continental collisional orogens: A systematic numerical study. J. Geophys. Res. Solid Earth 121, 5186–5211.
Liégeois, J.P., Navez, J., Hertogen, J., Black, R., 1998. Contrasting origin of post-collisional high-K calc-alkaline and shoshonitic versus alkaline and peralkaline granitoids. The use of sliding normalization. Lithos 45, 1–28.
Lindh, A., Gorbatschev, R., Lundegårdh, P.H., 1998. Beskrivning till berggrundskartan över Värmlands Län; Västra Värmlands Berggrund. Sveriges Geologiska Undersökning Ser. Ba 45 (2), 1–405.
Longhi, J., 2005. A mantle or mafic crustal source for Proterozoic anorthosites? Lithos 83, 183–198.
Longhi, J., Vander Auwera, J., Fram, M.S., Duchesne, J.C., 1999. Some phase equilibrium constraints on the origin of Proterozoic (massif) anorthosites and related rocks. J. Petrol. 40, 339–362.
Lorenz, H., Gee, D.G., Larionov, A.N., Majka, J., 2012. The Grenville-Sveconorwegian orogen in the high Arctic. Geol. Mag. 149, 875–891.
Loron, C., Moczydłowska, M., 2018. Tonian (Neoproterozoic) eukaryotic and prokaryotic organic-walled microfossils from the upper Visingsö Group, Sweden. Palynology 42, 220–254.
Lundmark, A.M., Corfu, F., 2008. Late-orogenic Sveconorwegian massif anorthosite in the Jotun Nappe Complex, SW Norway, and causes of repeated AMCG magmatism along the Baltoscandian margin. Contrib. Mineral. Petrol. 155, 147–163.
Lundmark, A.M., Lamminen, J., 2016. The provenance and setting of the Mesoproterozoic Dala Sandstone, western Sweden, and paleogeographic implications for southwestern Fennoscandia. Precambrian Res. 275, 197–208.
Lundqvist, I., Skiöld, T., 1993. U-Pb zircon dating of volcanic rocks of the Åmål Group, western Sweden. In: Lundqvist, T. (Ed.), Radiometric dating results. Sveriges Geologiska Undersökning, Research Papers, Uppsala, pp. 24–30.
Maijer, C., 1987. Day 7 - The metamorphic envelope of the Rogaland intrusive complex. In: Maijer, C., Padget, P. (Eds.), The geology of southernmost Norway: an excursion guide. Norges Geologiske Undersøkelse, pp. 68–73 Special Publication No 1.
Maijer, C., Verschure, R.H., 1998. Petrology and isotope geology of the Hunnedalen monzonoritic dyke swarm, SW Norway: a possible late expression of Egersund anorthosite magmatism. Norges Geol. Unders. Bull. 434, 83–107.
Marcantonio, F., McNutt, R.H., Dickin, A.P., Heaman, L.M., 1990. Isotopic evidence for the crustal evolution of the Frontenac Arch in the Grenville Province of Ontario, Canada. Chem. Geol. 83, 297–314.
Mattila, J., Viola, G., 2014. New constraints on 1.7 Gyr of brittle tectonic evolution in southwestern Finland derived from a structural study at the site of a potential nuclear waste repository (Olkiluoto Island). Journal of Structural Geology 67 (Part A), 50–74.
McLelland, J.M., Daly, J.S., Chiarenzelli, J., 1993. Sm–Nd and U–Pb isotopic evidence of juvenile crust in the Adirondack Lowlands and implications for the evolution of the Adirondack Mts. J. Geol. 101, 97–105.
Menuge, J.F., 1985. Neodymium, isotope evidence for the age and origin of the Proterozoic of Telemark, south Norway. In: Tobi, A.C., Touret, J.L. (Eds.), The deep Proterozoic crust in the north Atlantic provinces. Reidel, Dordrecht, pp. 435–448.
Menuge, J.F., 1988. The petrogenesis of massif anorthosites: a Nd and Sr isotopic investigation of the Proterozoic of Rogaland-Vest Agder, SW Norway. Contrib. Mineral. Petrol. 98, 363–373.
Merdith, A.S., Collins, A.S., Williams, S.E., Pisarevsky, S., Foden, J.D., Archibald, D.B., Blades, M.L., Alessio, B.L., Armistead, S., Plavsa, D., Clark, C., Müller, R.D., 2017. A full-plate global reconstruction of the Neoproterozoic. Gondwana Res. 50, 84–134.
Milne, K.P., Starmer, I.C., 1982. Extreme differentiation in the Proterozoic Gjerstad-Morkeheia complex of South Norway. Contrib. Mineral. Petrol. 79, 381–393.
Moczydłowska, M., Pease, V., Willman, S., Wickström, L., Agic, H., 2018. A Tonian age for the Visingsö Group in Sweden constrained by detrital zircon dating and biochronology: implications for evolutionary events. Geol. Mag. 155, 1175–1189.
Möller, C., 1998. Decompressed eclogites in the Sveconorwegian (-Grenvillian) orogen of SW Sweden: petrology and tectonic implications. J. Metamorph. Geol. 16, 641–656.
Möller, C., 1999. Sapphirine in SW Sweden: a record of Sveconorwegian (-Grenvillian) late-orogenic tectonic exhumation. J. Metamorph. Geol. 17, 127–141.
Möller, C., Andersson, J., 2018. Metamorphic zoning and behaviour of an underthrusting continental plate. J. Metamorph. Geol. 36, 567–589.
Möller, C., Söderlund, U., 1997. Age constraints on the regional deformation within the Eastern Segment, S Sweden: late Sveconorwegian granite dyke intrusion and metamorphic deformational relations. GFF 119, 1–12.
Möller, A., O'Brien, P.J., Kennedy, A., Kröner, A., 2002. Polyphase zircon in ultrahigh-temperature granulites (Rogaland, SW Norway): constraints for Pb diffusion in zircon. J. Metamorph. Geol. 20, 727–740.
Möller, A., O'Brien, P.J., Kennedy, A., Kröner, A., 2003. Linking growth episodes of zircon and metamorphic textures to zircon chemistry: an example from the ultrahigh-temperature granulites of Rogaland (SW Norway). In: Vance, D., Müller, W., Villa, I.M. (Eds.), Geochronology: linking the isotopic record with petrology and textures. London, Special Publications, Geological Society, pp. 65–81.
Möller, C., Andersson, J., Lundqvist, I., Hellström, F.A., 2007. Linking deformation, migmatite formation and zircon U-Pb geochronology in polymetamorphic gneisses, Sveconorwegian province, Sweden. J. Metamorph. Geol. 25, 727–750.
Möller, C., Andersson, J., Dyck, B., Antal Lundin, I., 2015. Exhumation of an eclogite terrane as a hot migmatitic nappe, Sveconorwegian orogen. Lithos 226, 147–168.
Morton, R.D., 1971. Geological investigations in the Bamble sector of the Fennoscandian Shield, S. Norway. No II. Metasediments and metapyroclastics (?) within the Precambrian metamorphic suite of the S Norwegian Skaergaard. Nor. Geol. Tidsskr. 51, 63–83.
Moyen, J.F., Laurent, O., Chelle-Michou, C., Couzinié, S., Vanderhaeghe, O., Zeh, A., Villaros, A., Gardien, V., 2017. Collision vs. subduction-related magmatism: two contrasting ways of granite formation and implications for crustal growth. Lithos 277, 154–177.
Mulch, A., Cosca, M.A., Andresen, A., Fiebig, J., 2005. Time scales of deformation and exhumation in extensional detachment systems determined by high-spatial resolution in situ UV-laser $^{40}Ar/^{39}Ar$ dating. Earth Planet. Sci. Lett. 233, 375–390.
Müller, A., Ihlen, P.M., Snook, B., Larsen, R., Flem, B., Bingen, B., Williamson, B.J., 2015. The chemistry of quartz in granitic pegmatites of southern Norway: petrogenetic and economic implications. Econ. Geol. 110, 1737–1757.
Müller, A., Romer, R.L., Pedersen, R.B., 2017. The Sveconorwegian Pegmatite Province – Thousands of pegmatites without parental granite. Can. Mineral. 55, 283–315.

Munz, I.A., 1990. Whiteschists and orthoamphibole-cordierite rocks and the P-T-t path of the Modum Complex, South Norway. Lithos 24, 181–200.
Munz, I.A., Morvik, R., 1991. Metagabbros in the Modum Complex, southern Norway: an important heat source for Sveconorwegian metamorphism. Precambrian Res. 52, 97–113.
Munz, I.A., Wayne, D., Austrheim, H., 1994. Retrograde fluid infiltration in the high-grade Modum Complex, South Norway - Evidence for age, source and REE mobility. Contrib. Mineral. Petrol. 116, 32–46.
Neilson, J.C., Kokelaar, B.P., Crowley, Q.G., 2009. Timing, relations and cause of plutonic and volcanic activity of the Siluro-Devonian post-collision magmatic episode in the Grampian Terrane, Scotland. J. Geol. Soc. Lond. 166, 545–561.
Nielsen, F.M., Campbell, I.H., McCulloch, M., Wilson, J.R., 1996. A strontium isotopic investigation of the Bjerkreim-Sokndal layered intrusion, Southwest Norway. J. Petrol. 37, 171–193.
Nijland, T.G., Maijer, C., 1993. The regional amphibolite to granulite facies transition at Arendal, Norway: evidence for a thermal dome. Neues Jahrbuch für Mineralogie, Abhandlungen 165, 191–221.
Nijland, T.G., Maijer, C., Senior, A., Verschure, R.H., 1993. Primary sedimentary structures and compositions of the high-grade metamorphic Nidelva Quartzite Complex (Bamble, Norway), and the origin of nodular gneisses. Proceedings Koninklijke Nederlandse Akademie van Wetenschappen 96, 217–232.
Nijland, T.G., Touret, J.L.R., Visser, D., 1998. Anomalously low temperature orthopyroxene, spinel, and sapphirine occurrences in metasediments from the Bamble amphibolite-to-granulite facies transition zone (South Norway): possible evidence for localized action of saline fluids. J. Geol. 106, 575–590.
Nijland, T.G., deHaas, G.J.L.M., Andersen, T., 2000. Rifting-related (sub)alkaline magmatism in the Bamble sector (Norway) during the 'Gothian'–Sveconorwegian interlude. GFF 122, 297–305.
Nijland, T.G., Harlov, D.E., Andersen, T., 2014. The Bamble Sector, South Norway: a review. Geosci. Front. 5, 635–658.
Nordgulen, Ø., 1999. Geologisk Kart Over Norge, Berggrunnskart Hamar, 1:250000. Norges Geologiske Undersøkelse.
Nystuen, J.P., Andresen, A., Kumpulainen, R.A., Siedlecka, A., 2008. Neoproterozoic basin evolution in Fennoscandia, East Greenland and Svalbard. Episodes 31, 35–43.
Olesen, O., Smethurst, M.A., Torsvik, T.H., Bidstrup, T., 2004. Sveconorwegian igneous complexes beneath the Norwegian-Danish Basin. Tectonophysics 387, 105–130.
Olivarius, M., Friis, H., Kokfelt, T.F., Wilson, J.R., 2015. Proterozoic basement and Palaeozoic sediments in the Ringkøbing–Fyn High characterized by zircon U–Pb ages and heavy minerals from Danish onshore wells. Bull. Geol. Soc. Den. 63, 29–43.
Page, L.M., Möller, C., Johansson, L., 1996a. $^{40}Ar/^{39}Ar$ geochronology across the Mylonite Zone and the Southwestern Granulite Province in the Sveconorwegian Orogen of S Sweden. Precambrian Res. 79, 239–259.
Page, L.M., Stephens, M.B., Wahlgren, C.H., 1996b. $^{40}Ar/^{39}Ar$ geochronological constraints on the tectonothermal evolution of the Eastern Segment of the Sveconorwegian Orogen, south-central Sweden. In: Brewer, T.S. (Ed.), Precambrian crustal evolution in the North Atlantic Region. London, Special Publications, Geological Society, pp. 315–330.
Paludan, J., Hansen, U.B., Olesen, N.O., 1994. Structural evolution of the Precambrian Bjerkreim–Sokndal intrusion, South Norway. Nor. Geol. Tidsskr. 74, 185–198.
Park, R.G., Åhäll, K.I., Boland, M.P., 1991. The Sveconorwegian shear-zone network of SW Sweden in relation to mid-Proterozoic plate movements. Precambrian Res. 49, 245–260.
Pasteels, P., Demaiffe, D., Michot, J., 1979. U-Pb and Rb-Sr geochronology of the eastern part of the south Rogaland igneous complex, southern Norway. Lithos 12, 199–208.
Pearce, J.A., Harris, N.B., Tindle, A.G., 1984. Trace element discrimination diagrams for the tectonic interpretation of granitic rocks. J. Petrol. 25, 956–983.
Peccerillo, A., Taylor, S.R., 1976. Geochemistry of eocene calc-alkaline volcanic rocks from the Kastamonu area, Northern Turkey. Contrib. Mineral. Petrol. 58, 63–81.
Pedersen, S., 1981. Rb-Sr age determinations on late Proterozoic granitoids from the Evje area, South Norway. Bull. Geol. Soc. Den. 29, 129–143.
Pedersen, S., Andersen, T., Konnerup-Madsen, J., Griffin, W.L., 2009. Recurrent Mesoproterozoic continental magmatism in South-Central Norway. Int. J. Earth Sci. 98, 1151–1171.
Persson-Nilsson, K., Lundqvist, L., 2014. Abstract. The Gillberga synform - and upper-crustal orogenic lid?, 31st Nordic Geological Winter Meeting. Geologiska Föreningen, Lund, Sweden.
Petersson, A., Scherstén, A., Andersson, J., Möller, C., 2015a. Zircon U-Pb and Hf isotopes from the eastern part of the Sveconorwegian Orogen, SW Sweden: Implications for the growth of Fennoscandia. In: Roberts, N.M.W., van Kranendonk, M., Parman, S., Shirey, S., Clift, P.D. (Eds.), Continent Formation Through Time. Geological Society, Special Publications, London, pp. 281–303.
Petersson, A., Scherstén, A., Bingen, B., Gerdes, A., Whitehouse, M.J., 2015b. Mesoproterozoic continental growth: U-Pb-Hf-O zircon record in the Idefjorden Terrane, Sveconorwegian Orogen. Precambrian Res. 261, 75–95.
Pettersson, C.H., Pease, V., Frei, D., 2009. U-Pb zircon provenance of metasedimentary basement of the Northwestern Terrane, Svalbard: implications for the Grenvillian-Sveconorwegian orogeny and development of Rodinia. Precambrian Res. 175, 206–220.
Piñán-Llamas, A., Andersson, J., Möller, C., Johansson, L., Hansen, E., 2015. Polyphasal foreland-vergent deformation in a deep section of the 1 Ga Sveconorwegian orogen. Precambrian Res. 265, 121–149.
Pisarevsky, S.A., Elming, S.Å., Pesonen, L.J., Li, Z.X., 2014. Mesoproterozoic paleogeography: Supercontinent and beyond. Precambrian Res. 244, 207–225.
Plank, T., Kelley, K.A., Zimmer, M.M., Hauri, E.H., Wallace, P.J., 2013. Why do mafic arc magmas contain c. 4 wt% water on average? Earth Planet. Sci. Lett. 364, 168–179.
Poudjom Djomani, Y.H., O'Reilly, S.Y., Griffin, W.L., Morgan, P., 2001. The density structure of subcontinental lithosphere through time. Earth Planet. Sci. Lett. 184, 605–621.
Pulsipher, M.A., Dehler, C.M., 2019. U-Pb detrital zircon geochronology, petrography, and synthesis of the middle Neoproterozoic Visingsö Group, Southern Sweden. Precambrian Res. 320, 323–333.
Rämö, O.T., 1991. Petrogenesis of the Proterozoic rapakivi granites and related basic rocks of southeastern Fennoscandia: Nd and Pb isotopic and general geochemic constraints. Geol. Surv. Finl. Bull. 355, 1–161.
Rey, P.F., Houseman, G., 2006. Lithospheric scale gravitational flow: the impact of body forces on orogenic processes from Archaean to Phanerozoic. Geol. Soc. Lond., Spec. Publ. 253, 153–167.
Rey, P., Vanderhaeghe, O., Teyssier, C., 2001. Gravitational collapse of the continental crust: definition, regimes and modes. Tectonophysics 342, 435–449.
Ripa, M., Stephens, M.B., 2020a. Chapter 9 - Continental magmatic arc and siliciclastic sedimentation in the far-field part of a 1.7 Ga accretionary orogen. Geol. Soc. Lond. Mem. 50, 253–268.
Ripa, M., Stephens, M.B., 2020b. Chapter 10 - Magmatism (1.6–1.4 Ga) and Mesoproterozoic sedimentation related to intracratonic rifting coeval with distal accretionary orogenesis. Geol. Soc. Lond. Mem. 50, 269–288.
Ripa, M., Stephens, M.B., 2020c. Chapter 12 - Dolerites (1.27–1.25 Ga) and alkaline ultrabasic dykes (c. 1.14 Ga) related to intracratonic rifting. Geol. Soc. Lond. Mem. 50, 315–323.
Ripa, M., Stephens, M.B., 2020d. Chapter 13 - Siliciclastic sedimentation in a foreland basin to the Sveconorwegian orogen and dolerites (0.98–0.95 Ga) related to intracratonic rifting. Geol. Soc. Lond. Mem. 50, 325–333.
Rivers, T., 2008. Assembly and preservation of lower, mid, and upper orogenic crust in the Grenville Province-Implications for the evolution of large hot long-duration orogens. Precambrian Res. 167, 237–259.
Rivers, T., 2012. Upper-crustal orogenic lid and mid-crustal core complexes: signature of a collapsed orogenic plateau in the hinterland of the Grenville Province. Can. J. Earth Sci. 49, 1–42.
Roberts, N.M.W., 2013. The boring billion? – Lid tectonics, continental growth and environmental change associated with the Columbia supercontinent. Geosci. Front. 4, 681–691.
Roberts, N.M.W., Slagstad, T., 2015. Continental growth and reworking on the edge of the Columbia and Rodinia supercontinents; 1.86–0.9 Ga accretionary orogeny in southwest Fennoscandia. Int. Geol. Rev. 57, 1582–1606.
Roberts, N.M.W., Slagstad, T., Parrish, R.R., Norry, M.J., Marker, M., Horstwood, M.S.A., 2013. Sedimentary recycling in arc magmas: geochemical and U-Pb-Hf-O constraints on the Mesoproterozoic Suldal Arc, SW Norway. Contrib. Mineral. Petrol. 165, 507–523.
Robins, B., Tumyr, O., Tysseland, M., Garmann, L.B., 1997. The Bjerkreim-Sokndal layered intrusion, Rogaland, SW Norway: Evidence from marginal rocks for a jotunite parent magma. Lithos 39, 121–133.
Rodhe, A., 1987. Depositional environments and lithostratigraphy of the Middle Proterozoic Almesåkra group, southern Sweden. Sveriges Geologiska Undersökning Ca 69, 1–80.
Roffeis, C., Corfu, F., 2014. Caledonian nappes of southern Norway and their correlation with Sveconorwegian basement domains. In: Corfu, F., Gasser, D., Chew, D.M. (Eds.), New perspectives on the Caledonides of Scandinavia and related areas. London, Special Publications, Geological Society, pp. 193–221.
Rogers, J.J.W., Santosh, M., 2002. Configuration of Columbia, a Mesoproterozoic Supercontinent. Gondwana Res. 5, 5–22.
Røhr, T.S., Bingen, B., Robinson, P., Reddy, S.M., 2013. Geochronology of Paleoproterozoic augen gneisses in the Western Gneiss Region, Norway: evidence for Sveconorwegian zircon neocrystallization and Caledonian zircon deformation. J. Geol. 121, 105–128.
Romer, R.L., Smeds, S.A., 1996. U-Pb columbite ages of pegmatites from Sveconorwegian terranes in southwestern Sweden. Precambrian Res. 76, 15–30.
Royden, L.H., Burchfiel, B.C., van der Hilst, R.D., 2008. The geological evolution of the Tibetan Plateau. Science 321, 1054–1058.
Rubatto, D., Hermann, J., Berger, J., Engi, M., 2009. Protracted fluid-induced melting during Barrovian metamorphism in the Central Alps. Contrib. Mineral. Petrol. 158, 703–722.
Ruiz, J., Patchett, P.J., Ortega-Gutierrez, F., 1988. Proterozoic and Phanerozoicbasement terranes of Mexico from Nd isotopic studies. Geol. Soc. Am. Bull. 100, 274–281.
Saintot, A., Stephens, M.B., Viola, G., Nordgulen, Ø., 2011. Brittle tectonic evolution and paleostress field reconstruction in the southwestern part of the Fennoscandian Shield, Forsmark, Sweden. Tectonics 30 (4). https://doi.org/10.1029/2010tc002781.
Schärer, U., Wilmart, E., Duchesne, J.C., 1996. The short duration and anorogenic character of anorthosite magmatism: U-Pb dating of the Rogaland complex, Norway. Earth Planet. Sci. Lett. 139, 335–350.
Scheiber, T., Viola, G., Bingen, B., Peters, M., Solli, A., 2015. Multiple reactivation and strain localization along a Proterozoic orogen-scale deformation zone: the Kongsberg-Telemark boundary in southern Norway revisited. Precambrian Res. 265, 78–103.
Scherer, E., Munker, C., Mezger, K., 2001. Calibration of the lutetium-hafnium clock. Science 293, 683–687.
Scherstén, A., Årebäck, H., Cornell, D., Hoskin, P., Åberg, A., Armstrong, R., 2000. Dating mafic-ultramafic intrusions by ion-microprobing contact-melt zircon: examples from SW Sweden. Contrib. Mineral. Petrol. 139, 115–125.
Schiellerup, H., Lambert, D.D., Prestvik, T., Robins, B., McBride, J.S., Larsen, R.B., 2000. Re–Os isotopic evidence for a lower crustal origin of massif-type anorthosites. Nature 405, 781–784.
Seydoux-Guillaume, A.M., Montel, J.M., Bingen, B., Bosse, V., de Parseval, P., Paquette, J.L., Janots, E., Wirth, R., 2012. Low-temperature alteration of monazite: Fluid mediated coupled dissolution-precipitation, irradiation damage, and disturbance of the U-Pb and Th-Pb chronometers. Chem. Geol. 330-331, 140–158.

Sigmond, E.M.O., 1975. Geologisk kart over Norge, berggrunnskart Sauda, 1:250000. Norges geologiske undersøkelse, Trondheim.
Sigmond, E.M.O., 1978. Beskrivelse til det berggrunnsgeologiske kartbladet Sauda 1: 250000. Norges Geol. Unders. Bull. 341, 1–94.
Sigmond, E.M.O., 1985. The Mandal–Ustaoset line, a newly discovered major fault zone in south Norway. In: Tobi, A.C., Touret, J.L. (Eds.), The Deep Proterozoic Crust in the North Atlantic provinces. Reidel, Dordrecht, pp. 323–331.
Sigmond, E.M.O., 1998. Geologisk kart over Norge, berggrunnskart Odda, 1:250000. Norges Geologiske Undersøkelse, Trondheim.
Sigmond, E.M.O., Ragnhildstveit, J., 2004. Berggrunnskart Kalhovd 1515 II, 1:50000. Norges Geologiske Undersøkelse, Trondheim.
Sizova, E., Gerya, T., Brown, M., 2014. Contrasting styles of Phanerozoic and Precambrian continental collision. Gondwana Res. 25, 522–545.
Slagstad, T., Roberts, N.M.W., Marker, M., Røhr, T.S., Schiellerup, H., 2013. A non-collisional, accretionary Sveconorwegian orogen. Terra Nova 25, 30–37.
Slagstad, T., Roberts, N.M.W., Kulakov, E., 2017. Linking orogenesis across a supercontinent; the Grenvillian and Sveconorwegian margins on Rodinia. Gondwana Res. 44, 109–115.
Slagstad, T., Roberts, N.M.W., Coint, N., Høy, I., Sauer, S., Kirkland, K.L., Marker, M., Røhr, T.S., Henderson, I.H.C., Stormoen, M.A., Skår, Ø., Sørensen, B.E., Bybee, G.M., 2018. Magma-driven, high-grade metamorphism in the Sveconorwegian Province, southwest Norway, during the terminal stages of Fennoscandian Shield evolution. Geosphere 14, 861–882.
Slagstad, T., Kulakov, E., Kirkland, C.L., Roberts, N.M.W., Ganerød, M., 2019. Breaking the Grenville–Sveconorwegian link in Rodinia reconstructions. Terra Nova 31, 430–437.
Slagstad, T., Marker, M., Roberts, N.M.W., Saalmann, K., Kirkland, C.L., Kulakov, E., Ganerød, M., Røhr, T.S., Møkkelgjerd, S.H.H., Granseth, A., Sørensen, B.E., 2020. The Sveconorwegian orogeny – Reamalgamation of the fragmented southwestern margin of Fennoscandia. Precambrian Res. 350, 105877.
Sláma, J., Walderhaug, O., Fonneland, H., Košler, J., Pedersen, R.B., 2011. Provenance of Neoproterozoic to Upper Cretaceous sedimentary rocks, eastern Greenland: Implications for recognizing the sources of sediments in the Norwegian Sea. Sediment. Geol. 238, 254–267.
Sobolev, A.V., Chaussidon, M., 1996. H_2O concentrations in primary melts from supra-subduction zones and mid-ocean ridges: implications for H_2O storage and recycling in the mantle. Earth Planet. Sci. Lett. 137, 45–55.
Söderlund, U., Ask, R., 2006. Evidence for two pulses (1215-1224 and ca. 1205 Ma) of bimodal magmatism along the Protogine Zone, S Sweden. GFF 128, 303–310.
Söderlund, U., Jarl, L.G., Persson, P.O., Stephens, M.B., Wahlgren, C.H., 1999. Protolith ages and timing of deformation in the eastern, marginal part of the Sveconorwegian orogen, southwestern Sweden. Precambrian Res. 94, 29–48.
Söderlund, U., Möller, C., Andersson, J., Johansson, L., Whitehouse, M.J., 2002. Zircon geochronology in polymetamorphic gneisses in the Sveconorwgian orogen, SW Sweden: ion microprobe evidence for 1.46-1.42 Ga and 0.98-0.96 Ga reworking. Precambrian Res. 113, 193–225.
Söderlund, P., Söderlund, U., Möller, C., Gorbatschev, R., Rodhe, A., 2004. Petrology and ion microprobe U-Pb chronology applied to a metabasic intrusion in southern Sweden: a study on zircon formation during metamorphism and deformation. Tectonics 23 (5), TC5005. https://doi.org/10.1029/2003TC001498.
Söderlund, U., Isachsen, C.E., Bylund, G., Heaman, L.M., Patchett, P.J., Vervoort, J.D., Andersson, U.B., 2005. U-Pb baddeleyite ages, and Hf, Nd isotope chemistry constraining repeated mafic magmatism in the Fennoscandian Shield from 1.6 to 0.9 Ga. Contrib. Mineral. Petrol. 150, 174–194.
Söderlund, U., Elming, S.Å., Ernst, R.E., Schissel, D., 2006. The Central Scandinavian Dolerite Group - Protracted hotspot activity or back-arc magmatism? Constraints from U-Pb baddeleyite geochronology and Hf isotopic data. Precambrian Res. 150, 136–152.
Söderlund, U., Hellström, F.A., Kamo, S.L., 2008a. Geochronology of high-pressure mafic granulite dykes in SW Sweden; tracking the P-T-t path of metamorphism using Hf isotopes in zircon and baddeleyite. J. Metamorph. Geol. 26, 539–560.
Söderlund, U., Karlsson, C., Johansson, L., Larsson, K., 2008b. The Kullaberg peninsula - a glimpse of the Proterozoic evolution of SW Fennoscandia. GFF 130, 1–10.
Solari, L.A., Ortega-Gutiérrez, F., Elías-Herrera, M., Ortega-Obregón, C., Macías-Romo, C., Reyes-Salas, M., 2014. Detrital provenance of the Grenvillian Oaxacan Complex, southern Mexico: a zircon perspective. Int. J. Earth Sci. 103, 1301–1315.
Spear, F.S., 1993. Metamorphic phase equilibria and pressure-temperature-time paths. Mineralogical Society of America, Monograph, Washington D.C.
Spencer, C.J., Kirkland, C.L., Prave, A.R., Strachan, R.A., Pease, V., 2019. Crustal reworking and orogenic styles inferred from zircon Hf isotopes: Proterozoic examples from the North Atlantic region. Geosci. Front. 10, 417–424.
Spencer, C.J., Roberts, N.M.W., Cawood, P.A., Hawkesworth, C.J., Prave, A.R., Antonini, A.S.M., Horstwood, M.S.A., 2014. Intermontane basins and bimodal volcanism at the onset of the Sveconorwegian Orogeny, southern Norway. Precambrian Res. 252, 107–118.
Stacey, J.S., Kramers, J.D., 1975. Approximation of terrestrial lead isotope evolution by a two-stage model. Earth Planet. Sci. Lett. 26, 207–221.
Starmer, I.C., 1985. The evolution of the south Norwegian Proterozoic as revealed by the major and mega-tectonics of the Kongsberg and Bamble sector. In: Tobi, A.C., Touret, J.L. (Eds.), The Deep Proterozoic Crust in the North Altantic Provinces. Reidel, Dordrecht, pp. 259–290.
Starmer, I.C., 1991. The Proterozoic evolution of the Bamble sector shear belt, southern Norway: correlations across southern Scandinavia and the Grenvillian controversy. Precambrian Res. 49, 107–139.
Stein, H.J., Bingen, B., 2002. 1.05-1.01 Ga Sveconorwegian metamorphism and deformation of the supracrustal sequence at Sæsvatn, South Norway: Re-Os dating of Cu-Mo mineral occurrences. In: Blundell, D., Neubauer, F., von Quadt, A. (Eds.), The Timing and Location of Major ore Deposits in an Evolving Orogen. Geological Society, Special Publications, London, pp. 319–335.
Stephens, M.B., 2020. Chapter 8 - Outboard-migrating accretionary orogeny at 1.9–1.8 Ga (Svecokarelian) along a margin to the continent Fennoscandia. Geol. Soc. Lond. Mem. 50, 237–250.
Stephens, M.B., Wahlgren, C.H., 2020a. Chapter 15 - Polyphase (1.9–1.8, 1.5–1.4 and 1.0–0.9 Ga) deformation and metamorphism of Proterozoic (1.9–1.2 Ga) continental crust, Eastern Segment, Sveconorwegian orogen. Geol. Soc. Lond. Mem. 50, 351–396.
Stephens, M.B., Wahlgren, C.H., 2020b. Chapter 17 - Accretionary orogens reworked in an overriding plate setting during protracted continent–continent collision, Sveconorwegian orogen, southwestern Sweden. Geol. Soc. Lond. Mem. 50, 435–448.
Stephens, M.B., Wahlgren, C.H., Weijermars, R., Cruden, A.R., 1996. Left lateral transpressive deformation and its tectonic implications, Sveconorwegian Orogen, Baltic Shield, Southwestern Sweden. Precambrian Res. 79, 261–279.
Stephens, M.B., Bergström, U., Wahlgren, C.H., 2020. Chapter 14 - Regional context and lithotectonic framework of the 1.1–0.9 Ga Sveconorwegian orogen, southwestern Sweden. Geol. Soc. Lond. Mem. 50, 337–349.
Strachan, R.A., Nutman, A.P., Friderichsen, J.D., 1995. SHRIMP U-Pb geochronology and metamorphic history of the Smallefjord sequence, NE Greenland Caledonides. J. Geol. Soc. Lond. 152, 779–784.
Strachan, R.A., Prave, A.R., Kirkland, C.L., Storey, C.D., 2013. U–Pb detrital zircon geochronology of the Dalradian Supergroup, Shetland Islands, Scotland: implications for regional correlations and Neoproterozoic–Palaeozoic basin development. J. Geol. Soc. Lond. 170, 905–916.
Thybo, H., 2001. Crustal structure along the EGT profile across the Tornquist Fan interpreted from seismic, gravity and magnetic data. Tectonophysics 334, 155–190.
Tobi, A.C., Hermans, G.A., Maijer, C., Jansen, J.B.H., 1985. Metamorphic zoning in the high-grade Proterozoic of Rogaland-Vest Agder, SW Norway. In: Tobi, A.C., Touret, J.L. (Eds.), The Deep Proterozoic Crust in the North Atlantic provinces. Reidel, Dordrecht, pp. 477–497.
Tohver, E., Bettencourt, J.S., Tosdal, R., Mezger, K., Leite, W.B., Payolla, B.L., 2004a. Terrane transfer during the Grenville orogeny: tracing the Amazonian ancestry of southern Appalachian basement through Pb and Nd isotopes. Earth Planet. Sci. Lett. 228, 161–176.
Tohver, E., van der Pluijm, B.A., Mezger, K., Essene, E., Scandolara, J.E., Rizzotto, G., 2004b. Significance of the Nova Bresilândia metasedimentary belt in western Brazil: redefining the Mesoproterozoic boundary of the Amazon craton. Tectonics, 23 TC6004. https://doi.org/10.1029/2003TC001563 001561-001520.
Tohver, E., van der Pluijm, B.A., Mezger, K., Scandolara, J.E., Essene, E., 2005. Two stage tectonic history of the SW Amazon craton in the late Mesoproterozoic: identifying a cryptic suture zone. Precambrian Res. 137, 35–59.
Tomkins, H.S., Williams, I.S., Ellis, D.J., 2005. In situ U-Pb dating of zircon formed from retrograde garnet breakdown during decompression in Rogaland, SW Norway. J. Metamorph. Geol. 23, 201–215.
Torgersen, E., Viola, G., Zwingmann, H., Henderson, I.H.C., 2015. Inclined K-Ar illite age spectra in brittle fault gouges: effects of fault reactivation and wall-rock contamination. Terra Nova 27, 106–113.
Torgersen, E., Henderson, I.H.C., Bingen, B., Svendby, K., Nasuti, A., 2018. Abstract. The Nisser Shear Zone – Discovery of a Sveconorwegian crustal-scale detachment zone in southern Norway 33rd Nordic Geological Winter Meeting. Geological Society of Denmark, Copenhagen, Denmark, p. 59.
Torsvik, T.H., 2003. The Rodinia jigsaw puzzle. Science 300, 1379–1381.
Torsvik, T.H., Smethurst, M.A., Meert, J.G., Van der Voo, R., Mc Kerrow, W.S., Brasier, M.D., Sturt, B.A., Walderhaug, H.J., 1996. Continental break up and collision in the Neoproterozoic and Paleozoic - A tale of Baltica and Laurentia. Earth Sci. Rev. 40, 229–258.
Touret, J.L., 1971a. Le facies granulite en Norvège méridionale. 1. Les associations minéralogiques. Lithos 4, 239–249.
Touret, J.L., 1971b. Le facies granulite en Norvège méridionale. 2. Les inclusions fluides. Lithos 4, 423–436.
Touret, J.L., 1987. Day 2 - The high-grade metamorphic Bamble sector. In: Maijer, C., Padget, P. (Eds.), The Geology of Southernmost Norway: An Excursion Guide. Norges Geologiske Undersøkelse, pp. 25–30 Special Publication No 1.
Tual, L., Piñán-Llamas, A., Möller, C., 2015. High-temperature deformation in the basal shear zone of an eclogite-bearing fold nappe, Sveconorwegian orogen, Sweden. Precambrian Res. 265, 104–120.
Tual, L., Pitra, P., Möller, C., 2017. P–T evolution of Precambrian eclogite in the Sveconorwegian orogen, SW Sweden. J. Metamorp. Geol. 35, 493–515.
Tucker, R.D., Krogh, T.E., Råheim, A., 1990. Proterozoic evolution and age - province boundaries in the central part of the Western Gneiss Region, Norway: results of U-Pb dating of accessory minerals from Trondheimsfjord to Geiranger. In: Gower, C.F., Rivers, T., Ryan, B. (Eds.), Mid-Proterozoic Laurentia-Baltica. Geological Association of Canada, pp. 149–173 Special Paper 38.
Ulmius, J., Andersson, J., Möller, C., 2015. Hallandian 1.45 Ga high-temperature metamorphism in Baltica: P-T evolution and SIMS U-Pb zircon ages of aluminous gneisses, SW Sweden. Precambrian Res. 265, 10–39.
Ulmius, J., Möller, C., Page, L., Johansson, L., Ganerød, M., 2018. The eastern boundary of Sveconorwegian reworking in the Baltic Shield, defined by 40Ar/39Ar geochronology across the southernmost Sveconorwegian Province. Precambrian Res. 307, 201–217.
Vaasjoki, M., 1981. The lead isotopic composition of some Finnish galenas. Geol. Surv. Finl. Bull. 316, 25.
Valentino, D.W., Chiarenzelli, J.R., Regan, S.P., 2019. Spatial and temporal links between Shawinigan accretionary orogenesis and massif anorthosite intrusion, southern Grenville province, New York, U.S.A. J. Geodyn. 129, 80–97.
Vander Auwera, J., Longhi, J., 1994. Experimental study of a jotunite (hypersthene monzodiorite): constraints on the parent magma composition and crystallization

conditions (P, T, fO_2) of the Bjerkreim-Sokndal layered intrusion (Norway). Contrib. Mineral. Petrol. 118, 60–78.
Vander Auwera, J., Longhi, J., Duchesne, J.C., 1998. A liquid line of descent of the Jotunite (Hypersthene Monzodiorite) suite. J. Petrol. 39, 439–468.
Vander Auwera, J., Bogaerts, M., Liégeois, J.P., Demaiffe, D., Wilmart, E., Bolle, O., Duchesne, J.C., 2003. Derivation of the 1.0-0.9 Ga ferro-potassic A-type granitoids of southern Norway by extreme differentiation from basic magmas. Precambrian Res. 124, 107–148.
Vander Auwera, J., Bogaerts, M., Bolle, O., Longhi, J., 2008. Genesis of intermediate igneous rocks at the end of the Sveconorwegian (Grenvillian) orogeny (S Norway) and their contribution to intracrustal differentiation. Contrib. Mineral. Petrol. 156, 721–743.
Vander Auwera, J., Bolle, O., Bingen, B., Liégeois, J.P., Bogaerts, M., Duchesne, J.C., DeWaele, B., Longhi, J., 2011. Sveconorwegian massif-type anorthosites and related granitoids result from post-collisional melting of a continental root. Earth Sci. Rev. 107, 375–397.
Vander Auwera, J., Charlier, B., Duchesne, J.C., Bingen, B., Longhi, J., Bolle, O., 2014b. Comment on Bybee et al. (2014): Pyroxene megacrysts in Proterozoic anorthosites: Implications for tectonic setting, magma source and magmatic processes at the Moho. Earth Planet. Sci. Lett. 401, 378–380.
Vander Auwera, J., Bolle, O., Dupont, A., Pin, C., Paquette, J.L., Charlier, B., Duchesne, J.C., Mattielli, N., Bogaerts, M., 2014a. Source-derived heterogeneities in the composite (charnockite-granite) ferroan Farsund intrusion (SW Norway). Precambrian Res. 251, 141–163.
Vanderhaeghe, O., 2012. The thermal–mechanical evolution of crustal orogenic belts at convergent plate boundaries: A reappraisal of the orogenic cycle. J. Geodyn. 56-57, 124–145.
Vermeesch, P., 2012. On the visualisation of detrital age distributions. Chem. Geol. 312, 190–194.
Verschure, R.H., Andriessen, P.A.M., Boelrijk, N.A.M., Hebeda, E.H., Maijer, C., Priem, H.N.A., Verdurmen, E.A.T., 1980. On the thermal stability of Rb-Sr and K-Ar biotite systems: evidence from coexisting Sveconorwegian (ca. 870 Ma) and (ca. 400 Ma) biotites in SW Norway. Contrib. Mineral. Petrol. 74, 245–252.
Villaseca, C., Barbero, L., Herreros, V., 1998. A re-examination of the typology of peraluminous granite types in intracontinental orogenic belts. Trans. R. Soc. Edinb. Earth Sci. 89, 113–119.
Viola, G., Henderson, I.H.C., 2010. Inclined transpression at the toe of an arcuate thrust: an example from the Precambrian "Mylonite Zone" of the Sveconorwegian orogen. In: Law, R., Butler, R., Holdsworth, R.E., Krabbendam, M., Strachan, R.A. (Eds.), Continental Tectonics and Mountain Building - The Legacy of Peach and Horne. Geological Society, Special Publications, London, pp. 715–737.
Viola, G., Venvik Ganerød, G., Wahlgren, C.H., 2009. Unraveling 1.5 Ga of brittle deformation history in the Laxemar-Simpevarp area, southeast Sweden: a contribution to the Swedish site investigation study for the disposal of highly radioactive nuclear waste. Tectonics 28 (5). https://doi.org/10.1029/2009TC002461 TC5007.
Viola, G., Henderson, I.H.C., Bingen, B., Hendriks, B.W.H., 2011. The Grenvillian-Sveconorwegian orogeny in Fennoscandia: Back-thrusting and extensional shearing along the "Mylonite Zone". Precambrian Res. 189, 368–388.
Viola, G., Zwingmann, H., Mattila, J., Käpyaho, A., 2013. K-Ar illite age constraints on the Proterozoic formation and reactivation history of a brittle fault in Fennoscandia. Terra Nova 25, 236–244.
Viola, G., Bingen, B., Solli, A., 2016. Berggrunnskart Kongsberg lithotectoniske enhet, Kongsberg-Modum-Hønefoss - Bedrock geology map of the Kongsberg lithotectonic unit, Kongsberg-Modum-Hønefoss. Norges Geologiske Undersøkelse - Geological Survey of Norway Scale 1:100000, 1 sheet.
Wahlgren, C.H., Page, L., Kübler, L., Delin, H., 2016. ^{40}Ar-^{39}Ar biotite age of a lamprophyre dyke and constraints on the timing of ductile deformation inside the Idefjorden terrane and along the Mylonite Zone, Sveconorwegian orogen, south-west Sweden. GFF 138, 311–319.
Wahlgren, C.H., Stephens, M.B., 2020. Chapter 11 - Reworking of older (1.8 Ga) continental crust by Mesoproterozoic (1.5–1.4 Ga) orogeny, Blekinge–Bornholm orogen, southeastern Sweden. Geol. Soc. Lond. Mem. 50, 291–312.
Wahlgren, C.H., Cruden, A.R., Stephens, M.B., 1994. Kinematics of a major fan-like structure in the eastern part of the Sveconorwegian orogen, Baltic Shield, south-central Sweden. Precambrian Res. 70, 67–91.
Wallace, P.J., 2005. Volatiles in subduction zone magmas: concentrations and fluxes based on melt inclusion and volcanic gas data. J. Volcanol. Geotherm. Res. 140, 217–240.
Wang, X.D., Söderlund, U., Lindh, A., Johansson, L., 1998. U-Pb and Sm-Nd dating of high-pressure granulite- and upper amphibolite facies rocks from SW Sweden. Precambrian Res. 92, 319–339.
Weber, B., Köhler, H., 1999. Sm–Nd, Rb–Sr and U–Pb geochronology of a Grenville Terrane in Southern Mexico: origin and geologic history of the Guichicovi Complex. Precambrian Res. 96, 245–262.
Weber, B., Scherer, E.E., Schulze, C., Valencia, V.A., Montecinos, P., Mezger, K., Ruiz, J., 2010. U-Pb and Lu-Hf isotope systematics of lower crust from central-southern Mexico - Geodynamic significance of Oaxaquia in a Rodinia Realm. Precambrian Res. 182, 149–162.
Weis, D., 1986. Genetic implications of Pb isotopic geochemistry in the Rogaland anorthositic complex (Southwest Norway). Chem. Geol. 57, 181–199.
Wickström, L.M., Stephens, M.B., 2020. Chapter 18 - Tonian–Cryogenian rifting and Cambrian–Early Devonian platformal to foreland basin development outside the Caledonide orogen. Geol. Soc. Lond. Mem. 50, 451–477.
Wiest, J.D., Jacobs, J., Ksienzyk, A.K., Fossen, H., 2018. Sveconorwegian vs. Caledonian orogenesis in the eastern Øygarden Complex, SW Norway – Geochronology, structural constraints and tectonic implications. Precambrian Res. 305, 1–18.
Wilmart, E., Demaiffe, D., Duchesne, J.C., 1989. Geochemical constraints on the genesis of the Tellnes ilmenite deposit, southwest Norway. Econ. Geol. 84, 1047–1056.
Zhang, S., Li, Z.-X., Evans, D.A.D., Wu, H., Li, H., Dong, J., 2012. Pre-Rodinia supercontinent Nuna shaping up: a global synthesis with new paleomagnetic results from North China. Earth Planet. Sci. Lett. 353-354, 145–155.
Zhang, W., Roberts, D., Pease, V., 2015. Provenance characteristics and regional implications of Neoproterozoic, Timanian-margin successions and a basal Caledonian nappe in northern Norway. Precambrian Res. 268, 153–167.
Zhang, W., Roberts, D., Pease, V., 2016. Provenance of sandstones from Caledonian nappes in Finnmark, Norway: implications for Neoproterozoic–Cambrian palaeogeography. Tectonophysics 691, 198–205.